CD8+ T Cell Receptor Characterization in HPV Associated Head and Neck Cancer

by

Peaches Rebecca Ulrich

A Dissertation Presented in Partial Fulfillment
of the Requirements for the Degree
Doctor of Philosophy

Approved November 2020 by the
Graduate Supervisory Committee:

Karen S. Anderson, Chair
Douglas Lake
Carlo Maley
Arvind Varsani

ARIZONA STATE UNIVERSITY

December 2020

ABSTRACT

The human papillomavirus (HPV) is a double-stranded DNA virus responsible for causing upwards of 80% of head and neck cancers in the oropharyngeal region. Current treatments, including surgery, chemotherapy, and/or radiation, are aggressive and elicit toxic effects. HPV is a pathogen that expresses viral-specific oncogenic proteins that play a role in cancer progression. These proteins may serve as potential targets for immunotherapeutic applications. Engineered T cell receptor (TCR) therapy may be an advantageous approach for HPV-associated cancers. In TCR therapy, TCRs are modified to express a receptor that is specific to an immunogenic antigen (part of the virus/cancer capable of eliciting an immune response). Since HPV-associated oropharyngeal cancers typically express unique viral proteins, it is important to identify the TCRs capable of recognizing these proteins. Evidence supports that head and neck cancers typically experience high levels of immune cell infiltration and are subsequently associated with increased survival rates. Most of the immune cell infiltrations in HPV+ HNSCC are CD8+ T lymphocytes, drawing attention to their prospective use in cellular immunotherapies. While TCRs are highly specific, the TCR repertoire is extremely diverse; enabling the immune system to fight off numerous pathogens. In project 1, I review approaches to analyzing TCR diversity and explore the use of DNA origami in retrieving paired TCR sequences from a population. The results determine that DNA origami can be used within a monoclonal population but requires further optimization before being applied in a polyclonal setting. In project 2, I investigate HPV-specific T-cell dysfunction; I detect low frequency HPV-specific CD8+ T cells, determine that they are tumor specific, and show that HPV+HNSCC patients exhibit increased epitope-specific levels of CD8+T cell exhaustion. In project 3, I apply methods to expand and isolate TCRαβ sequences derived from donors stimulated with a previously identified HPV epitope. Single-cell analysis provide ten unique

TCRαβ pairs with corresponding CDR3 sequences that may serve as therapeutic candidates. This thesis contributes to fundamental immunology by contributing to the knowledge of T cell dysfunction within HPV+HNSCC and further reveals TCR gene usage within an HPV stimulated population, thus identifying potential TCR pairs for adoptive cell therapies.

DEDICATION

This degree is dedicated to my Ohana: James, Becky, and Jaimis Ulrich. You selflessly paved the way for me to pursue my passions and in doing so, have made me who I am today. Daddy, thank you for teaching me to prioritize our faith, family, and education; thank you for teaching me to be humble and stubborn, it has brought me a long way. Mama, you are the most radiant and resilient person that I know; to you I owe every success and because of you, I stood up again after every failure, thank you. To my heart, best sister friend, and forever life-coach, Meeshie. You are my biggest advocate and cheerleader, thank you for lifting me up and keeping me going every step of the way; I wouldn't want to life with anyone else by my side, thank you for helping me to see the world in the most vibrant of colors. Ohana, I love you.

To my nephews and nieces, Drake, Caydin, Avery and Bellamy (the lost boys), Clover, Jordan, Enzo, Milo, Maddie, Brady, Caleb, and Jacob, Devin, and CJ. You can do anything in this world, all you have to do is believe. Remember that Goonies never say die and if you ever feel lost in this world all you have to do is look to the sky; second star to the right and straight on till morning. To my sister Gina and every aunt, uncle, cousin, and friend that cheered me on, thank you, I love you.

To my person, Heather Hrach, this thesis would not have happened without you. You helped me to grow both scientifically and personally in more ways than I could count, and I will never be able to repay you. You, Aaron, and Leica made me feel less alone throughout this process and were always there to encourage, support, and love me. I love you. To best friend Brittany Ulloa, thank you for being able to predict my every movement and never hesitate to knock sense into me, I love you.

To Kim Emfield, Jamie Slingluff, and Trish Montano thank you for your love and prayers. Ash, thank you for traveling this great state with me and reminding me how

remarkably wild and free this world can be. To the Ochoa, Wharton, and Vallas family, I cannot thank you enough for your support and love over the years. To my BFF Mateo, my best boy Lennan, and my best girl Ellion I really couldn't have asked for better rascals to spend my nights and weekends with. Thank you for keeping the kid in me alive with your laughter and imagination. I love you this much.

To Dr. Sylvia Vetrone, Dr. Hector Valenzuela, Dr. Kathy Barlow, Dr. Erica Fradinger, Dr. Dave Bourgaize, Dr. Cheryl Swift, Dr. Andrea Rehn, Mrs. Alvarado, and Mrs. Dodge. You sparked and fueled my passion for learning, creating, and thinking "outside the box." Dr. Vetrone, not only did you introduce me to the subject of Immunology but without you I never would have thought to pursue a PhD; you are a phenomenal professor and a great friend, thank you. Dr. Valenzuela, you continually inspire me with your excitement for science and your consistent encouragement in my studies, thank you. Dr. Barlow, this pear would have expired long ago if I didn't have you to keep me on my toes, thank you.

To those who are no longer with me but never fail to propel me forward, Amanda Parks, Lupe Arredondo, and Bema. Amanda, you are still my greatest loss in this world, I fight every day for you. Being surrounded by such talented scientists I truly believe that one day we will provide personalized diagnostics, preventative care, and treatments that will replace despair with hope. Grandma Lupe, your little genius made it and I made it because of you. I miss you. Bema, I think of you every day, I love you. Thank you all for believing in me.

ACKNOWLEDGMENTS

I would like to thank my dissertation committee, Dr. Karen Anderson, Dr. Douglas Lake, Dr. Carlo Maley, and Dr. Arvin Varsani. Dr. Anderson, you have provided me with an environment to learn, create, and grow in my passion for Science; thank you for your consistent enthusiasm for research. Dr. Lake, thank you for showing interest in my research and for your intellectual input. Dr. Maley, thank you for showing me the importance of looking at the bigger picture. Dr. Varsani, thank you for always welcoming conversations and probing me to think of the "why" behind every question. To Dr. Wilson-Rawls, thank you for being a mother hen to all of the MCB graduate students, we could not ask for a better advocate. To Dr. Mangone, thank you for helping me to see the light at the end of the tunnel.

To Dr. Krishna, thank you for modeling the dedication, & resilience required for being a successful scientist. To Dr. Schoettle, you taught me resilience and so much of what I know about Immunology; thank you for always coming to the rescue when I needed it the most. To Dr. Yaron, thank you for being a "breath of fresh air" and continually providing encouragement, you are going to change the face of academia for the better. To my past and present lab mates: Dr. Katchman, Dr. Chen, Dr. Chowell-Puente, Dr. Ewaisha, Dr. Ferdosi, Dr. Hou (my lab mom), Eric Wilson (my forever plus one), Jacqueline Carmona, Mark Knappenberger, Alex Roesler, Marika Hopper, Padhma Yuvarai, and Gillian Reynoso. Thank you for imparting your knowledge, sharing in laughter, and indulging in my coffee addiction. To Nolan Vale, Gabrielle Hirneise, and Charles Marquardt, thank you for bringing color into my world; I hope you make as profound a mark on this world as you have on my heart. This degree was a team effort, and I could not have done it without each of you. To the individuals I met as strangers and have become best friends: my MCEats Kevin Klicky, Cindy Xu, Alex

Andre, Mark Reynolds, Kavita Manhas, Carrie Jenkins, Nicole Appel, Evelyn Luna, Matt Epp, and Piper, I love you guys.

To Kerri Robinson and Mr. and Mrs. Maslick, thank you for supporting me in my graduate studies; this research would not have been possible without you. To the Genomics Core (Joy, Dee, Nick, and Brandon) thank you for your endless help and nerf gun barricades. To the Biodesign facilities and security team, thank you for every warm smile.

TABLE OF CONTENTS

CHAPTER Page

LIST OF TABLES

LIST OF FIGURES

Figure Page

CHAPTER 1

INTRODUCTION

Human papillomaviruses (HPVs) are responsible for an array of diseases affecting areas of cutaneous and mucosal epithelia, typically inducing hyperproliferative lesions [1, 2]. The severity of disease ranges from warts on the skin and genitals, to invasive cancers like cervical cancer and head and neck cancer. Initially, HPV was originally thought to only affect women as it was first recognized in cervical cancers [3]. In the 1970s, Dr. Harald zur Hausen won the Nobel Prize for identifying HPV in cervical cancer but it was not until 1983 that the connection between HPV infection and oropharyngeal cancers was identified, highlighting the susceptibility of both men and women to HPV-associated cancers [3, 4]. While extensive research has been conducted to investigate the role of adaptive immunity in the context of chronic infections, there is still very little that is understood about HPV infections and immune clearance [5]. Specifically, it is still unknown as to why some individuals can clear HPV infections while others develop persistent infections and HPV associated cancers. The HPV genome, which is mostly conserved between strains, expresses viral-specific oncogenic proteins that have the potential to propagate cancer progression [1]. Recent studies have investigated the use of HPV protein fragments (epitopes) as targets for T-cell based immunotherapies [6]. Expanding on these known epitopes and characterizing the immune cells that recognize and respond to these epitopes may further advance our ability to generate targeted therapies.

Immune System Overview

Immunology

Immunology is the study of how the body, through a range of physical, biological, and chemical defenses, combats infections [7, 8]. The immune system is equipped with effector

mechanisms that function to destroy invading pathogens and eliminate toxic or allergenic particles [9].

As a whole, the key functions of the immune system include discrimination, diversity, specificity, rapidity, and memory [10]. In the context of immunology, discrimination refers to the immune system's ability to differentiate between infectious microorganisms and the host's own molecular makeup, a concept referred to as "self" versus "non-self" [10, 11]. In addition to being able to discriminate between self and non-self, immune responses must be diverse enough to respond to a wide range of pathogens while also maintaining specificity to that pathogen [10, 11]. The speed of the immune response is important because it must occur quickly enough to contain and prevent the spread of infection [10, 11]. Lastly, upon successful recognition and removal of a pathogen, the host is provided with long-lasting immunity to subsequent infections from that pathogen [10, 11]. Broadly, the immune system is divided into two compartments: innate and adaptive immunity. These two branches of the immune system are primarily distinguished by the speed and specificity of their reaction to a pathogen [10, 12].

Innate immunity, the initial respondent to a pathogen, produces a general, rapid response but does not confer any immune memory[10]. Importantly, the innate immune system is also responsible for activating the adaptive immune response [10–12]. Upon activation, the goal of the adaptive immune system is to induce a more rapid and specific response to the invading pathogen [10, 12]. Once the infection is controlled, adaptive immune cell subsets specific to that pathogen remain and circulate throughout the body to provide a swift response to any potential subsequent infections [10, 12]. Although distinct from one another, these two branches of immunity are inherently complementary.

General Response to Infection

In most instances, the body's first defense against pathogens is a physical barrier such as skin or the mucosal epithelium [7]. Epithelial cells produce a number of natural antimicrobial defenses, including defensins and cathelicidins, which are responsible for damaging the cell walls of microbes [7, 10]. Depending on the location of the infection (i.e. the gastrointestinal tract), an invading pathogen may also need to overcome secretions of sebum, lactic acid, and/or lysozymes, which also work to trap and demolish the integrity of the pathogen [7, 10]. Throughout the duration of the immune response, an individual may experience redness, swelling, heat, and/or pain, which may fluctuate in intensity [10]. Upon successfully breaching both the physical and biochemical barriers, the invading pathogen begins to replicate, at which point, it may be recognized by innate immune cells [7]. Once activated (occurring within minutes to hours), different types of innate cells implement a diverse set of mechanisms to destroy the pathogen [7, 10]. The response of the innate immune system to infection is typically ample enough to clear infections. However, when the innate system is not successful in clearing infectious pathogens, the adaptive immune response is required.

Innate Immunity

The innate immune system is comprised of antimicrobial proteins (lysozymes, defensins, complement proteins), small bioactive molecules (cytokines, chemokines, etc), and a subset of immune cells [7, 9]. The complement system is one of the most critical elements of innate immunity. Briefly, once activated via the recognition of pathogen-associated molecular patterns (PAMPs), molecules of the complement system puncture holes into the membranes of bacterial pathogens [7, 12–14]. This interaction leads to a local inflammatory response and further promotes phagocytosis of the pathogen [7, 10]. If complement is not sufficient in

destroying the pathogen, then cells such as tissue macrophages will activate innate immune cells via the secretion of cytokines [7, 10, 12]

Cells of the innate immune system derive from myeloid progenitor cells and include neutrophils, eosinophils, basophils, monocytes, and macrophages [7, 15]. Neutrophils, eosinophils, and basophils are polymorphonuclear leukocytes that have cytoplasmic granules [9–11]. These cells express receptors on their cell surface (scavenger, complement, Fc receptors) that help to recognize targets on extracellular pathogens, complement proteins, and antibodies, respectively [8, 10, 15]. After recognition, neutrophils, eosinophils, and basophils attack the pathogen primarily via phagocytosis and/or degranulation. Similar to neutrophils, eosinophils, and basophils, macrophages and monocytes express cell surface receptors to recognize and kill pathogens[10, 15, 16]. However, these cells also play a key role in regulating inflammation and cytokine production [10, 11]. Macrophages are tissue residents whereas monocytes circulate throughout the body. Dendritic cells and macrophages are unique cell subsets responsible for activating adaptive immune cells via antigen presentation through the Major Histocompatibility Complex (MHC) I or MHC II (further discussed in subsequent sections)[10–12]

Adaptive Immunity

Adaptive immunity evolved nearly 450 million years ago, with the emergence of the first jawed vertebrates [17]. The evolution was marked by the presence of diverse lymphoid-derived cell subsets and molecules, including natural killer (NK) cells, NK-T cells, lymphocytes (B and T cells), major histocompatibility complexes (MHC I and MHC II), and immunoglobulin (Ig) molecules [9, 17]. NK cells are granular lymphocytes that recognize and kill viral/tumor-infected cells via degranulation and have the capability to proliferate in response to microbes [10]. NK-T cells are hybrids of NK and T cells in that they have

characteristics of both, including being able to recognize surface antigens in the absence of MHC [9]. T and B lymphocytes are adaptive immune cells that express cell surface receptors responsible for binding to and identifying antigens, or the components (molecule, macromolecule, virus particle, etc) of a pathogen recognized as non-self [10, 18, 19].

Adaptive immune responses can be partitioned into humoral and cell-mediated immunity and are differentiated by active cell type and the microbe of interest being targeted [11, 16]. In short, humoral immunity is facilitated by B cells and associated antibodies. B cells express B cell receptors (BCRs) that are responsible for recognizing soluble antigens, leading to differentiation into either plasma or memory B cells [9, 10, 16, 20]. Plasma cells produce antibodies (secreted Ig molecules) that neutralize pathogens; whereas, memory cells circulate the body in wait of subsequent infection. B cell subsets can be further defined by the type of antigen they recognize, and the resulting antibody produced [9, 20].

Cell-mediated immunity is characterized by T cells. Similar to B cells, T cells are classified by their T cell receptors (TCRs) which are responsible for recognizing microbes that have been previously digested and presented on MHC proteins via antigen-presenting cells (APCs) (i.e. dendritic cells) [18]. Two major subsets of T cells are CD4+ (helper) T cells and CD8+ T cells (the focus of this dissertation). CD4 (helper) T cells respond to digested extracellular pathogens and produce cytokines that work to control the type and intensity of the response [9, 10]. Briefly, upon stimulation by peptide:MHC II (p:MHC) complexes, CD4+ T cells secrete pro-inflammatory cytokines (such as Th1, Th2, Th17) that lead to eliminating intracellular/extracellular pathogen. CD4+ T cells can also aid B cells and CD8+ T cells in their effector function [16]. CD8+ T cells, also regarded as cytotoxic T cells or CTLs, are stimulated by pMCH I complexes via APCs [10, 18]. Once stimulated, CTLs travel to the site of infection and induce apoptosis of the infected or malignant cells[9, 10, 16]. Apoptosis by

CTLs can occur through effector molecules including Perforin and Granzyme or Fas-ligand (FasL) binding [16]. Upon CTL recognition of target cells, secretory granules comprised of Granzyme B and Perforin, move toward the TCR:MHC immunologic synapse and are released[21]. Another method of CTL killing is through the binding of FasL located on CTLs to the Fas protein expressed on target cells [10]. CD8+ T cells

Major Histocompatibility Complex (MHC) and Antigen Processing

Human leukocyte antigen (HLA) molecules are membrane bound glycoproteins that are located on the surface of almost all cells [10, 22]. HLA molecules are encoded by the genetic loci of major histocompatibility complexes (MHC). In 1987, Bjorkman et al elucidated the crystal structure of the human MHC HLA-A*02:01-B2M complex [22]. Figure 1.1 shows the original schematic representation of the HLA-A2 structure (left) and the MHC I crystal structure with peptide bound (right). The MHC I molecules (HLA-A, B, and C) are made up of two polypeptide chains, a heavy chain (30KD) and a light chain (β_2m, 11KD) [22]. The heavy chain, which extends into the membrane bilayer, is divided into three domains: α_1, α_2, and α_3. The α_1 and α_2 subunits form the antigen binding cleft for peptide binding and α_3 binds to CD8α co-receptor during TCR:pMHC interactions.

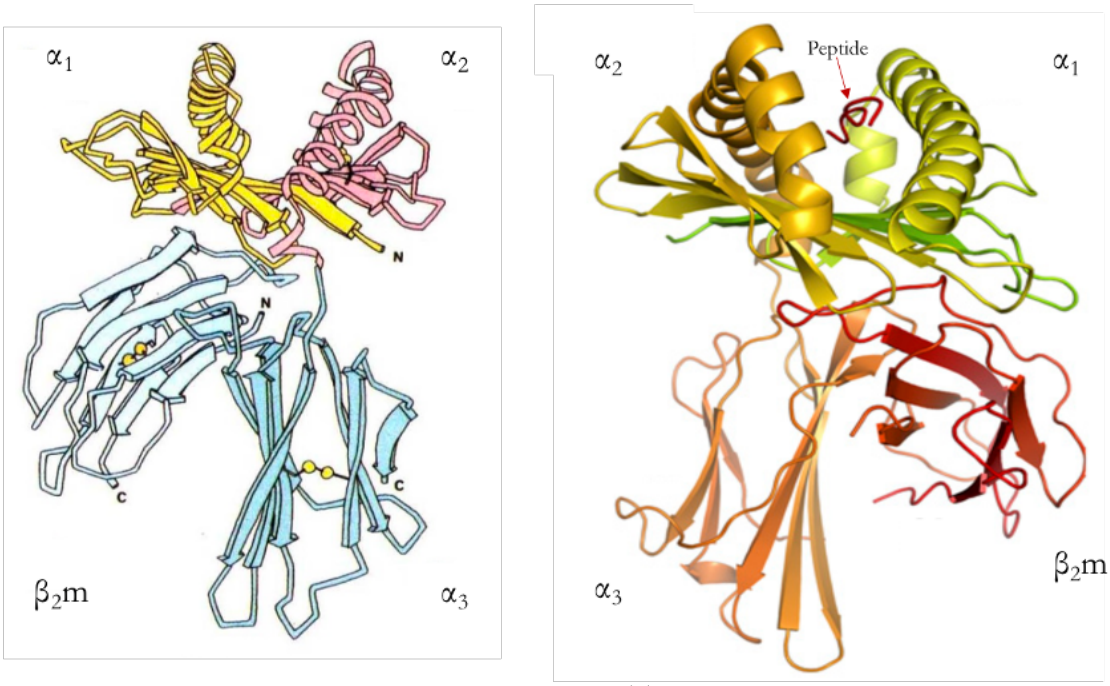

Figure 1.1: Ribbon Diagram of MHC I Complex. The figure to the right is a representation of the four HLA-A2 domains: α_1, α_2, α_3, and β_2m. The immunoglobulin-like domains α_3 and β_2m are located at the bottom and are proximal to the cell membrane. Polymorphic domains α_1, α_2, are shown on top. The ribbon structure (right) of the MHC class I molecule displays the interaction between the three alpha subunits and β2m with peptide. The alpha helices of the α1 and α2 subunits form an antigen binding cleft for peptide binding. Figure (left) adapted Bjorkman, *et al* 1987 [22] and figure (right) adapted from Zhang *et al* 2012 [23].

MHC molecules play a significant role in immune recognition of antigens as they serve to present antigen fragments to T cells [24]. Classical antigen processing postulates that CTLs are presented intracellular peptides (antigen fragments) via MHC class I (HLA-I) molecules; whereas, CD4+ helper T cells are presented peptides by MHC class II (HLA-II) molecules [10, 25, 26]. While nearly all nucleated cells express MHC I molecules, MHC II are generally present on specialized cells, including APCs [27]. Antigen processing generally occurs in one of two ways, through the intracellular proteolysis of cytosolic proteins via the immunoproteosome (MHC I pathway) or exogenous proteins are fragmented via lysosomes (MHC II pathway) [25–27]. For the purpose of this dissertation, MHC I antigen processing will be emphasized for its ability to harness the power of CD8+ T cells.

During MHC I processing, cytosolic proteins are degraded in the proteosome, producing long peptides ([25, 26]. These peptides are then transported by transporter-associated-with-antigen-processing (TAP) molecules to the endoplasmic reticulum (ER) of the cell [28]. Once in the ER, the long peptides are further cut by ER aminopeptidase (ERAAP) to produce short peptides (9-11 amino acids)[28]. Peptides bind to their respective MHC (forming a p:MHC complex) and travel to the cell surface via the Golgi complex. CTLs (via their TCR) then interact with the peptide generated, which may be self-peptide or non-self antigenic epitopes [25, 26]. Upon TCR:pMHC recognition, T cell activation occurs (discussed in subsequent sections).

TCRs have the capability of interacting with p:MHC complex but will only respond when the peptide is bound to a specific MHC molecule; TCR reactivity to peptide bound to a specific MHC molecule is referred to as MHC-restricted recognition [27]. T cell MHC restriction occurs during T cell development, when T cells undergo positive selection (only T cells that bind MHC with appropriate affinity go on for further development) [27]. The germline and selection models suggest different There are two models that explain how MHC restriction originated. The germline model argues that there is a preexisting germline TCR repertoire that is inherently specific for MHC whereas the selection model suggests that there is no inherent TCR bias to MHC [29].

T Cell Structure and Function

CD8+ T cells are the critical mediators in both eliminating pathogens and surveying the environment for infected cells [10, 19, 26]. Like other immune cells, an important role of CTLs is to be able to distinguish between self and non-self antigens [10, 19]. Unlike innate immunity, where cells can recognize pathogens via a fixed subset of cell-surface receptors, adaptive immunity relies on surface receptors of one molecular type: B cell receptors (BCR)

found on B cells or T cell receptors (TCR) located on T cells [26]. The majority of T cells in the human body, express classical TCRs that have a TCRα and TCRβ chain, which are co-expressed withCD3 chains (γ, δ, ε and ζ) [10, 19, 30, 31]. CD3 proteins have long cytoplasmic tails that help assist with signal transduction during TCR activation (Figure 1.2) [30, 31].

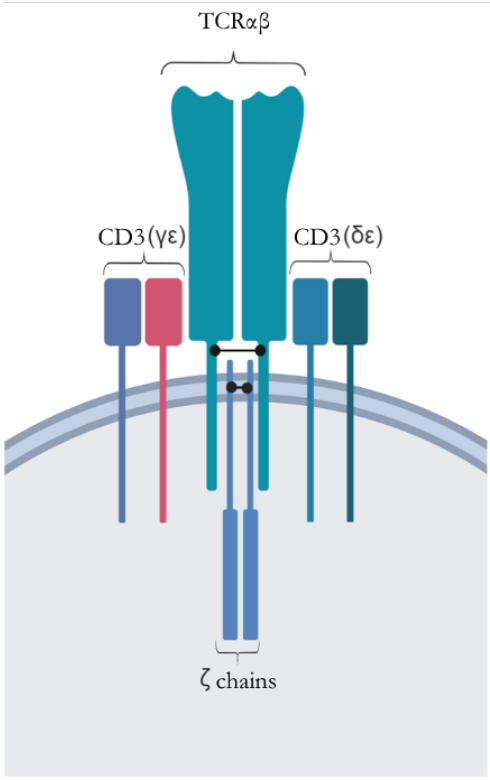

Further, TCRαβ are heterodimeric proteins that recognize MHC:peptide ligands [31, 32]. The α and β chains of the TCR are each composed of a constant and variable region. Each variable region of the TCR consists of variable (TRAV) and joining (TRAJ) gene segments for the alpha chain and variable (TRBV), diversity (TRBD), and joining (TRBJ) gene segments for the beta chain. In order to create a functional TCR, each gene must undergo a process of gene rearrangement known as somatic recombination [31].

Figure 1.2: Human TCR Complex. TCRαβ is a heterodimeric dimeric structure that is made up of two type-I glycoprotein chains that are connected by disulfide bridges. Each chain of the TCR is composed of two extracellular domains, a transmembrane region and a short intracytoplasmic region. The multimeric complex, referred to as CD3 complex, is responsible for mediating signal transduction upon antigen recognition. There are three CD3 dimers (εγ, δε and ζζ) that have acidic transmembrane residues, allowing for them to interact with the basic residues on the transmembrane portion of the TCR chains. Intracellular tyrosine activation motifs (ITAMs), found on the intracellular CD3 region, facilitate signal transduction. The CD3 dimers (εγ, δε and ζζ) each contain ITAMs; γ, δ and ε have one ITAM and ζ subunits contain three. Following TCR activation, the phosphorylated ITAMS recruit tyrosine kinases, initiating a signaling cascade to induce further T cell activation and/or effector functions [10, 26, 30]. Image created using BioRender.

Somatic recombination is the process of gene rearrangement in T cells [31, 33]. Briefly, every V-region recombination event is initiated by 12bp and 23bp recombination signal

sequences (RSSs), which flank V-region gene segments, coming together. From there, lymphoid specific recombinases, known as RAG-1 and RAG-2, bind to the 12 and 23 RSS and bring them together [34, 35]. Rag proteins further cleave the DNA between the coding segment and its RSS, producing hairpins in the coding ends of the genes. Repair protein, Ku70/80, then bind to the hairpin and the Artemis protein randomly cleaves the hairpin [31, 33–35]. Terminal deoxynucleotidyl transferase (TdT) then performs random nucleotide additions to the ends of the cleaved DNA. From there, exonucleases remove nucleotides from the ends of the cleaved DNA while DNS repair enzymes correct for unpaired nucleotides. After this, DNA ligase IV ligates the two coding ends. Collectively, the process of somatic recombination plays a large role in TCR diversity [31, 33–35].

Following the somatic recombination of V, D, and J gene segments, the functional TCR is comprised of variable regions at each distal end of TCRα and TCRβ chains, forming what is known as the antigen-binding site [31, 33]. The antigen-binding site functions to recognize antigen fragments via MHC presentation[19]. Each variable region of the TCR chains has three highly diverse loops known as complementarity-determining regions (CDRs) 1, 2, and 3. CDR1 and 2 are primarily encoded by the V gene segment whereas CDR3 is encoded by a portion of V and J genes (for the alpha chain) and V, D, J genes (for the beta chain)[16]. Additionally, CDR3 also contains the random P- and N- nucleotides junctions within the V-J, V-D-J gene rearrangements, making the CDR3 region the most diverse [10, 26]. CDR3 typically makes the most contact with peptide during TCR recognition, and consequently determines specificity (Figure 1.3).

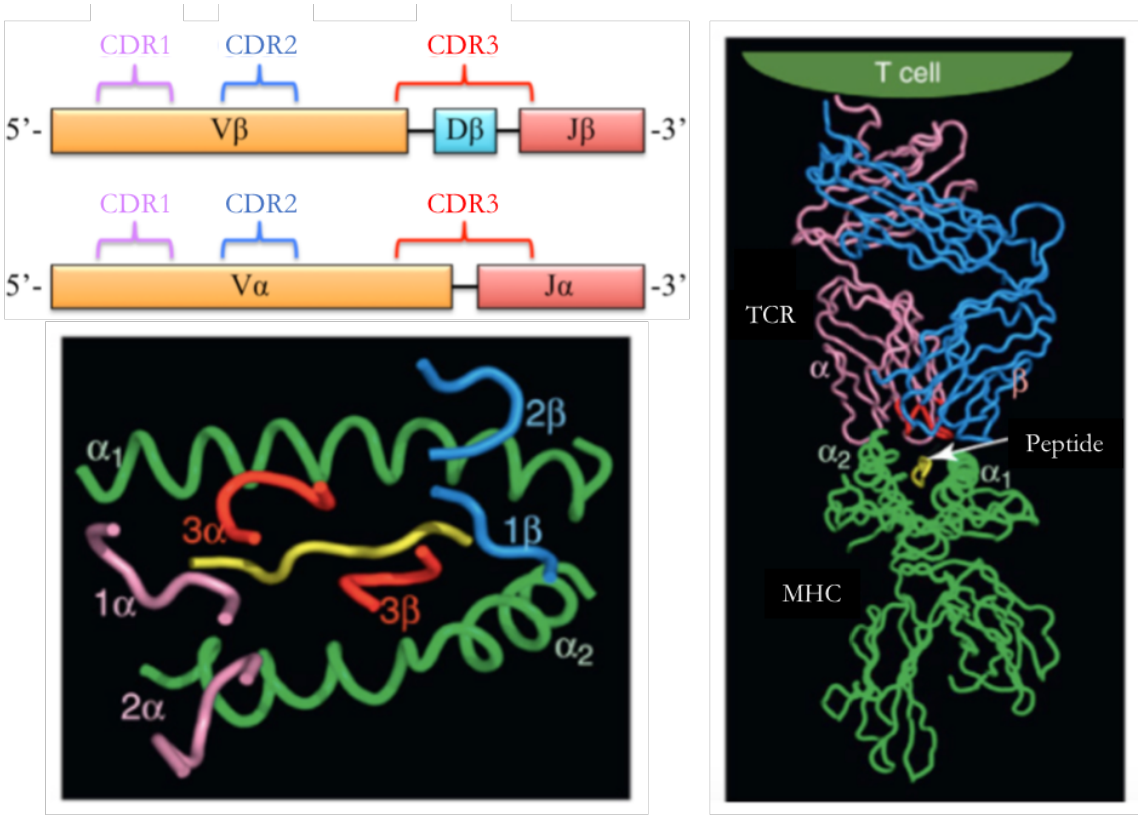

Figure 1.3 : Complementarity Determining Regions (CDRs) Interaction with MHC. The coding sequences for the CDR regions correspond to three hypervariable regions of DNA for each TCR chain. CDRs 1 and 2 are germline encoded within each given V gene while CDR3 is encoded by the imprecise junction of the V-D-J gene segments or V-J for TCRβ and TCRα, respectively. [B] Crystal structures of TCR:pMHC complexes show that even though CDR1, 2, and 3 can all make contact with both MHC and bound peptide epitopes, it is CDR1 and 2 (pink and blue, respectively) that primarily make contact with MHC protein (green). At the same time, CDR3 (red) is typically centered over the bound peptide (shown in yellow). [C] Crystal structure of the complete TCR:pMHC complex. Crystal structures adapted from Garcia *et al.* 2012 [32].

There exists a high level of diversity and specificity amongst TCRs. Much of TCR diversity is accredited to three primary factors. First, there are numerous copies of V, D, and J gene segments encoded in the genome, allowing for different combinations of rearranged V-J or V-D-J during somatic recombination (known as sequence diversity). Secondly, during somatic recombination, non-templated nucleotide additions and/or deletions are introduced at gene junctions (junctional diversity), further contributing to TCR diversity. Lastly, the different combinations of TCRα and TCRβ chain pairing further contributes to a diverse

repertoire of TCRs. In 1999 Arstilla published a study reporting that through the process of somatic recombination, an estimated 10^6 unique TCRβ can be produced [36]. With similar TCRα estimates, the theoretical prediction of unique TCRαβ combinations was 10^{12}. Using spectratyping technology, it was estimated that the human repertoire contained $2.5x10^7$ TCR clonotypes whereas more advanced technology has projected there to be roughly $3\text{-}4x10^6$ unique TCRβ alone, suggesting greater diversity than once expected [36, 37]. The true extent of TCR diversity is relatively unknown, with estimates ranging from 10^{12} - 10^{16} TCR clonotypes (TCR specific to particular antigen) [36, 38]. With the advancement of high-throughput sequencing, studies suggest that a more conservative range (10^{11} - 10^{12}) may actually be more reflective of unique TCR clonotypes [37]. Important to note, at adulthood humans have about 10^{12} T cells and since some will express the same TCR, it's likely that humans will actually go on to express less than 10^{12} unique TCR at any given time [36, 39–41]. Overall, the TCR repertoire in any given individual is highly diverse; current approaches to analyze TCR diversity will be further addressed in this thesis.

Furthermore, the interaction between TCR and peptide:MHC complex (TCR-pMHC) is critical for adaptive immunity. Once a TCR-pMHC interaction is established, forming an immunologic synapse the constant domain regions of TCRαβ interact with the CD3 complex proteins, initiating recruitment of signal transducing molecules (Figure 1.4) [16]. Signal transducing molecules such as LCK are recruited, resulting in phosphorylation of CD3 ITAMs [42]. Upon phosphorylation of the ITAMs, subsequent phosphorylation occurs resulting in

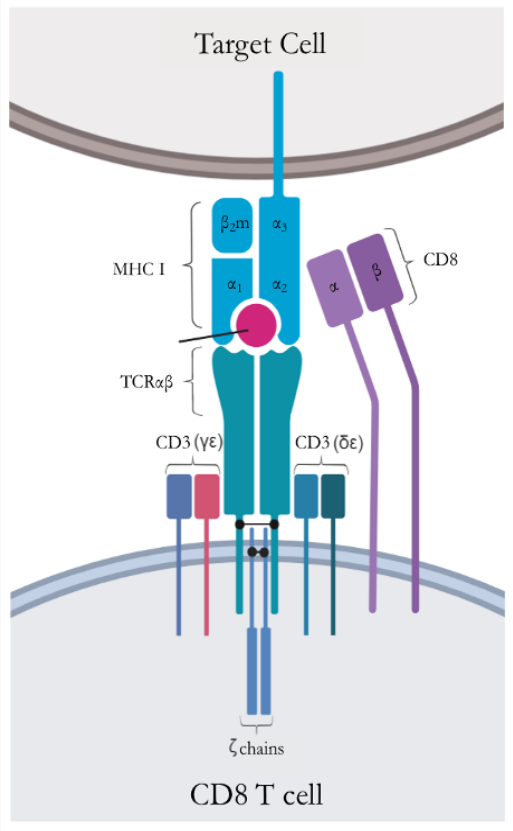

the assembly of a multiprotein complex known as LAT-signalosome [30, 42]. This complex includes co-receptors CD8 and CD28; CD8 co receptor binds to the α3 subunit of the MHC I complex and enhances intracellular signaling while CD28 enhances cell proliferation, cytokine production, and cell survival [43]. Collectively, this highly complex signaling network results in the upregulation of genes that are further required for proliferation, the recruitment and secretion of cytokines (Interleukin-2) and effector functions, including cytolysis of target cells [42, 43].

Figure 1.4: Immunological Synapse of the TCR-pMHC Interaction. TCR:pMHC with CD8 co-receptor (bottom) and antigen presenting cell (APC) at the top. The α domain of the CD8 co-receptor makes contact with the α3 subunit of the MHC I complex, enhancing the TCR;pMCH interaction and signal transduction. Following TCR activation, phosphorylated ITAMS of the TCR recruit tyrosine kinases, initiating a signaling cascade to induce further T cell activation and/or effector functions [10]. Image created using BioRender.

Adoptive Cell Therapeutic Approaches to Cancer

Harnessing the anti-tumor properties of the immune system to treat cancer has gained significant attention over the last several decades [36] The cytotoxic capabilities of CD8+ T cells in combination with their ability to target cancer-derived neoantigens has made them particularly provocative for developing immunotherapies [45]. The development and success of immune checkpoint inhibitors to essentially release the 'breaks' on T cells has further demonstrated the potential power of using T cells to combat cancer [46]. Immunotherapies in combination with immune checkpoint blockades have proven successful in increasing survival amongst patients with melanoma and non-small cell lung cancer [47]. However, for many late-

stage cancers, the development of new immunotherapeutic approaches is not just beneficial – it's necessary [48]. New immunotherapies, such as adoptive cell transfer, are being developed and refined for these hard-to-treat cancers

Adoptive cell therapy (ACT) is an immunotherapeutic approach that modifies T cells to target different tumor types [49]. Broadly, with some ACT, a patient's CD8+T cells are isolated and amplified to be re-infused into the patient, or human cell lines are engineered to express TCR for the recognition of a desired cancer antigen. Three common approaches encompassed by ACT include the use of tumor-infiltrating lymphocytes (TIL), modified T cell genes to express a novel TCR, and chimeric antigen receptors (CAR) that specifically target tumor cells [48]. Dr. Stevan Rosenberg first portrayed the successful use of TIL while at the National Institute of Health (NIH) [50]. In his studies, TIL were isolated from murine tumors and demonstrated *in vivo* anti-tumor activity. TIL therapy has proven successful in numerous cancer types including melanoma, cervical, renal, breast, and non-small cell lung cancer [51]. In addition to ACT with TIL, TCR and CAR therapies have shown promise.

TCR gene therapy, in which T cells are reprogrammed to recognize specific antigens via the modification of TCR genes, was first shown to have clinical relevance in targeting metastatic melanoma in 17 patients [48]. This therapeutic approach entails isolating antigen-specific TCR, learning their TCRαβ gene usages within a sample population and then determining which would be most functional (a topic that is further exploited in this thesis). In addition to melanoma, B-cell malignancies and synovial cell sarcoma have shown encouraging results in clinical trials with the use of TCR and CAR therapies [6]. However, attempting to apply these approaches to epithelial cancers has remained challenging. Many antigens targeted for epithelial cancers are shared by both healthy and tumor tissues, thus

increasing the likeliness of off-tumor toxicity [6, 45]. As more progress is made in discerning tumor antigens from healthy tissue antigens, toxicity issues could be diminished.

Targeting tumor-specific neoepitopes, derived from genetic alterations in tumor cells, has shown enhanced cytotoxic T-cell targeting of multiple solid tumors via ACT [52–54]. However, there are only certain overexpressed antigens that are known, thus limiting the amount of targets and potentially conferring the emergence of treatment-resistant cells [55]. Thus, there is renewed interest in determining a repertoire of HLA-restricted antigens that could be potentially targeted by TCR for ACT [52]. Accordingly, peptide databases have been created as active repositories for these antigens, to further accelerate the development of associated immunotherapies.

Human Papillomavirus (HPV) Genotypes

There are more than 130 species of HPV that have been identified according to the gene encoding the L1 protein and placed into five major phylogenetic genera: alpha, beta, gamma, mu, and nu [56]. New HPV types are classified when the sequence encoding their L1 protein has less than 90% similarity with previously identified L1 sequences [2]. Amongst the HPV genera, gamma comprises the majority of known HPV subtypes, followed by alpha and beta. Broadly, alpha HPV corresponds to mucosal infective strains; whereas, beta HPV tends to infect cutaneous epithelia [1]. HPV strains can be further classified into low and high risk types, dependent on their likelihood to cause malignant cancers. HPV 6, 11, 26, 53, 66, 67, 68, 70, 73, and 82 are generally considered low-risk; whereas, HPV 16, 18, 31, 33, 35, 39, 45, 51, 52, 56, 58, and 59 are recognized as high-risk types [56]. While low-risk HPV are most commonly responsible for benign genital warts, the high-risk types are known to contribute to the development of cancers including cervical, vaginal, anal, penial, and oropharyngeal [3]. Amongst all HPV strains, HPV-16 and HPV-18 are most associated in malignant HPV

cancers, with HPV16 contributing to more than 90% of HPV-associated head and neck cancers [56, 57].

HPV Genome

HPV is a small (50-60 nm) non-enveloped double stranded DNA virus comprised of a circular eight thousand base pair genome [1, 56, 58]. The HPV genome is made up of three primary regions described as the early (E), late (L), and noncoding long control region (LCR) or upstream regulatory region (URR)(Figure 1.5) [1, 56, 58, 59]. There are typically eight or nine open reading frames (ORFs) that are designated as early or late, depending on their time of expression [2, 60]. The early regions consist of six major proteins (E1, E2, E4, E5, E6, and E7), which play regulatory roles in HPV (Table 1.1). Broadly, E1 and E2 are involved in viral [6] replication and DNA replication whereas E4, E5, E6, and E7 play a more dominant role in driving cell cycle, immune evasion, and viral release [60]. The late region encodes for two major structural proteins, L1 and L2, which together make up the viral capsid necessary for viral packaging, transmission, viral spread, and survival [1, 60]. The majority of the early proteins are known to be expressed early during the infectious cycle and reduced later during infection. Of these proteins, E4 is the first to be expressed during late infection followed by L1 and L2 proteins [1]. The LCR, located between L1 and E6, contains promoter elements, binding sites for repressors, transcription factors, and the viral origin of replication [60].

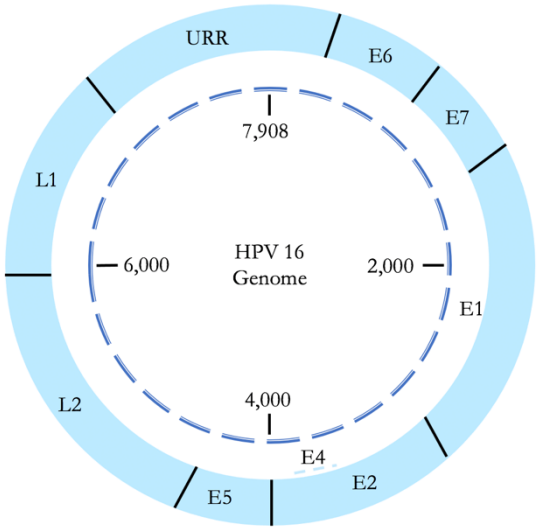

Figure 1.5: HPV Genome Organization.
Figure adapted from Riemer *et al* 2010

Importantly, E2 plays a vital role in suppressing the expression of oncogenes E6 and E7 [1, 2, 61]. In a healthy cell, retinoblastoma protein (pRB) binds to transcription factor E2f and prevents it from activating the transcription of genes that are necessary for cell division [2, 62]. Oncogenic E7 binds to the Rb protein product and E2F is released which leads to the progression of the cell cycle [62, 63]. Typically, in response to the release of E2F, p53 is eventually released to initiate apoptosis. E6 thus binds and degrades p53, inhibiting apoptosis. Together, increased expression of both E6 and E7 proteins leads to genetic changes contributing to genomic instability and mutations within infected cells that may lead to cancer progression[62, 63].

HPV Protein	**Protein Function in Viral Replication**
E1	Replication of viral episome and gene transcription.
E2	DNA replication and transcription. Regulates cell cycle, gene expression, and apoptosis.
E3	Function not known.
E4	Genome amplification, viral assembly, cell cycle arrest.
E5	Growth stimulation, interferes with apoptosis
E6	Oncoprotein- inhibits apoptosis
E7	Oncoprotein- cell cycle control via pRB interaction
E8	Function not known
L1	Major capsid protein
L2	Minor capsid protein, recruits L1 capsid

Table 1.1: The Roles of HPV Proteins in Viral Replication [1, 2, 61]

HPV Life Cycle: Replication and Integration

The life cycle of HPV is tightly linked to the host tissue that it is infecting (i.e. differentiating skin or mucosal epithelia [2, 64]. HPV accesses dividing cells through small wounds in the epithelium and upon entering the cell, the HPV genome gets transported to the nucleus [1, 2, 64]. The replication cycle of HPV is generally divided into the latent and lytic infections. Within latent infections, the HPV genome undergoes replication at low copy

numbers (20-100 copies) [1, 64]. E1 and E2 proteins play an essential role in the replication process and are thought to be the only proteins expressed at this stage in order to maintain limited replication [61]. Upon persistent infection, infected daughter cells travel to the upper epithelium layers, indicative of lytic infection. Within the lytic infection stage, the late genes are produced, inducing the amplification (resulting in thousands of copies) of the HPV genome [61]. At this point, the oncogenic properties of E6 and E7 play a major role in driving continuous cell division and inhibiting apoptosis [1, 2].

Integration of HPV genomes into host genomes has been seen in the majority of both invasive cervical and HPV+ head and neck cancers [61]. Within cervical cancer, there is a correlation between HPV integration and disease progression; HPV integration increased from 53.8% to 81.7% as disease progressed from cervical intraepithelial neoplasia to carcinomas [61]. Thirty-six HPV+HNSCC samples from TCGA that underwent whole-genome and transcriptome sequencing provided evidence that host genome integration occurs in these tumors as well, although at lower rates than that of cervical cancer [61, 65]. Although HPV integration is seen in later stages of cancer progression, it is not yet confirmed whether it is a result of E6 and E7 oncogenic activity or if it was present before. Evidence shows that both E1 and E2 proteins are typically lost once viral integration occurs while oncogenic E6 and E7 are maintained post integration [61, 66]. Other studies have demonstrated that there is less interruption of E2 upon integration in HPV+HNSCC [67]. In the context of HPV+HNSCC, evidence supports that E2 and E6 are predominantly expressed and recognized in low-grade lesions while E7 is most present in high-grade lesions [68].

HPV-associated Head and Neck Squamous Cell Carcinoma (HPV+HNSCC)

Head and neck cancer is the sixth most common cancer worldwide with an estimated 880,000 annual diagnoses and 300,000 deaths [57, 68, 69]. HPV infection is now considered a

primary cause of head and neck squamous cell carcinomas (HNSCC) [57, 67]. Within the United States alone, 40-80% of head and neck cancers in the oropharynx are due to HPV (HPV+HNSCCs) [3]. While the number of HNSCC incidences has decreased with a decline in tobacco use, the number of HPV+HNSCC cases have increased by more than 225%, predominantly amongst younger white men [57, 70]. Generally, head and neck cancers derive from the mucosal epithelia that lie in the oropharynx, nasopharynx, hypopharynx, sinonasal tract, and oral cavity [56, 57, 71]. HPV+HNSCCs tend to rise from the reticulated epithelium of the tonsillar crypts and are often morphologically distinct from HPV-HNSCC [71]. Unlike most HNSCCs, HPV+HNSCCs lack keratinization, exhibit lobular growth, and have an increased infiltration of lymphocytes [57].

HNSCC cases can be categorized into two groups based on risk factors. Individuals younger than 40 years old who report to be non-smokers/drinkers are low risk while individuals older than 40 years old who smoke/drink are high risk [65, 72]. HNSCC cases typically have poor prognosis due to late stage (III or IV) discovery, but risk factors (HPV infection, smoking, and alcohol use) tend to have a significant influence on this prognosis [65, 73]. Briefly, individuals who lack an HPV infection but drink and smoke have the worst prognosis and poor survival. Contrary, patients who do have a persistent HPV infection but abstained from drinking and smoking had the best survival rates. Individuals who presented with an HPV infection and reported intermittent use of alcohol and tobacco use had intermediate overall survival rates. Overall, patients with HPV+HNSCC tend to have higher survival rates compared to individuals diagnosed with tobacco and alcohol related HNSCC [73]. Less than 50% of individuals with HPV- oropharyngeal cancer have a 5 year survival rate compared to 70% of HPV+ cases [73, 74].

Although it is possible to contract a non-sexual mucosal HPV infection, most infections are a result from sexual exposures in early adulthood [56]. Differences in when individuals have their first sexual contacts in combination with an increase in the number of oral sex partners could contribute to the rise of HPV-associated HNSCCs [57]. Differences in sexual behavior between men and women may also play a role in why more HPV HNSCC diagnosis are seen among men. Though HPV+HNSCC incidence is seen in individuals who report having few sexual partners, control studies have shown that the risk of HPV+HNSCC increased by two-fold with having between 1 and 5 oral sex partners and five-fold in individuals with six or more oral sex partners [57, 75, 76].

Though upwards of 90% of sexually active individuals will contract an HPV infection within their lifetime, nearly 80% of HPV infections within the head and neck are cleared within 2 years via the immune system [57, 77]. A minority of HPV infections are symptomatic and become persistent, increasing the chances of developing cancer. The majority (85%) of HPV+HNSCC incidences worldwide are a result of HPV16 and HPV18 strains; whereas, HPV33, HPV35, HPV52, HPV45, HPV39, and HPV58 contribute to the remaining 15% of cases [78]. Some factors that may contribute to persistent HPV infections include alcohol consumption, tobacco use, poor oral hygiene, genetic risk factors, defective immune responses, and HLA specificity [56, 57].

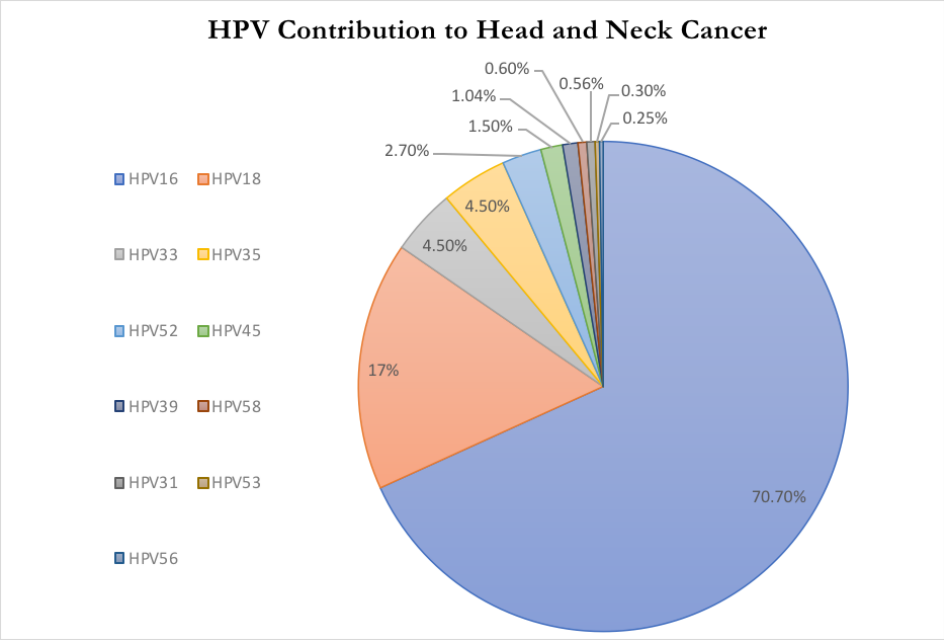

Figure 1.6: Distribution of HPV Strains in Head and Neck Cancer [78].

HPV and CD8+ T Cell Immunity

The majority of women that contract an HPV infection clear the virus via recognition of viral antigens by CD8+ T lymphocytes [77]. Yet, persistent infection is still observed in upwards of 15% of women [65, 68]. The rationale behind why and how some individuals are capable of clearing HPV infections whereas others are not is still unclear. The replicative nature of HPV and varying aspects of the immune system contribute to viral escape and insufficient elimination of the virus [65]. Both HPV+ cervical cancer and head and neck cancer cell lines have been shown to elude T-cell recognition via impaired antigen processing and presentation [6]. The ability of HPV to maintain low copy numbers helps it evade the immune system [79, 80]. In conjunction, the limited expression of viral genes limits antigen presentation by MHC I for immune recognition [79, 80].

Cytotoxic T lymphocytes play an important role in anti-tumor immunity – the effector function of CD8+ T cells is to recognize and kill infected cells [16]. Different studies have demonstrated the importance of these cells within the context of HPV+HNSCCs. Regardless

of HPV status, most oropharyngeal cancers experience high immune cell infiltration [81]. The infiltration of immune cells, in the context of oropharyngeal cancers, is commonly associated with increased overall survival and disease-free survival [65, 82]. When differentiating between HPV+ and HPV-HNSCCs, numerous other studies report a greater infiltration of CD8+ TILs in the HPV+ fraction [65].

Current Methods of Prevention, Detection and Treatments for HPV+HNSCC

Vaccines currently approved in the United States to help protect HPV infections include Cervarix and Gardasil-9. Cervarix is designed to protect against HPV16 and HPV18 while Gardasil-9 is designed not only to protect HPV16, HPV18, HPV6, and HPV11 but also HPV31, 33, 45, 52, and 58 [83, 84]. While Cervarix has been approved for use in females ranging from 9 and 25 years old, Gardasil-9 is approved for males and females within the ages of 9 and 26 years old [84]. Studies have provided evidence of neutralizing anti-HPV antibody production within the saliva following immunization, suggesting that current vaccines may provide some protection against HPV+HNSCCs [85–87]. In comparing vaccinated and unvaccinated groups, individuals who received Gardasil-9 had lower prevalence of the HPV types covered by the vaccine. Nevertheless, more studies are necessary to determine the true efficacy of these vaccines against HPV infections in areas of the head and neck.

Routine screening for head and neck cancer has become more necessary with a growing number of incidences. However, to date, there is no standard method to screen for early stages of HPV-associated carcinomas in the head and neck [57]. Processing oral swab samples may be used to detect HPV in some instances but is not always reliable because not every swab will provide enough cells for analysis. In order to efficiently detect HPV, a highly sensitive assay is required.

Current methods of detecting HPV infection include nested-PCR assays, DNA in-situ hybridization (ISH), serum tests for detecting antibodies against HPV epitopes, and immunohistochemical detection of specific biomarkers [57, 88, 89]. Of these methods, PCR is typically used to determine the presence of HPV although this method cannot distinguish between whether the infection is transcriptionally active or inactive [57]. ISH is routinely used for diagnostic assessments of oropharyngeal carcinomas as it allows for direct visualization of HPV within a tissue sample; ISH can discriminate between HPV presence in all tumor cells versus low viral copy in a subset of cells [57, 88]. Serological tests that target E2, E6, and E7 HPV proteins are sometimes used as an early diagnostics tool, but this remains challenging. The challenge lies in that not every HPV+HNSCC patient will test positive for E2, E6, and E7 antibodies; whereas, those who do may not necessarily go on to develop cancer [57, 75]. p16, a protein involved in slowing down cell cycle progression, is commonly used as a surrogate marker for HPV infection[90]. P16 expression increases as a downstream effect of oncogenic E7 protein binding to the Rb gene product and can be easily detected via immunohistochemistry [57, 90]. Detection of p16 expression in combination with ISH may prove to be a superior method of diagnosis to determine HPV status [57, 64, 91].

Treatments for HPV+HNSSC include surgery, chemotherapy, or radiotherapy [57]. For locally advanced oropharyngeal cancers, the standard-of-care includes a combination of surgery, radiotherapy, and chemoradiation. Combination therapy proved to result in lower rates of recurrence and death [57]. Nevertheless, nearly half the number of patients who undergo treatment still die of the disease [65]. The efficacy of HPV vaccines in preventing associated cancers will play a large role in diminishing these cancer types [70, 92]. However, slow vaccine uptake in combination with decades worth of time between infection and

diagnosis will result in thousands of HPV-associated cancer cases in the interim [93]. In order to better treat HPV+HNSCCs, the development of novel therapeutic strategies is crucial.

To date, the FDA has approved nivolumab and pembrolizumab for checkpoint blockade immunotherapy (CKB) in HNSCC [92, 94, 95]. Further, identifying and targeting tumor-specific epitopes in solid tumors has been found to improve CD8+T cell cytotoxicity [52–54]. Thus, more targeted therapies, including the use of adoptive T cell therapy (ACT), is being heavily explored for HNSCC. ACT exploits an individual's own immune system by identifying and isolating the CD8+ T lymphocytes that target the epitope of interest and either 1) expand and reinfuse them back into the patient or 2) characterize the epitope-specific CD8+TCR, engineer human cell lines to express this TCR, and re-infuse those cells back into the patient [96]. HPV16-E2, E6, and E7 are often found following integration in HPV+HNSCC and serum antibodies are detectable in HPV+HNSCC patients, making these proteins immunogenetic candidates for ACT therapies [61, 97]. Oncoproteins E6 and E7 serve as ideal targets since they are constitutively expressed and play important roles in virus survival within HPV-associated cancers [6, 48]. Our previous work investigated potential immunogenic E2, E6, E7 epitopes, providing possible TCR targets, as further discusses in this thesis [92]. Although previous clinical studies using vaccines to target E6 and E7 have been conducted, they have shown little evidence that the T cell-specific targeting of these antigens in killing HPV tumor cells was effective [6, 48]. However, in 2015 a promising clinical trial demonstrated the successful targeting of HPV-16 tumors by E6-specific engineered TCR, renewing interest in discovering TCR candidates for gene therapy for HPV-associated cancers [6].

CHAPTER 2

METHODS FOR ANALYZING TCR DIVERSITY

Overview:

Throughout one's lifetime, their immune system will encounter numerous pathogens that it must be able to recognize and eliminate to preserve his/her health. To do this, the human body is equipped with an extensive set of T cell receptors (TCR) located on the surface of T cells, referred to as the TCR repertoire [10, 38, 98]. T cell function is dependent on the ability of TCRs to recognize antigen presented to them via major-histocompatibility complex (MHC) molecules; requiring the TCR repertoire to highly diverse yet specific to antigen. The wide range of TCRs within an individual is produced via the recombination of the genes that encode each TCR chain (TCRα and TCRβ), known as somatic recombination [35]. In short, TCRα are made up of variable (V) and joining (J) genes while TCRβ has an additional diversity (D) gene segment. During somatic recombination, the respective V-J or V-D-J genes for each TCR chain are rearranged to include random insertions, deletions, and a substitutions [35, 38]. The rearrangement of V-J and V-D-J make up hypervariable complementarity-determining regions (CDR1, CDR2, and CDR3) for each respective TCR chain [16, 38]. The CDR1 and CDR2 are primarily encoded by the V gene of each chain whereas CDR3 is encoded by portions of V(D)J, including the junctional diversity in between. The V(D)J junction, which encodes CDR3, also forms the antigen recognition site of the TCR; thus, making CDR3 not only the most diverse but also highly specific to particular antigen [16]. In addition to the diversity created through gene rearrangement, the pairing of each TCRα and TCRβ to form a functional heterodimer provides combinatorial diversity. This process of somatic recombination and TCRαβ pairing is highly important because it produces exceedingly diverse TCR that have the capability of recognizing millions of pathogens [10, 35, 38]. Studies trying

to quantify TCR diversity have led to rather high estimations (upwards of 10^{20}) TCR combinations [98]. However, since the human body on average has 10^{12} T cells, the theoretical diversity of 10^{20} is unlikely [37, 38].

Interestingly, some TCRs are generated more commonly than others [38, 99]. As a result, there are frequency variations (the incidence of a particular TCR pair) between individuals. However, TCR-clonotypes can also be found shared amongst individuals, referred to as a "public" TCR repertoire [38, 99]. The sharing of identical TCRs between individuals in response to the same epitope has been seen across numerous immune responses such as in the context of human cytomegalovirus (CMV), Herpes simplex virus, Human immunodeficiency syndrome (HIV), melanoma, prostate cancer, etc [99]. Importantly, public TCRs have been associated with favorable outcomes in some cancers [99, 100].

In addition to further defining the role of public TCR repertoire between individuals, characterizing the TCR repertoire in cancer may provide more insight into prognosis, immune monitoring, as well as immunotherapies. Some studies investigating the TCR repertoire in the context of breast cancer, glioma, hepatocellular cancer, and cervical cancer have confirmed that the TCR repertoire could serve as a tool for monitoring immune responses [101–103]. For instance, when studying patients with cervical cancer, it was observed that cancer progression was associated with a decrease in TCR diversity; likewise, the TCR repertoires between patients were similar to one another in comparison to healthy individuals [104]. The decrease in TCR diversity with worsening prognosis highlights the importance of characterizing TCR clonotypes specific for given antigenic epitopes that can be engineered for targeted therapy.

Further, high tumor mutational load, or a high range of mutations within a tumor environment, may be an important factor in therapeutic responses in patients [105]. Studies

have found high mutation burden to play a significant role in some cancers because these cancers are commonly associated with the presence of tumor-specific antigens (neoantigens) that can be targeted by cytotoxic T cells (CD8+ T cells) [105]. Tumor mutation load varies between tumor types; lower grade malignancies usually have lower tumor mutation burden whereas cancers associated with DNA damage from environmental sources (smoking, alcohol use, etc), are highly mutated [105–107]. In the context of head and neck squamous cell carcinomas (HNSCC), both human papillomavirus associated HNSCC (HPV+HNSCC) and HPV- HNSCC had a comparable occurrence of somatic mutations [108]. However, in addition to somatic mutations, HPV+HNSCC also express antigenic viral protein. With a higher mutational burden, significantly more immune cell infiltration, and CD8+ T cell activation, HPV+HNSCCs are deemed immune "hot" and may be more susceptible to targeted treatments [108].

Together, these studies emphasize the importance of assessing CDR3 diversity and determining antigen specific TCRs within cancer. To do so, reliable and robust techniques for determining CDR3 TCR sequences and their specific αβ pairing is exceedingly necessary. Over the last several decades, tremendous efforts have been put forth to develop methods to identify and sequence TCR, providing a more comprehensive overview of the immune repertoire [109].

Methods of Analyzing TCR Diversity

One method originally used to assess TCR repertoire diversity is Immunoscope, or CDR3 spectratyping. The technique of CDR3 spectratyping involves multiplex reverse transcription polymerase chain reaction (RT-PCR) of the TCRβ chain [110]. Briefly, messenger RNA (mRNA) is isolated from T-cells, reverse transcribed to produce the complementary DNA (cDNA) sequence encompassing the CDR3 region, then further amplified by PCR. The

PCR products are then run via polyacrylamide gel electrophoresis (PAGE) where they are separated based on their length and further purified for sequence analysis. The technique of spectratyping further provides a means to study the clonal composition of T-cell populations during immune responses [110]. When analyzing the TCR repertoire of bone marrow transplant patients compared to healthy individuals, studies found that the TCR repertoire was reflective of immune function; Patients who experienced recurrent infections had a decrease in TCR diversity [111, 112]. CDR3 spectratyping provided some of the first quantified estimations of T cell diversity and insight into repertoire fluctuations during disease. However, many studies were limited to a small sample set or TCRβ measurements alone and thus not truly reflective of the larger T cell repertoire [112]. Due to technological advances, we can take a more comprehensive approach to investigating TCR diversity.

The development of next generation sequencing (NGS) based technologies has revolutionized the ways that we can assess TCR CDR3 diversity and gather paired TCR sequences [113]. NGS platforms provide deeper sequencing, which was not feasible with capillary-based sequencing. The Illumina Genome Analyzer (GA) system provides massively parallel sequencing of short templates, providing increased read lengths and number of reads for every sample [113]. Briefly, a library of PCR adapters are ligated to fragmented DNA templates. The DNA is then loaded onto a flow cell containing nanowells which contain oligonucleotides complementary to the previously ligated adapters. After hybridization, PCR is then performed to amplify the template library, producing thousands of copies of each DNA fragment. Following PCR, dye-termination chemistry is used to sequence the template at 30-54 nucleotide intervals until the full DNA template is sequenced. Exploiting NGS advancements, researchers have developed bulk and single-cell approaches for analyzing the TCR repertoire [114].

Through adaptations to the GA system, Harlan Robins and his team developed the ImmunoSEQ platform for simultaneous sequencing of TCRαβ CDR3 from genomic DNA using a multiplex primer approach [113, 114]. ImmunoSEQ technology implements the use of multiplex primer sets to allow for efficient sequencing of target genes in immune cells [109, 113]. These primer sets contain Vα forward and Jα reverse or Vβ forward and Jβ reverse primers combinations for TCRα or TCRβ, respectively. Universal primer sequences are ligated to the 5' end of each primer to allow for downstream sequencing. Through sequencing, a 200bp amplicon is produced which allows for ample coverage of the CDR3 region. Other bulk methods, including pariSEQ, use algorithms to pair TCRα and TCRβ based off of their given frequency in a sample population [114, 115]. Direct TCR CDR3 sequencing at a much larger scale is now possible allowing for a deeper analysis of diversity and relative frequency of individual CDR3. Since the development of ImmunoSeq, several other companies have developed services and kits for TCR repertoire analysis with varying modifications in starting material, library preparation, target sequence, and sequencing platform (Table 2.1) [109, 113–115].

Company	Starting Material	Library Preparation	Target CDR Chain	Sequencing Platform
Adaptive Biotechnologies ImmunoSeq PairSEQ	gDNA cDNA	Multiplex PCR (V-J primer set)	TCRα, TCR β CDR3	Illumina: HiSeq, MiSeq
BGI	gDN RNA	Multiplex PCR (V-C primer set)	TCRα, TCR β CDR3	Illumina: HiSeq (100x 2bp) MiSeq (150/300 x 2bp)
	RNA	5' RACE	TCRα, TCR β CDR1, 2, 3	
iRepertoire	gDNA	Multiplex PCR V-J primer set)	TCR β CDR3	Illumina: HiSeq, MiSeq (100/150 x 2bp)
	RNA	Multiplex PCR (V-C primer set)	TCRα, TCR β CDR2,3	HiSeq, MiSeq (100/150/250 x 2bp)
Takara Bio	RNA	5' RACE	TCRα, TCR β CDR1,2,3	Illumina: HiSeq, MiSeq (300 x 2bp)

Table 2.1: Overview of Company Products for Assessing the Immune Repertoire. Adapted from Rosati, *et al* [109]

One of the prominent issues when trying to asses TCR diversity is that many of these platforms sequence TCRα and TCRβ separately (bulk sequencing) providing insight into individual CDR3 diversity and gene repertoire analysis but not specific TCR pairing [114]. Since TCRαβ are heterodimeric proteins, the CDR3 regions of both are necessary for understanding the specificity of the receptor for antigen. Recognizing this issue, many researchers have turned to single-cell methods to isolate and amplify TCR populations of interest. Single-cell methods include TCR enrichment, microfluidics, and fluorescence-activated cell sorting (FACS) [114]. During TCR enrichment, TCR transcripts are enriched by a multiplex PCR set spanning Vα and Vβ regions in conjunction with Cα and Cβ regions. An additional PCR is then performed to incorporate barcoded adaptors that could then be used for downstream pairing and sequencing [116]. With microfluidics, cells are suspended in oil-

in-water droplets containing specific RT and PCR reagents. TCR mRNA transcripts are reverse transcribed and amplified in the cell suspension and ultimately fused together by overlap extension, producing a single amplicon containing both TCRαβ sequences [117]. An additional method of single-cell sorting requires labeling target cells with fluorophore-conjugated antibodies and then separating the populations based off of their emission [118]. Labeled cells can be deposited into a 96-well plate and then RT-PCR performed directly in each well. Like the previously mentioned methodologies, specific adapters and unique barcodes are incorporated into each TCR transcript so they can be paired downstream [114, 118].

Limitations of Current Approaches

While advancements in high throughput sequencing and specific immune profiling platforms has allowed for the analysis of larger sampling of the immune repertoire, these methods still present limitations. The multiplex PCR primer sets utilized by platforms including ImmunoSeq, BGI, and iRepertoire present two problems: new V gene allele variants may not be detected and inherent differences in primer kinetics may result in amplification biases[109, 119]. As a result, some gene alleles could potentially be amplified better than others which would distort the true CDR3 frequency in the sample population. 5'RACE methods are also susceptible to amplification bias. To help compensate for these biases, some techniques incorporate unique molecular identifiers (UMIs) [109, 120]. The UMIs are incorporated into the oligonucleotide used for template-switching during cDNA synthesis. Thus, each cDNA can get uniquely barcoded allowing for downstream tracing of sequences that came from the same mRNA. Mispairing of TCRαβ chains during sorting or forming microfluidic droplets also presents as a problem for downstream results [114]. Collectively, each of these platforms is also very expensive and often require rigorous preparation.

New Approach- DNA Origami

Although there are really great technologies available that allow for the identification of T cells, they each have some limitations, whether it's low-throughput, the chance of false-pairing, and/or the inability to detect very low frequency clones. Even more, many of these technologies are reliant on some form of single-cell sorting. In an effort to develop a more efficient method of identifying and sequencing paired TCRαβ, we sought to develop a platform that we could easily get into cells, use as a to tool to capture and link genes, and also modulate for downstream isolation and purification purposes. Based on those characteristics, we decided to use DNA Origami.

DNA nanotechnology exploits the specificity of Watson-Crick base pairing to use oligonucleotides as a platform for the self-assembling of two and three -dimensional structures [121]. In 2006 Paul Rothemund demonstrated how a combination of 216 short 'staple' strands of DNA can direct the folding of a longer single strand of DNA (M13mp18 bacteriophage). Through a 'one-pot' method, he demonstrated that over 10^{14} nanostructures could be produced in an array of shapes and patterns, thus coining the methodology as 'scaffold DNA origami [121]. More so, the scaffold platform is highly adaptable and allows for staple strands to be substituted for your own oligonucleotides of interest. Knowing that the platform is not only very modifiable but small enough to get into cells and has low toxicity, we incorporated several modifications to use the scaffold as a mode of a delivery into cells to capture and isolate paired human TCRαβ mRNA (Figure 2.1) [122]. The initial validation experiments were performed on P14 transgenic mice by the lead graduate student and collaborator Dr. Schoettle. The first array of experiments and optimizations that he performed on the mouse model that I then adapted for the human model can be found in his dissertation titled, "Bowties,

Barcodes, and DNA Origami; A Novel Approach for Paired-Chain Immune Receptor Repertoire Analysis" [123].

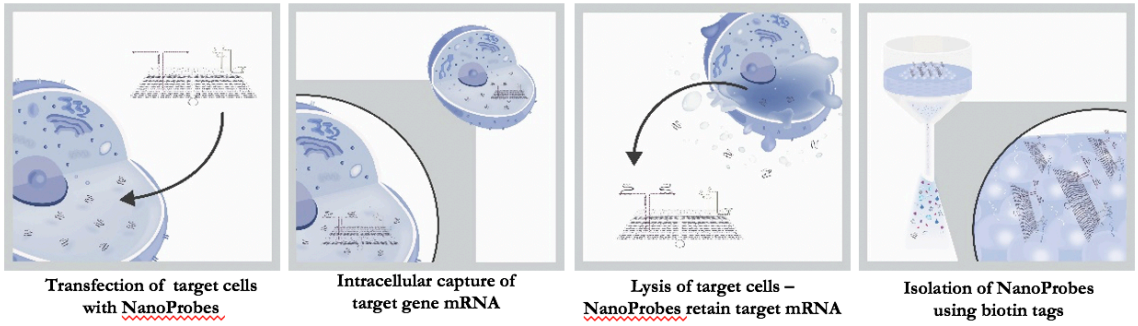

Figure 2.1: Schematic of DNA Origami Transfection Strategy for Linking Sequences from Individual Cells. Simultaneous transfection of millions of CD8 T cells with DNA origami nanostructures containing barcoded mRNA capture strands that can bioinformatically link captured TCRα and TCRβ CDR3 sequences from individual T cells without the need for any form of single-cell presorting. Following transfection, cells are lysed and nanostructures with bound mRNA are re-isolated using integral biotin tags in an avidin column purification step.

Materials and Methods:

Scaffold Design

The long ssDNA M13mp18 bacteriophage (7.4kb) was modified to include a 5'-5' bowtie linkage that would allow for each end to run directionally from 5' to 3' (synthesized and ordered from IDT). Importantly, the bowtie linkage has a sequence complimentary to the M13mp18 scaffold backbone while the 3' ends has a primer site (X" and 'Y') for downstream amplification, complimentary barcodes, and mRNA capture sites complimentary to the conserved constant domains of TCRα and TCRβ that therefore serve as our Cα and Cβ capture probes and downstream RT primers (Figure 2.2). The barcodes can be used to bioinformatically link captured TCRα and TCRβ gene information from the same cell during downstream sequencing. We then substituted several staple strands to incorporate a

fluorescein isothiocyanate (FITC) fluorophore that would allow for validation of successful transfection. Additionally, biotin labels for downstream isolation from cell lysates.

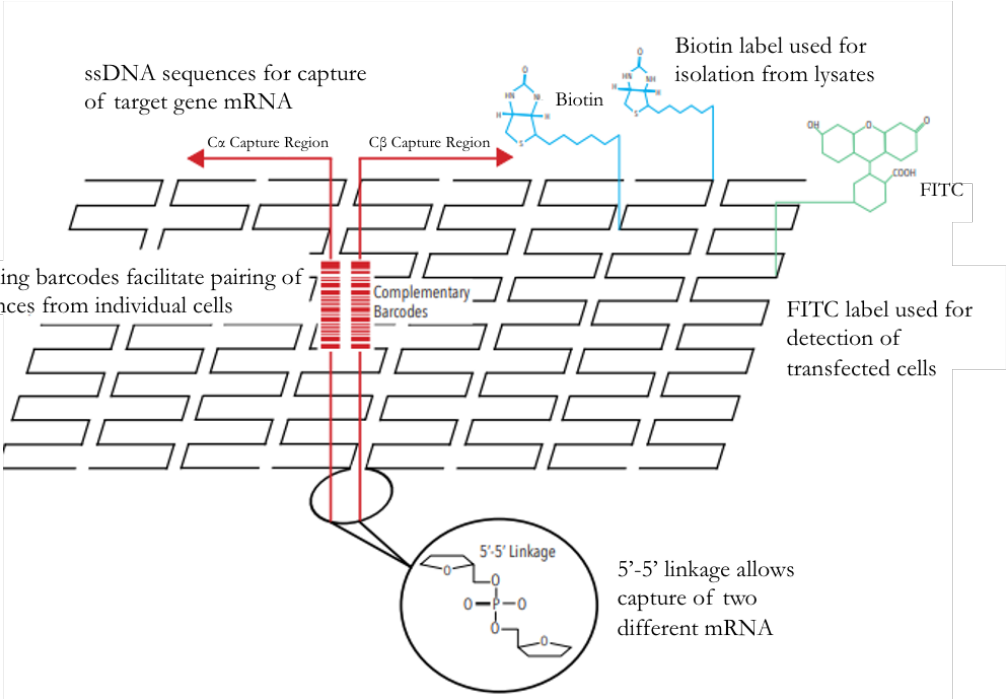

Figure 2.2: DNA Origami Nanoprobe Design for Bowtie Strand Barcoding of Captured mRNA Sequences. Organization of 5'-5' bowtie mRNA nanoprobe includes a region complementary to the M13mp18 phage ssDNA that includes a 5'-5' phosphodiester or "bowtie" linkage, resulting in both ends of the bowtie strand to have 5'-3' directionality. These two ends are designed to be complementary to the constant regions of either the TCRα or TCRβ mRNAs and therefore serve as our Cα and Cβ capture probes and downstream RT primers. Additionally, each capture probe includes a 12-mer "barcode" upstream from the capture sequence that retains sequence complementarity to one another. These barcodes can be used to bioinformatically link captured TCRα or TCRβ gene information from the same cell during downstream sequencing. The locations of four biotinylated strands used for purification as well as a FITC conjugated strand used for FACS assessment of transfection are included as well.

Origami Scaffold and Nanoprobe Synthesis

The nanoprobes were synthesized through an oil-in-water emulsion and overlap extension elongation protocol established and described by [123]. Additionally, the DNA origami scaffold and annealing of the nanoprobe complex was also synthesized as previously described by [123]. Briefly, the long ssDNA M13mp18 bacteriophage (7.4kb) and shorter

'staple' strands were synthesized by and ordered from Integrated DNA Technologies (IDT). Once received, the staple strands were mixed in equimolar concentrations. The specific nanoprobe containing the TCR Cα and Cβ capture sites as well as the biotin/FITC staples were first PAGE-purified then mixed with the scaffold M13 ssDNA and staple DNA (50 nM scaffold, 250 nM staples, 150 nM mRNA probes/biotinylated tags/fluorophore tags) in aqueous buffer (1x TAE with 12 mM Mg^{2+}). The folding of the DNA was then synthesized through a thermal denaturation (90°C) and gradual annealing (to 20°C) over 12 hours. 100K Amicon filters were then used to purify the synthesized origami from any excess staple strands.

Total RNA Isolation

The Jurkat E6.1, an immortalized CD4+ human T cell line, was used for validation of this approach as it expresses a monoclonal T cell receptor on its surface. Jurkat cells were harvested at 1 x 10^6 cells per sample using RPMI media supplemented with 10% fetal bovine serum (FBS) and washed in phosphate buffered saline (PBS) at 1200rpm for 3 minutes (Gibco, USA). Total RNA was extracted using an endotoxin free RNA extraction kit (Qiagen). Following extraction, RNA was DNAse treated and RNA quality was analyzed by measuring A_{260}/A_{280} absorbance ratios (ThermoFisher, USA).

Nanoprobe Capture Sites Binding to Human TCRα and TCRβ mRNA Lysate

In order to assess the ability of the capture regions of the nanoprobes to bind Jurkat RNA, an RT-PCR was performed. ssBC' and ssBC nanoprobe strands (specific for the constant regions of TCRα and TCRβ, respectively) were used as RT primers. As a positive control, a primer specific for each respective TCRαβ constant region (Cα or Cβ) was used. Following the Maxima RT kit protocol (50°C incubation for 30 minutes followed by an 85°C incubation for 5 minutes, ThermoFisher Scientific, MA, USA). Following RT, each sample

was treated with RNase A at 1ul of RNase A to 20ul of sample incubated at 37°C for 10 minutes (Sigma-Aldrich). For PCR, primers specific to either the Jurkat TCRα variable region (Vα) or TCRβ variable region (Vβ) were used in combination with either an 'X' or 'Y' primer sequence (DreamTaq, ThermoFisher Scientific, MA, USA). 'X' and "Y' priming sites were previously incorporated upstream of each Cα, Cβ capture region on the nanoprobe. For the positive controls, Cα or Cβ reverse primers were used.

DNA Origami Nanoprobe Complex Binding to Human TCRα and TCRβ mRNA Lysate

In order to assess the ability of the nanoprobes to bind Jurkat RNA once annealed to the DNA origami platform, an RT-PCR was performed. The origami nanoprobe complex was incubated with Jurkat mRNA while ssBC was used as the positive control. Following the Maxima RT kit protocol, samples were incubated at 50°C for 30 minutes followed by an 85°C incubation for 5 minutes, (ThermoFisher Scientific, MA, USA). Following RT, each sample was treated with RNase A at 1ul of RNase A to 20ul of sample incubated at 37°C for 10 minutes (Sigma-Aldrich). For PCR, primers specific to either the Jurkat TCRα variable region (Vα) or TCRβ variable region (Vβ) were used in combination with either an 'X' or 'Y' primer sequence (DreamTaq, ThermoFisher Scientific, MA, USA). For the positive controls, 'X' or 'Y' were used. To confirm that the individual nanoprobes specifically captured the Jurkat *TCRα and TCRβ* mRNA, Sanger sequencing of the RT-PCR products was performed and compared to the known Jurkat TCR sequences.

DNA Origami Transfection into Jurkat E6.1 Cell Line

Jurkat cells ($1x10^6$ cells/sample) were pelleted at 1200 rpm for 3 minutes then washed in MACs buffer (Miltenyi Biotec) then resuspended in a mixture of 75 μL MACs buffer and 25 μL DNA Origami (50nM in 1X TAE-Mg^{2+}) or a mock transfection mixture of 25 μL 1X

TAE-Mg^{2+} buffer. For electroporation, the Neon syringe transfection system was used (ThermoFisher Scientific, MA, USA). The parameters for electroporation include 100ul syringe tips, 2000 V, 10 ms, and 2 pulses. Post transfection, each sample was transferred to 100ul prewarmed RPMI supplemented with 10%FBS in a 96-well plate. Samples were incubated overnight at 37°C for 18-24 hours. Transfection efficiency was analyzed using an Attune flow cytometer (ThermoFisher Scientific, MA, USA); the FITC tag incorporated into each origami structure allowed for successfully transfected cells to be identified by flow cytometry (488 nm excitation, 518 nm emission).

Transfected Origami Nanoprobe Complex Binding to Human TCRα and TCRβ mRNA

DNA origami with the extended mRNA nanoprobes specific for human TCRαβ constant regions was isolated and purified from transfected Jurkat cells using the biotinylated staple strands incorporated into the origami scaffold. At 18-24 hours post-transfection, cells were lysed in 100ul of 1% NP-40 buffer and 2ul Ribolock RNase inhibitor for 30 minutes on ice (Invitrogen). The bound TCRαβ mRNA was then filtered through a streptavidin conjugated resin column (Pierce Streptavidin UltraLink Resin, Sigma Prep Columns, 7-20μM pore size). The columns were washed three times at 2000 rpm for 30 seconds with 1x TAE-MG^{2+} to remove any cellular debris. Following purification, reverse transcription (RT) was performed in the columns using the TCRαβ capture region on the nanoprobes as RT primers. Following the Omniscript RT kit protocol, 40μL of the RT mastermix was added directly to column and incubated for 30 minutes at 50°C then spun at 2000rpm for 10 seconds (Qiagen). After incubation, the RNA was removed by addition of an RNase and eluted via an incubation of 95°C for 5 min, followed by a centrifugation at 10,000 rpm for 5min. Following RT, PCR was performed using a single primer specific for the constant sequences on either end of the

TCRαβ mRNA capture probes and an additional primer specific for the known Jurkat TCRα and TCRβ variable regions sequences. To confirm that the DNA-nanoprobe complex specifically captures the Jurkat *TCRα and TCR*β mRNA, Sanger sequencing of the RT-PCR products was performed and compared to the known Jurkat TCR sequences.

Results:

Individual nanoprobes can capture and amplify human TCRα/β mRNA. In order to decide whether the nanoprobe containing the capture region specific for *TCR*αβ would bind mRNA and act as a reverse transcription (RT) primer, we used Jurkat mRNA for validation. The nanoprobe capture region sequences were designed to bind the conserved TCRα and TCRβ constant (Cα and Cβ) domain regions of each mRNA species. The origami-nanoprobe complex was designed to bind complimentary to the 3' sites of the CDR3 sequences of interest. To determine if the capture regions would specifically bind and reverse transcribe the mRNA, we used one-sided capture sites ssBC' to capture TCRα and ssBC for TCRβ. Following RT, the products were amplified using Va and Vb gene primers specific for the expressed Jurkat TCR. Specific binding of TCRα or TCRβ mRNA with their respective capture probe was observed (Figure 2.3) and mirrored the positive controls that used sequence specific Cα and Cβ RT primers.

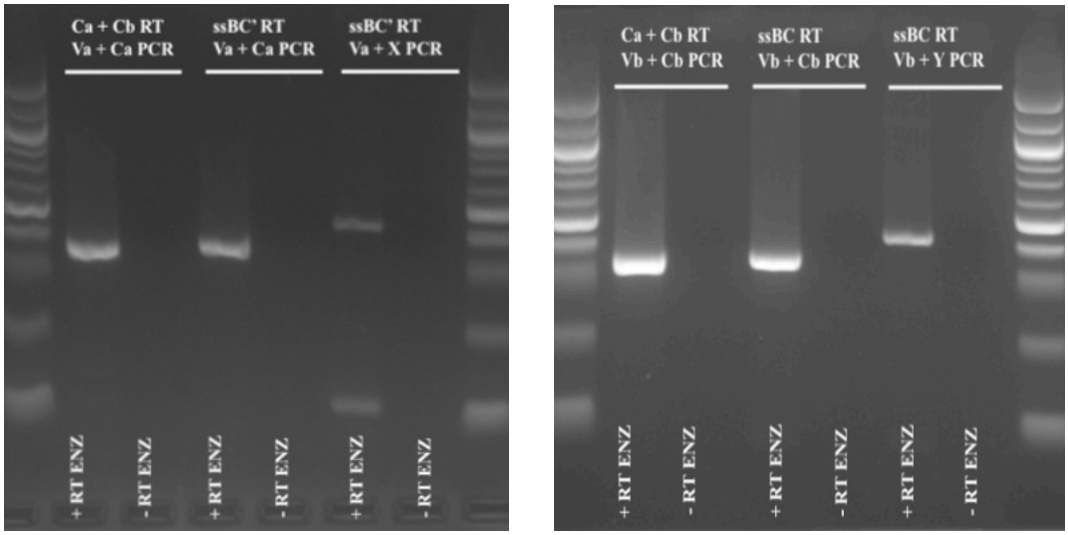

Figure 2.3: One-sided Capture and Amplification of Human TCRα/β mRNA using Nanoprobes. Agarose gel electrophoresis of TCRα and TCRβ RT-PCR products amplified from mRNA lysate captured by nanoprobes (ssBC/ssBC'). Using Cα and Cβ specific RT primers as positive controls. ssBC/ssBC' nanoprobes were able to bind TCRα/β mRNA and act as reverse transcription primers. Following PCR, the amplified products yielded identical bands as controls (left: lanes 2 vs 4 and 6 and right: lanes 2 vs 4 and 6). Gel purification and sanger sequencing confirmed homology between RT-PCR products from both control and experimental samples.

DNA origami nanoprobe complex can capture both TCRα and TCRβ mRNA from mRNA lysate. Upon validating that the designed nanoprobe capture regions would act as an RT primer, we moved forward in annealing the DNA origami-nanoprobe complex and testing the ability of the entire complex to bind the TCR mRNA. Prior to testing intracellular binding, we used Jurkat cell lysate. RNA was extracted and purified from Jurkat cells and incubated with the origami-nanoprobe complex. V region specific primers were used for the PCR reaction along with respective 'X' and 'Y' reverse primers. After running the DNA products on an agarose gel, the results demonstrated that the origami-nanoprobe complex mirrored the positive control. Sanger sequencing results confirmed >90% homology between the Jurkat reported TCT sequence and the origami-nanoprobe captured sequence (Figure 2.4).

High transfection efficiency can be achieved by Neon syringe transfection system. Following these validations, we moved forward with testing the transfection efficiency of the DNA origami nanoprobe complexes into Jurkat cells. To do this, we used a syringe based electroporation system followed by analysis on the Attune flow cytometer. The origami nanoprobe complexes had an incorporated FITC tag annealed previously and was used as a marker of successfully transfected cells. Upon determining the optimal transfection parameters, we yielded results providing >89% transfection efficiency (Figure 2.5).

DNA origami nanoprobes complex can be transfected and capture both TCRα and TCRβ mRNA from Jurkat T cells. Successful transfection of the DNA origami nanoprobe complex led us to start testing the ability of the nanoprobes to bind and link the TCRαβ mRNA species intracellularly. Purified origami nanoprobe complexes were transfected into Jurkat cells using the optimized parameters. Following an 18-24 hour incubation, the DNA origami nanoprobe complexes were isolated and purified. The resulting RT product was then used in a PCR reaction with Jurkat specific TCRα and TCRβ V region primers. Gel electrophoresis and sanger sequencing confirmed TCR mRNA capture, isolation, and amplification of Jurkat TCRαβ mRNA (Figure 2.6).

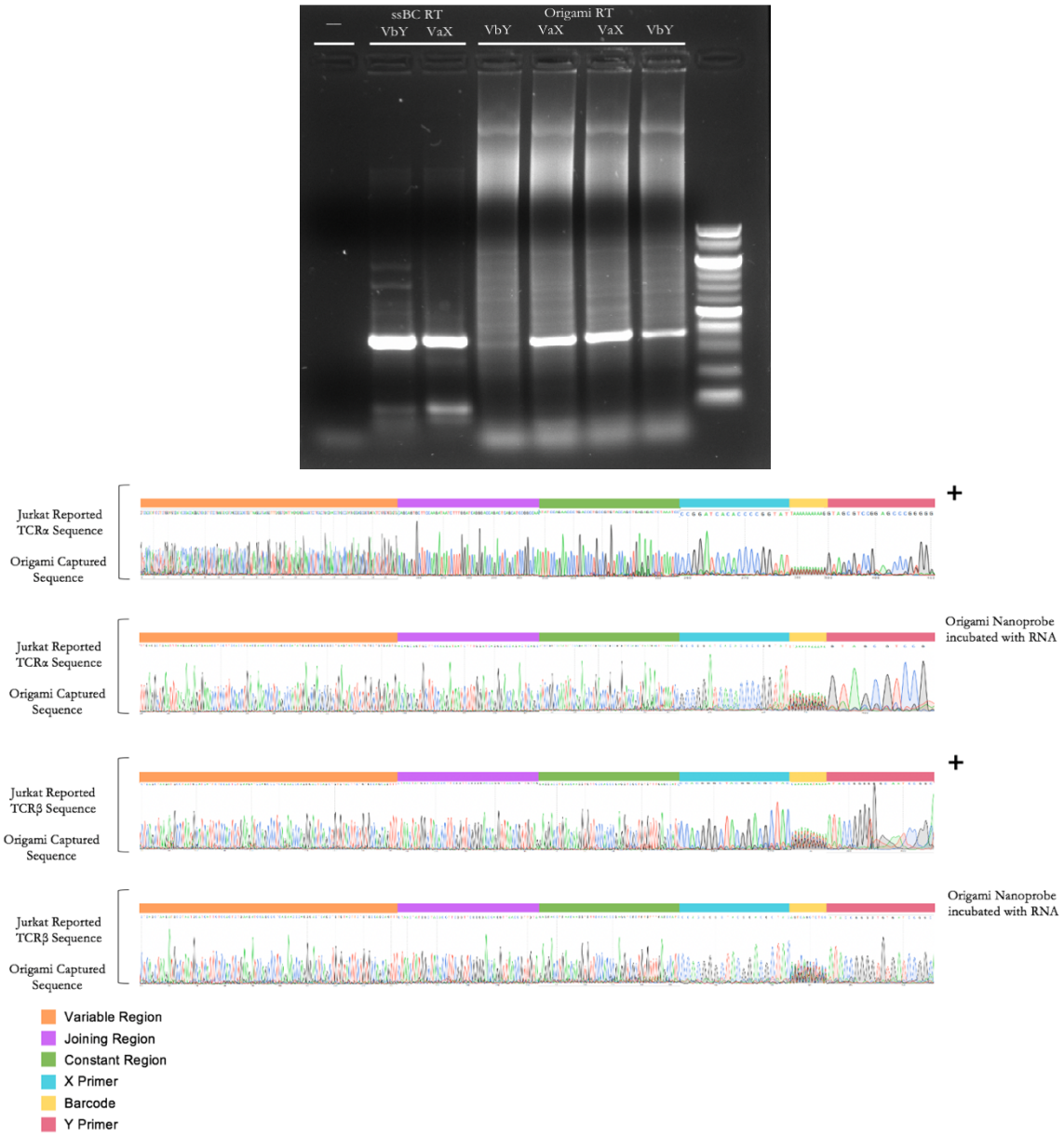

Figure 2.4: RT-PCR and Sequencing Confirm the Ability of DNA origami Nanoprobes to Capture both TCRα and TCRβ mRNA from mRNA Lysate. Agarose gel electrophoresis of TCRα and TCRβ RT-PCR products amplified from mRNA captured by nanoprobes (ssBC/ssBC') or origami-nanoprobe complexes. *In vitro* transcribed TCRα/β mRNA was used as positive controls. Origami with TCRα/β probes incubated with Jurkat cell mRNA were able to bind TCRα/β mRNA that was then reverse transcribed and amplified yielding identical bands as controls (lanes 2 vs 4 and 7 and lanes 3 vs 5 and 6). Sequencing traces of both TCRα (top two) and TCRβ (bottom two) from RT-PCR products from Jurkat T cells with reported TCRα and TCRβ gene sequences listed above. 100% homology was observed between reported Jurkat sequences and traces generated from RT-PCR products (right).

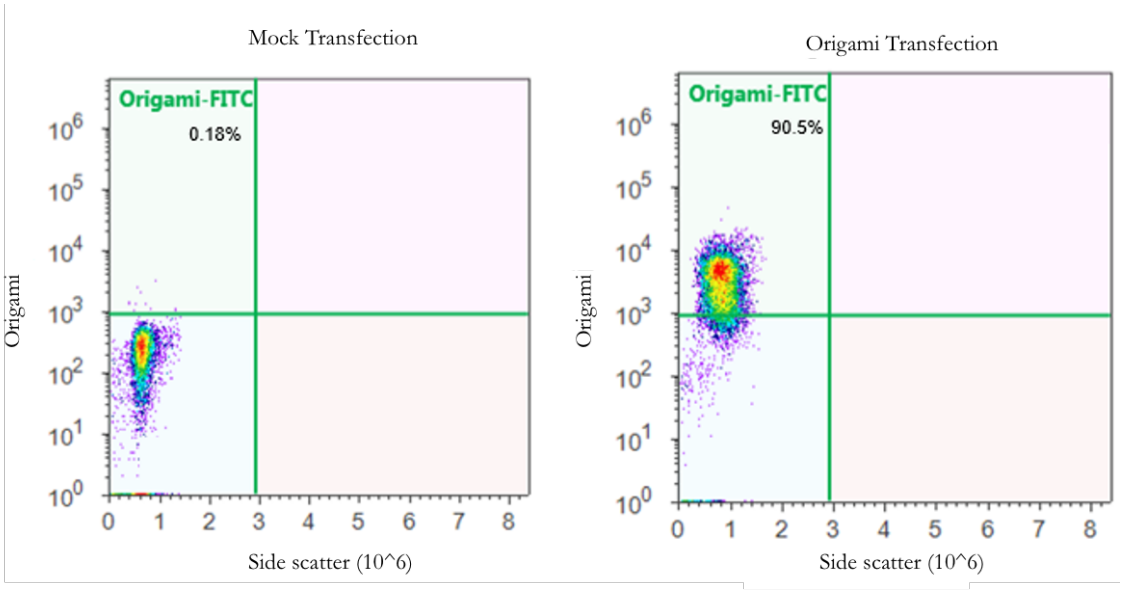

Figure 2.5: High Transfection Efficiency chieved by Neon syringe transfection system. Flow cytometry analysis of electroporation samples of Jurkat T cells with DNA origami using the Neon Syringe electroporation system demonstrates transfection efficiency of >90% after 24 hour incubation (right) when compared to mock transfection controls (left). Samples consisted of $1x10^6$ cells in 75 μL MACS buffer and 25 μL DNA Origami (50nM) in 1X TAE-Mg2+ and were compared to negative control mock transfections of $1x10^6$ cells in 75μL MACS buffer and 25 μL 1X TAE-Mg2+.

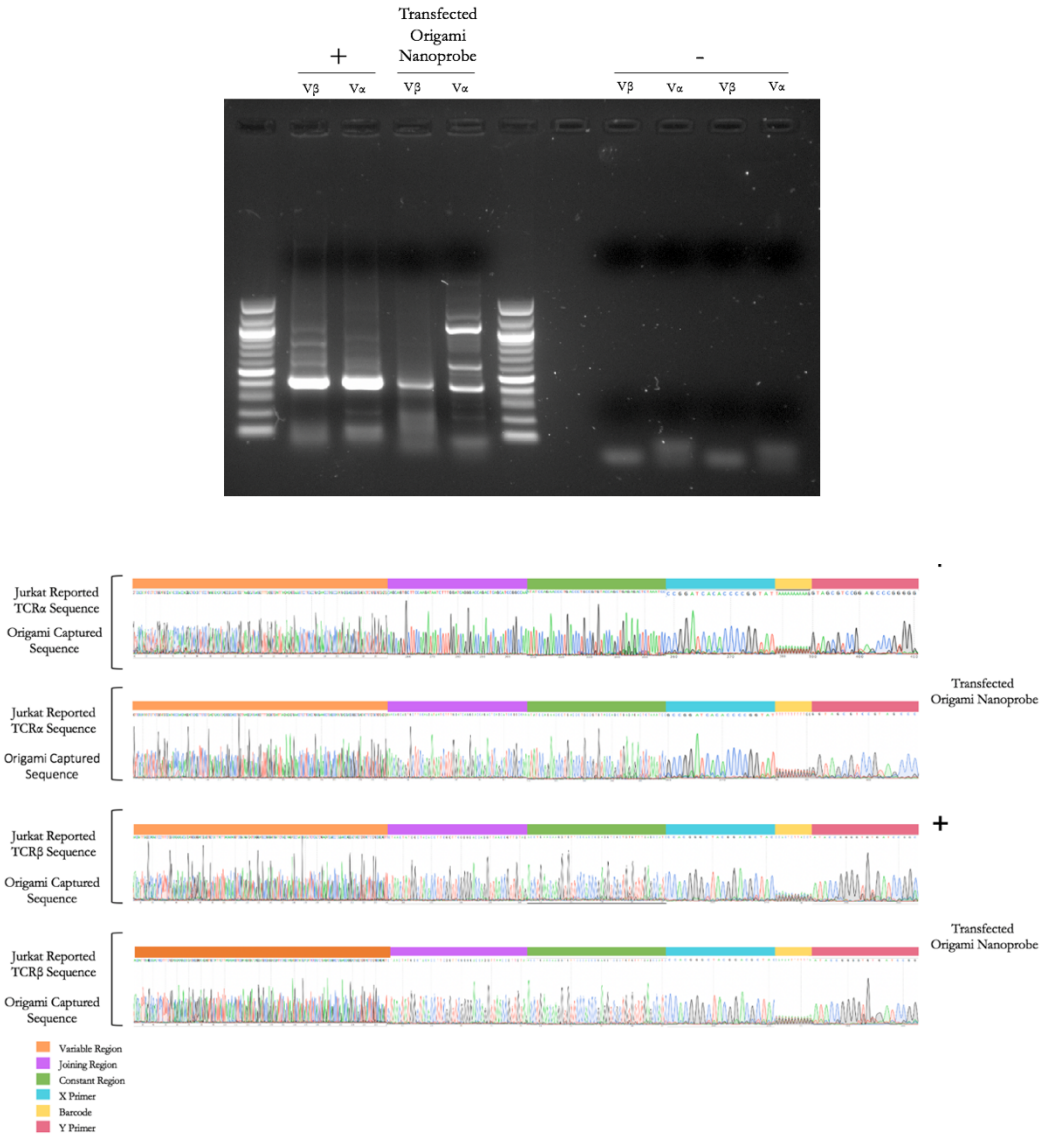

Figure 2.6 RT-PCR and Sequencing Confirm Ability of DNA Origami Nanoprobes to be Transfected and Capture both TCRα and TCRβ mRNA from Jurkat T cells. Agarose gel electrophoresis of TCRα and TCRβ RT-PCR products amplified from mRNA captured by origami purified from post-transfected cell lysate. *In vitro* transcribed TCRα/β mRNA was used as positive controls. Origami with TCRα/β probes transfected into Jurkat T cells were able to bind, protect, and be re-isolated with TCRα/β mRNA that was then reverse transcribed and amplified yielding identical bands as controls (lanes 2 vs 4 and lanes 3 vs 5). Sequencing traces of both TCRα (top two) and TCRβ (bottom two) from RT-PCR products from Jurkat T cells with reported TCRα and TCRβ gene sequences listed above. 100% homology was observed between reported Jurkat sequences and traces generated from post-transfected RT-PCR products.

Discussion:

As previously discussed, a major problem in identifying TCRαβ pairs from cells for has been the lack of high-throughput methods for obtaining CDR3 sequence information from individual cells. Current techniques focused on assessing the human TCR repertoire are limited by the need for single cell isolation and sequencing of individual TCRs. Even more, the technology is limited to providing estimates of CDR3 diversity of either the TCRα chain or TCRβ chain but not TCRαβ pairs. Retrieving information from a single chain of the TCR serves to provide estimates of lymphocyte diversity. However, without sequencing information of paired TCRα and TCRβ, accurate antigen specificity of a TCR cannot be obtained. In order to overcome these limitations, we aimed to modify DNA origami nanostructures to simultaneously capture TCRα and TCRβ mRNA from individual cells.

Modifications to the DNA origami nanostructures were made to incorporate extended capture probes complementary to the conserved regions of human TCRα or TCRβ mRNA species. We demonstrated that our modified nanoprobes are capable of binding TCR mRNA and act as gene specific reverse transcription primers to synthesize cDNA. Upon synthesizing origami-nanoprobe structures, we further confirmed capture of specific TCR mRNA that was validated with sanger sequencing. Moving forward, we demonstrated that these origami nanostructures with TCR–specific nanoprobes are capable of being transfected into T cells with high efficiency using the Jurkat E6.1 cell line. Jurkat cells transfected with the origami scaffold and custom nanoprobes, resulted in the successful capture and amplification of TCRαβ sequences. Validation using Sanger sequencing confirmed the capture of barcoded TCRα and TCRβ CDR3 sequences.

While the DNA origami scaffold proved to be a successful tool for the capture and linking of TCRαβ mRNA species at the single cell level, these experiments were done in a monoclonal TCR cell line. In order to prove truly useful for capturing and barcoding paired TCRαβ mRNA at the single-cell level, this methodology needs to be further optimized and tested in a polyclonal population.

CHAPTER 3

CD8+ T CELL DYSFUNCTION IN HPV ASSOCIATED HEAD AND NECK CANCER

Publication Note

The research reported in this chapter was submitted for publication in Cancer Research. Sri Krishna, Eric Wilson, and Karen Anderson. All authors and co-authors have granted permission for this work to be included in this dissertation.

Overview:

Antiviral Immunity

Viruses, which are made up of either DNA or RNA and surrounded by a protein coat, are responsible for an array of acute and chronic infections [124]. During acute infections, viruses are typically cleared within a week, however in some cases the virus may persists in the host without being recognized by the immune system [125]. While some persistent infections are harmless within a healthy individual, some turn into chronic infections. The immune system plays a primary role in inhibiting and clearing viral infections. B cells secrete antibodies that work to neutralize viral particles before they can infect cells [10]. If B cells fail to neutralize the viral particles, the virus can infect and hijack the host cells protein-synthesis machinery so they can begin synthesizing their own viral proteins[125]. During this process, viral proteins get degraded into peptides that could be loaded onto MHC I molecules and further presented to cytotoxic T cells (CTLs) for targeted killing of the virus [125, 126]. Once activated, the naïve CD8+ cells expand and differentiate into effector cells that then travel through the hosts lymphatic and bloodstream to target infected cells and eliminate the infection [125, 126]. After successful clearance of the infection the population of CD8+ effector T cells contract and an estimated 5% remain as memory T cells that can be activated upon a secondary infection [126].

The importance of T cell responses in controlling viral infections was highlighted in early studies in the context of measles, cytomegalovirus (CMV), hepatitis C virus (HCV), and HIV; depletion of CD8+ T cells results in the inability to clear infection [127]. In early studies investigating the role of T cells in acute and chronic infections, T cell responses were observed in mice deficient in CD8+ T cells infected with lymphocytic choriomeningitis virus (LCMV) [128]. The study found that while immune competent mice would normally be able to control the infection, the lack of CD8+ T cells resulted in persistent infection [127, 128]. Further studies exemplifying the need for a substantial magnitude of T cells for viral clearance was show in chimpanzees [125]. When chimpanzees were depleted of CD8+T cells then infected with hepatitis B virus (HBV), they failed to clear the viral infection; however, when CD8+ T cells were reintroduced, upwards of 98% of viral DNA was eliminated [125, 129]. The importance of T cells in viral clearance can be further seen in the context of immunocompromised individuals whose fail to completely clear viral infections as a result of decreased CD8+ T cell levels and/or T cell dysfunction [130].

While the mammalian immune system has evolved to control many different viral infections, some viruses have developed mechanisms to circumvent immune recognition. The inability of the immune system to sufficiently recognize and clear an infectious virus is a signature of chronic infections [131]. Mechanisms by which viruses escape immune recognition, coined as immune evasion, include immune modulation and altering immune cell function [126, 131]. While some viruses restrict the expression of viral antigens, others may interfere with MHC antigen processing and presentation, inhibit cell apoptosis, destroy T cells, and/or induce immune cell exhaustion in order to evade an immune response [5, 126].

The Role of HPV Oncogenic Proteins in Immune Evasion

Human papillomaviruses (HPVs), which are capable of inducing cancers in multiple origins of the body including the cervix and regions of the head and neck, have evolved immunoevasion strategies that contribute to persistent infection [5]. The primary mechanism of immune evasion in the context of HPV is tightly linked to modulation of viral gene expression and inhibiting antigen presentation by MHC I molecules [2, 126, 131]. During its latent phase, HPV proteins limit replication and maintain low copy numbers, reducing the likelihood of detection [64]. Studies have shown that HPV protein E7 significantly decreases cell surface expression/antigen presentation of MHC as thus limiting cytotoxic killing [2, 132]. E7 inhibits the phosphorylation of the signal transducer and activator of transcription 1 (STAT1) factor resulting in inhibited expression of interferon regulatory factor-1 (IRF-1) and transporter associated antigen processing subunit (TAP-1); consequently inhibiting the interferon-γ (IFN-γ) facilitated MHC I antigen processing/presentation [132, 133]. Likewise, E6 has also been shown to interfere with STAT signaling, thus interfering with IFN-γ mediated processes [132]. Although the exact mechanisms of how HPV evades the immune system have not been completely elucidated, we know that HPV proteins work to maintain low level expression of viral antigens, downregulate MHC presentation/processing, and moderate an anti-inflammatory environment [60].

Targeting HPV Epitopes to Characterize Preexisting CD8+ T cells in HPV+HNSCC

As previously described, oncogenic proteins E6 and E7 play a prominent role in the pathogenesis of HPV associated head and neck cancer (HPV+ HNSCC) and are maintained after viral integration into the host genome [61]. While E2 is often lost in cervical cancers where there is a high level of integration, studies have demonstrated E2 to be maintained in

HPV+HNSCC [67]. Studies have demonstrated that serum antibodies against HPV16-E2, E6, and E7 can be detected in patients with HPV+ HNSCC [97, 134]. The ability to detect antibodies to these viral proteins confirms their immunogenic nature and potential usefulness for immune targeting [92]. Therapeutic vaccines and adoptive cell therapies targeting antigen-specific epitopes have exhibited enhanced T cell killing in solid tumors [52]. With renewed interest in identifying immunogenic HPV epitopes, we worked expand on previously identified immunogenic targets and bioinformatically predict potential immunogenic HLA class I restricted epitopes from HPV16 E2, E6, and E7 [92]. In doing so, we further aimed to investigate potential T cell dysfunction in HPV+ HNSCC donors by cell surface phenotyping

T-cell exhaustion, defined as T cells acquiring an altered differentiation state or the physical loss of T cells, is characterized by the loss of effector function and sustained expression of inhibitory receptors [135, 136]. T-cell exhaustion is seen in multiple cancer types as well as in viral infections derived from HIV, hepatitis B virus (HBV), and hepatitis C virus (HCV) [137]. Unlike in acute infections, CD8+ T cells typically have severe defects in their ability to differentiate and respond in chronic viral infections [138]. Although CTLs initially generate effector functions, over time and increased viral load, functionality is lost [138]. While mechanisms behind T cell exhaustion are still being explored, the observed primary driver is continuous antigen exposure; the lack of CD4+ T cell help and upregulated inhibitory receptor signaling may also be contributing factors [135]. Prior studies performed in chronic lymphocytic choriomeningitis virus (LCMV) mouse models have demonstrated that the severity of T cell exhaustion is associated with levels of antigen stimulation [135, 136]. The study found that the presence of persistent epitopes at high levels eventually resulted in T cell deletion whereas decreased levels of epitope persistence led to exhaustion (diminished T cell function) [136]. Exhausted CD8+T cells were also found to be "addicted" to their cognate

antigen, requiring continual stimulation for T cell maintenance [136] . Pathways that are further implicated in T cell exhaustion include prolonged cell-to-cell signals, persistent levels of inflammatory and suppressive cytokines, and fluctuations in chemokine receptor expression levels [135].

Continuous CTL exhaustion is detrimental in fighting off persistent viral infections. In 2007, Wherry et al. described the molecular signature of CD8+ T-cell exhaustion [137, 139]. In the context of LCMV, exhausted CD8+ T cells elicited the following differences: overexpression of cell-surface inhibitory receptors including programmed cell death protein 1 (PD-1) and downregulation of transcription factors involved in TCR and cytokine receptor signaling [139, 140]. Exhausted T cells may express other inhibitory molecules in addition to PD-1 including T cell immunoglobulin domain and mucin domain-containing protein 3 (TIM3), lymphocyte activation gene 3 protein (LAG3), ecto-nucleoside triphosphate diphosphohydrolase-1 (CD39), cytotoxic T lymphocyte antigen 4 (CTLA4) as well as a variety of others [135, 141]. Co-expression of multiple inhibitory receptors is indicative of T cell exhaustion [135]. In an initial effort to determine if phenotypically exhausted CTL populations could be functionally restored in a murine model, Barber et al. introduced a PD-L1 blockade and the results demonstrated an enhanced CTL responses [140]. Recognizing that there are commonalities between different viral infections and immune interactions, we wanted to investigate potential CD8+ T cell dysfunction in HPV+HNSCC. Thus, after screening our predicted HPV epitopes for immunogenic potential, I worked to further detect preexisting HPV-specific CD8+ T cells from patients with HPV+HNSCC and examine them for markers of exhaustion.

Materials & Methods:

HPV16 Epitope Predictions and Epitope Mapping from HPV+ HNSCC PBMCs

Predictions for HPV16 CTL-epitopes were made using previously described strategies and performed by my colleagues Sri Krishna and Eric Wilson [92, 142, 143]. They restricted epitope predictions to the globally frequent HLA-class I alleles: HLAs A*01:01, A*02:01, A*03:01, A*11:01, A*24:02, B*07:02, B*08:01, B*15:01, B*27:05, B*35:01, B*40:01, B*40:02, B*44:02 B*51:01, and B*57:01. Candidate epitopes were 9-mer or 10-mer in derived from the HPV16 proteins E2, E6, and E7. Five independent prediction algorithms were used and normalized with the top 4-5 candidate peptides/HLA-allele further used for the in vitro experiments.

Epitope mapping from HPV+ HNSCC PBMCs was also performed as previously described [92]. Briefly, PBMCs, obtained from stage III or stage IV HPV+ HNSCC patients. were thawed, rested with 1μg/mL of CKB antibodies anti-PD1 (eBosciences, USA), anti-CTLA4 (eBosciences, USA) for 1 hour at 37°C. HPV16-peptides (Proimmune, UK) were added in pool or individually in biological triplicates, along with recombinant human IL-2 (20U/mL), human IL-7 (5ng/mL). On day 5, a media exchange was performed to replace half media with fresh media along with fresh IL-2 and peptide pool. On day 8, another media exchange was performed with fresh media, IL-2, and peptide then replated into a 96-well enzyme-linked immune absorbent spot (Elispot) plate for downstream Elispot detection. The same procedure was repeated to determine individual epitope mapping and deconvoluted using the selected candidate epitopes and the patient's HLA-restriction.

HPV-CTL stimulation for phenotyping

To generate HPV-specific T-cells, autologous HPV+ HNSCC patient B-cell APCs were stimulated by with either peptide pulsing with HPV16-epitopes, or transfection with

whole HPV-antigen encoded in mammalian expression plasmid pCDNA3.2 (Invitrogen, CA, USA) as previously described in Krishna *et al* [92]. APCs were washed and incubated with thawed whole HPV+ HNSCC PBMCs at a ratio of 1:2 (200,000 APCs : 400,000 PBMCs) supplemented with 20U/mL recombinant human IL-2 (R&D Systems, MN, USA), 5ng/mL IL-7 (R&D Systems, MN, USA). Checkpoint antibodies were not added for phenotyping experiments. On day 5, a partial media exchange was performed and on day 10, expanded HPV-CTLs were restimulated with peptide-pulsed or transfected APCs similar to day 1. CTLs were immunophenotyped after day 14 or 20.

Tetramer staining and HPV-CTL phenotyping

Staining for tetramer and CTL phenotyping were performed as previously described [92]. HPV16-tetramers TLQDVSLEV E2 (93-101), YICEEASVTV E2 (138-147), ALQAIELQL E2 (69-77), KLPQLCTEL E6 (18-26), TIHDIILECV E6 (29-38), FAFRDLCIV E6 (52-60), YMLDLQPET E7 (11-19), and YMLDLQPETT E7 (11-20) were obtained from NIH Tetramer Core Facility at Emory University. Positive controls Flu-M1 and BMLF1 pentamers were obtained from Proimmune, UK. For multimer staining, cells were resuspended in 100µL staining buffer with 5% human serum and 1mM Dasatanib (ThermoFisher Scientific, MA, USA), and each multimer was added at concentration of 1:100 for 30 minutes at room temperature. Cells were washed twice and restained with anti-CD8-PC5, anti-CD4-FITC, anti-CD14-FITC and anti-CD19-FITC for exclusion gates, and either a combination of anti-PD1-BV605 and anti-CD39-BV-421 or anti-PD1-BV-605 and anti-TIM3-BV-421 for 30 minutes on ice. For memory markers, CCR7-BV421, anti-CD45RO-BV605 and anti-CD45RA-FITC were stained for 30 minutes on ice after multimer staining. Samples were then washed twice in 1x PBS, and analyzed by Attune flow cytometer (ThermoFisher Scientific, MA, USA).

Results:

HPV+HNSCC patient CTL's are responsive to predicted HPV16 epitopes. To determine if the HPV+HNSCC patient PBMC would be responsive to the range of predicted HPV E2, E6, and E7 peptides, we did an enzyme-linked immune absorbent spot (ELISpot) assay to measure the frequency of IFNγ secretion. The Elispot results, measured by spot forming units (SFUs) per 10^6 PBMCs, showed that fifty-one out of the fifty-nine total predicted peptides were able to produce a T-cell response within at least one patient [92]. In comparison to E2 and E6 peptides, the E7 peptides provided subdominant CTL responses. Overall, the E2, E6, and E7 were ranked according to their immunogenicity across donors; peptides that elicited an average response frequency of less than ten SFUs were considered as low immunogenic, those with an average response frequency between ten and one hundred were considered as moderately immunogenic, and epitopes with an average frequency response equal to or greater than one hundred SFU were deemed strongly immunogenic (Figure 3.1) [92]. Overall, six peptides were categorized as low immunogenic, twenty-nine were moderately immunogenic, and sixteen were strongly immunogenic. Importantly, most of the peptides that stimulated a moderate to high immunogenic response were either first predicted by us and/or first described in the context of HLA restriction [92]. Collectively, these results provided a panel of newly identified immunogenic HPV epitopes in an HLA-restricted landscape.

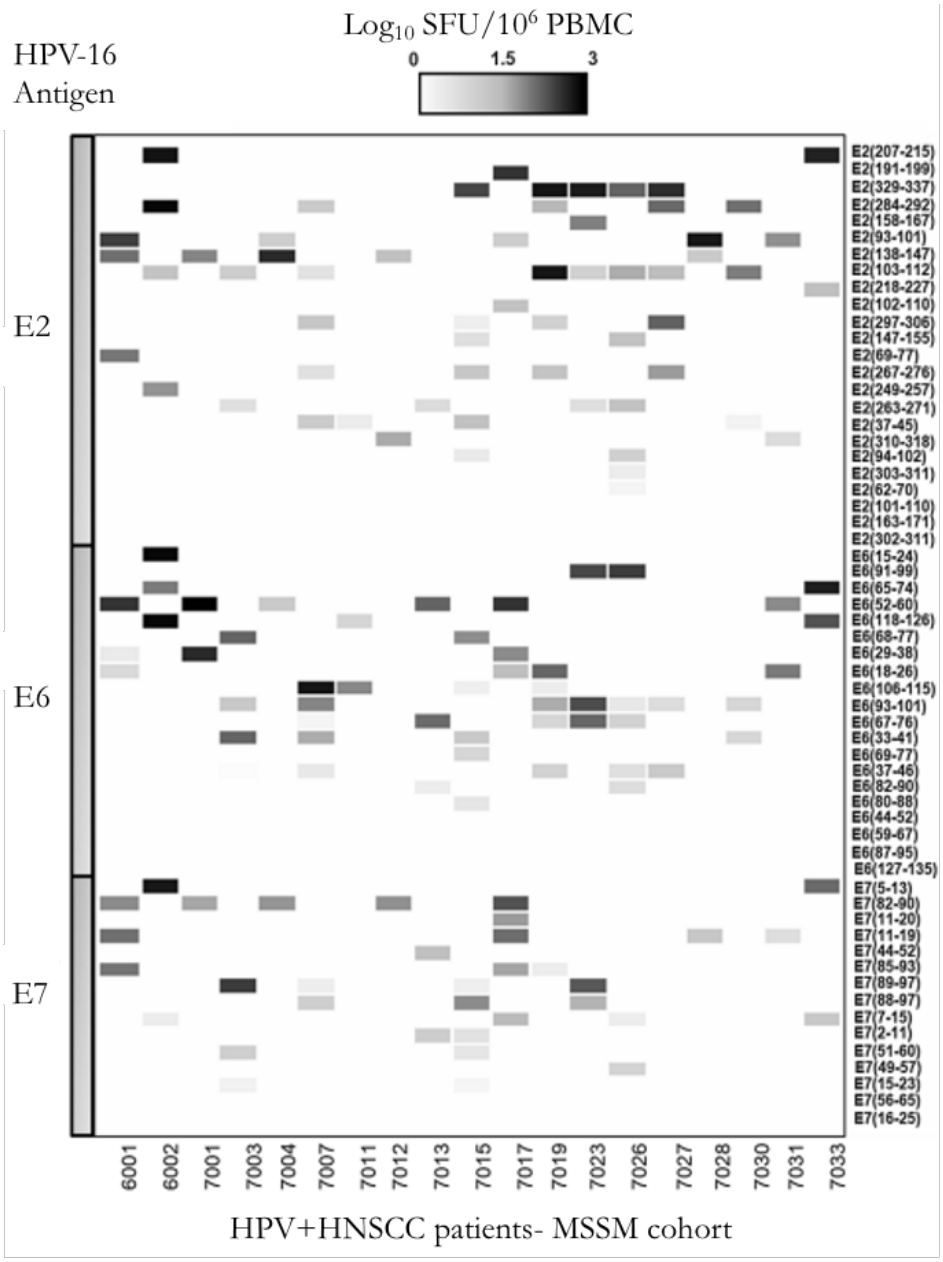

Figure 3.1: The Distribution of Immunogenic CTL-Epitopes Derived from HPV16 E2, E6, and E7 in HPV_HNSCC Patients. Elispot deconvolution screen across 19 HPV+ HNSCC patients (columns) against 59 HPV16 E2, E6, and E7 peptides (rows) in log scale. Twenty-four E2 peptides, twenty E6, and fifteen E7 peptides were screened. For each antigen, peptides are ranked from highest (top) to lowest (bottom) immunogenicity. Figure adapted from Krishna *et al* [92].

HPV-specific T-cells display a memory phenotype in HPV+ HNSCC patients. To determine if stimulated HPV-specific CTLs in HPV+HNSCC were naïve or memory T-cells, we performed ex vivo stimulations with autologous APCs presenting cognate HPV16-antigens [92]. After one round of stimulations, upwards of seventy-nine percent of HPV-specific CTLs, detected by using HLA-A*02:02 tetramers, exhibited a memory phenotype. Effector memory T cells (T_{EM}), responsible for providing an immediate response to previously encountered antigen, were defined as $CD45RO^{hi}$ and $CCR7^{lo}$ [144]. Central memory T cells (T_{CM}), responsible for sustaining the T cell response, were defined as exhibiting a $CD45RO^{hi}$ and $CCR7^{hi}$ phenotype (Figure 3.2) [144]. E2-specific CTLs were seen at higher frequencies in the T effector memory compartment whereas E6 and E7 were more comparable. Although the HPV+HNSCC patient samples were stimulated ex vivo, we were able to identify that memory CTLs were indeed present within the population; demonstrating that the patient had previously elicited an immune response to HPV antigen [92].

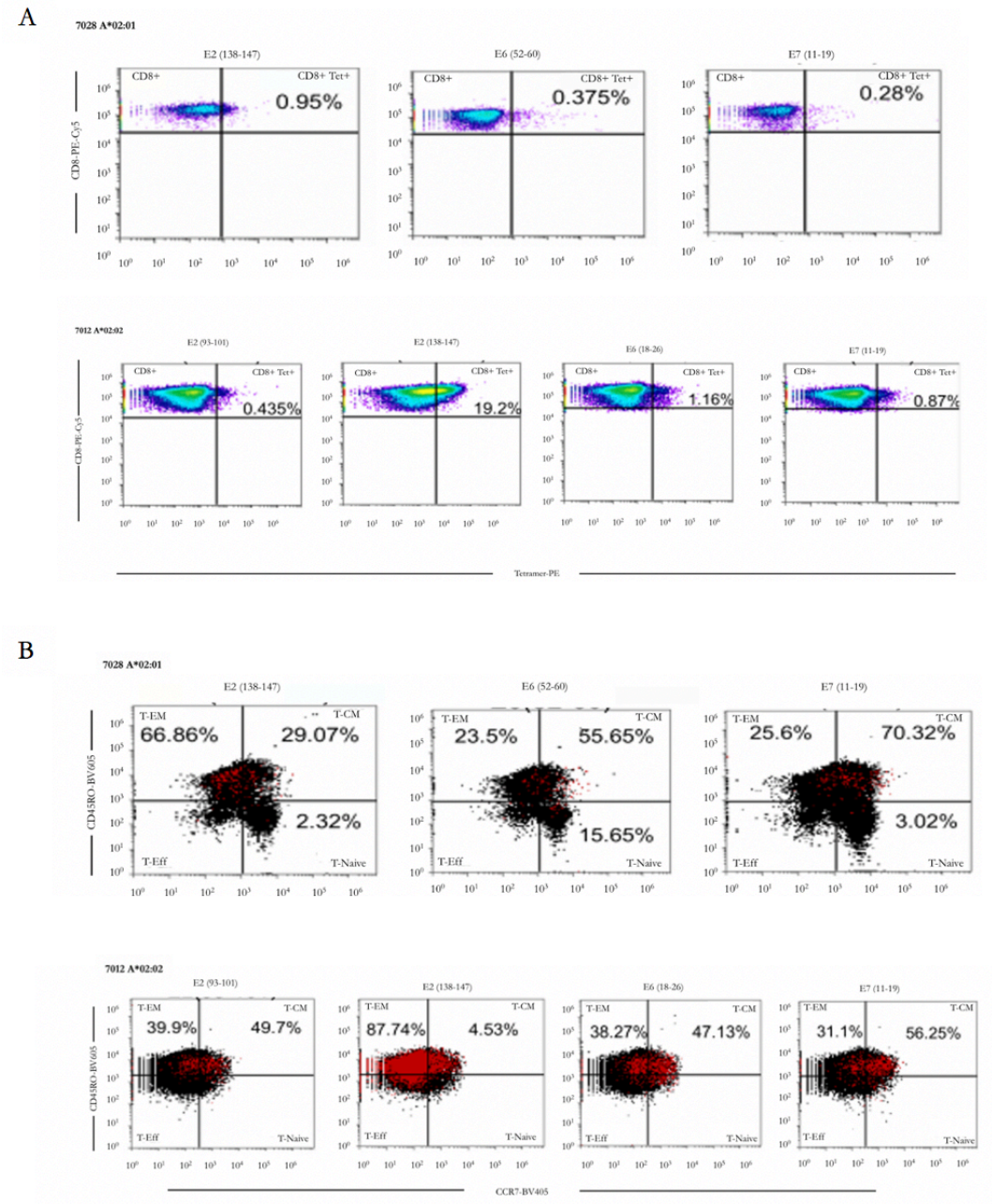

Figure 3.2: Memory HPV-CTLs can be Detected in HPV+ HNSCC Patients. Flow cytometry plots from HPV^{+} HNSCC patients (7028, 7012) CTLs after ex vivo stimulation. **A**. HPV-antigen specific CTLs can be detected using tetramer specific for given HPV-antigen after stimulation. **B**. Stimulated CTLs from HPV+HNSCC donor exhibits memory phenotype. CD8+ phenotypes (black); back-gated CD8+tetramer+ phenotypes (red). Percentage represented is back gated CD8+Tetramer+ events. Figure adapted from Krishna *et al* [90].

HPV-specific T-cells display a dysfunctional phenotype in HPV+ HNSCC patients. As previously described, T cell dysfunction is pervasive in many chronic infections and cancers [138]. Recognizing that HPV can lead to persistent chronic infections and sometimes cancer, we wanted to investigate CTL dysfunction in HPV+HNSCC. Stimulated HPV-specific CTLs from HPV+HNSCC patients that co-expressed multiple inhibitory markers (TIM3+PD-1+ or CD39+PD-1+, double positive exhausted phenotype DP^{EX}) were defined as exhausted. We first validated this approach by comparing chronic (EBV-BMLF1) CTLs with acute (Flu-M1); the chronic CTL exhibited a higher DP^{EX} phenotype [92]. Moving forward, we were able to detect HPV-specific CTLs in four patients (HLA-A*02:01) by antigen-specific tetramers after stimulating with autologous APC transfected with cognate antigen (Figure 3.3, top). Within this patient CTL population, E2 specific CTLs were at the highest frequency; E6 and E7 specific CTLs were comparable to one another. As predicted, E2, E6, and E7 specific CTLs presented multiple inhibitory markers, signifying substantial exhaustion (Figure 3.3, bottom) [92]. E7-CTLs exhibited the highest levels of exhaustion in this patient, followed by E2 CTLs then E6 CTLs. While similar results were reflected in three additional HPV+HNSCC patient samples, two other donors exhibited higher exhaustion in E2-CTLs whereas E6-CTLs remained relatively low. These data suggest that HPV-CTL dysfunction may be higher in E2 and E7-CTLs compared to E6 in HPV+HNSCC.

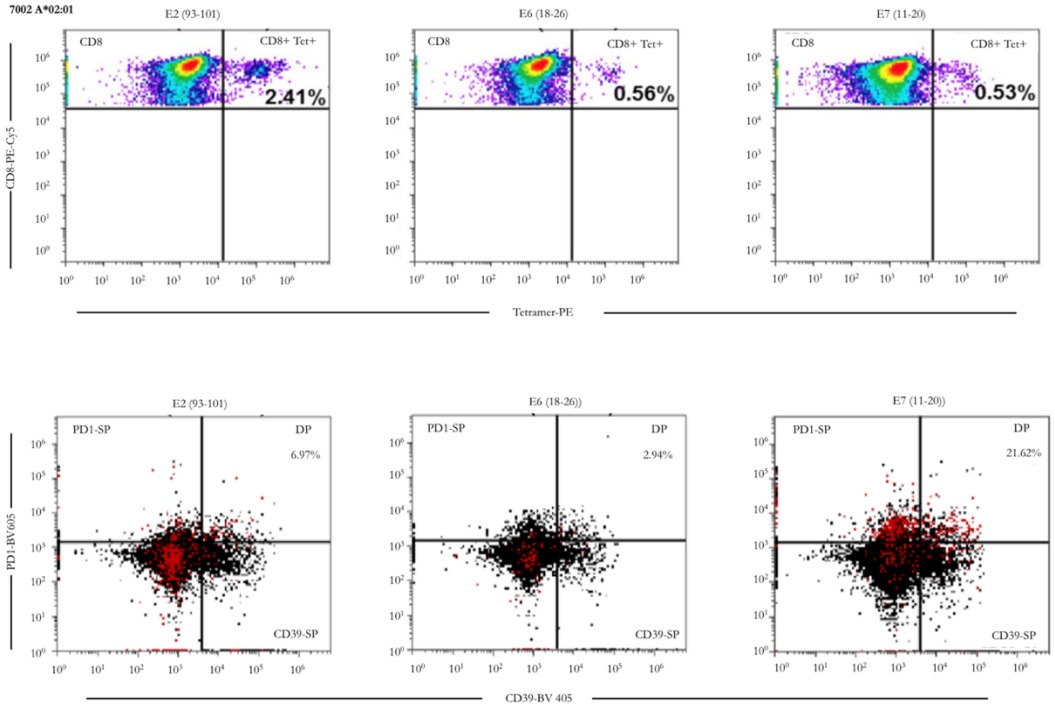

Figure 3.3: HPV16-Specific T cells Present a Dysfunctional Phenotype when Stimulated *Ex Vivo*. Flow cytometry plots from an HLA-A*02:01 HPV^{+} HNSCC patient CTLs that were stimulated with autologous APCs transfected with cognate antigen. Top, HPV16-Tetramer^{+}CD8^{+} T cells are one example for each HPV16-antigen; labels correspond to HPV16-epitope; percentages indicate tetramer^{+} events within the CD8^{+} gated population. Bottom, CD8^{+}PD1^{+}CD39^{+} (black) or CD8^{+}Tetramer^{+}PD1^{+}CD39^{+} (red). Percentage represented is back gated CD8^{+}Tetramer^{+}DP^{Ex}. Figure adapted from Krishna *et al* [90].

Discussion:

Both DNA and RNA viruses contribute to the development of an estimated 15% of human cancers worldwide [145]. While HPV are typically the culprit of benign papillomas and warts, persistent infection may lead to cancers in the cervix, head and neck, and anogenital regions [64]. Being able to detect the expression of oncogenic proteins E6 and E7 along with E2 after they integrate into the host genome make them potential candidates for immune targeting [61, 66, 67, 146]. While studies have previously predicted epitopes derived from E6 and E7, our study expanded the spectrum of potential targets to include E2 derived epitopes. Additionally, we broadened our epitope predictions to cover globally frequent HLA supertypes. From our studies, we identified an array of novel high, medium, and low immunogenic epitopes across HPV E2, E7, and E7 antigens. The results suggest that E2 and E6 antigens are capable of inducing higher CTL responses in comparison to E7. While E6 and E7 are the typical candidates for T-cell targeted therapies, our findings suggest that HPV E2 antigen may also provide valuable target [6].

Thus far, we know that T cell dysfunction is prevalent in many chronic viral infections as well as cancer, but it has not been extensively studied in the context of HPV+HNSCC. Upon identifying a landscape of immunogenic epitopes, we further aimed to develop a method to detect low frequency HPV-specific CTLs, determine whether these CTLs were tumor specific, and assess overall T cell dysfunction. Our ex vivo stimulation protocol, which included the addition of PD-1 and CTLA-4 checkpoint blockade antibodies, helped in being able to detect low-frequency HPV-CTL-responses. After the ex vivo stimulation, we were able to detect HPV-specific CTLs by antigen-specific tetramers, allowing us to determine relative HPV-CTLs frequencies across donors. From our experiments, it was evident that

HPV16 E2 CTLs were present at higher frequencies, again suggesting that E2 could be an important target for HPV+HNSCC targeted therapies. When we further went on to phenotype stimulated HPV-CTLs, we found that the majority expressed cell surface markers specific for effector memory (T_{EM}, $CD45RO^{hi}CCR7^{lo}$) and central memory (T_{CM}, $CD45RO^{hi}CCR7^{hi}$) differentiation, signifying that the donor had previously generated a T cell response and memory specific to our given epitopes. I further went on to investigate HPV-specific CTL dysfunction in HPV+ HNSCC. We found substantial dysfunction in E2, E6, and E7-specific CTLs ($CD8+CD39^{+}PD\text{-}1^{+}$ or $CD8+ TIM\text{-}3^{+}PD\text{-}1^{+}$ phenotype). Finding HPV16-antigen specific CTLs in the T cell memory compartment in conjunction with a high dysfunction phenotype together suggest specificity to HPV+ HNSCC tumor in these samples. While E2 and E6-specific CTLs presented a dysfunction phenotype, E7-CTL dysfunction was at higher frequency and E7-CTL dysfunction rarely occurred in conjunction with E2/E6-CTL dysfunction; suggesting variations in HPV viral load within these patients. Prior to these experiments, HPV-specific T cell dysfunction in HNSCC had not been previously described.

Further work done by my colleagues went on to investigate the role of Indoleamine 2,3-dioxygenase (IDO-1), a catabolizing enzyme, in HPV+HNSCC. Our interest in IDO-1 stemmed from IDO-1 inhibitors being evaluated to enhance tumor immunity [141, 147]. Through differential gene expression signatures, we found that IDO-1 was strongly expressed in HPV+ samples compared to HPV-HNSCC. We then tested the ability of IDO-1 inhibition to overcome HPV specific CTL exhaustion. What we found was that a combination of PD-1 blockade with IDO-inhibition was able to enhance T-cell targeting of HPV+HNSCC, proposing its potential use in targeted immunotherapy.

While the first HPV vaccine was licensed and recommended for women in 2006, it was not until 2009 that an HPV vaccine was licensed for men [148]. Almost 14 years later,

HPV infections and associated cancers remain a global issue. This research not only provides a larger pool of immunogenic epitopes that could potentially be immune therapeutic targets in HPV+HNSCC but confirms a dysfunctional phenotype in HPV+HNSCC that is observed in other viral chronic infections and cancer. Even more, we demonstrate the importance of further exploring checkpoint blockade in combination with IDO-1 inhibitors in HPV+HNSCC.

CHAPTER 4

SINGLE-CELL ANALYSIS OF HPV-SPECIFIC TCR

Overview:

Nearly 80 percent of HPV+ HNSCCs are linked to the high-risk HPV16 subtype [93]. Although we have seen a gradual increase in the uptake of HPV vaccines in both men and women, the impact of vaccination may not be prevalent for several more decades [149]. Recognizing the increasing prevalence of HPV associated cancers and understanding that specific HPV viral antigens can be detected in these cancers has attracted a growing interest in identifying immunogenic epitope targets and their TCR counterparts. Several vaccines and immune therapies have already been developed to target oncogenic proteins E7 and E6 and have been successful in regression of HPV derived cervical cancer [150, 151]. The identification of HPV-derived epitopes in combination with advancements in adoptive cell therapeutics have revamped efforts to identify HPV- specific cytotoxic T-cell receptors (CD8+ TCR) that can target and eliminate HPV associated head and neck cancers.

The composition of an antigen-specific T cell repertoire can be extremely diverse within any given individual and varies during healthy and disease states [152]. A diverse T cell repertoire is important, allowing for a wide range of potential pathogens that could be recognized and eliminated [153]. Within the context of cervical cancer, cancer progression was strongly associated with lower TCR diversity [104]. The association between decreased TCR diversity and worsening prognosis in disease states emphasizes the importance of characterizing TCR clonotypes specific for given antigenic epitopes that could be used for targeted therapy.

There are few studies that have investigated the T cell repertoire in the context of HPV+HNSCC derived antigens. In this study, we used a previously identified HPV16-E6

immunogenic epitope to stimulate donor PBMCs and characterize the generated TCR for the identification of unique clonotypes, providing potential TCR targets.

Materials and Methods:

Autologous APC generation from healthy individual PBMCs

Autologous CD40L-activated B cell APCs were generated from healthy donors by incubating whole PBMCs with irradiated (32 Gy) K562-cell line expressing human CD40L (KCD40L) at a ratio of 4:1 (800,000 PBMCs to 200,000 irradiated KCD40Ls) in each well. The cells were maintained in B cell media (BCM) consisting of IMDM (Gibco, USA), 10% heat-inactivated human serum (Gemini Bio Products, CA, USA), 100mM HEPES (Sigma-Aldrich, CA, USA), and 2mM L-Glutamine (Gibco, USA). BCM was supplemented with 10ng/mL recombinant human IL-4 (R&D Systems, MN, USA), 2μg/mL Cyclosporin A (Sigma-Aldrich, CA, USA), and insulin transferrin supplement (ITES, Lonza, MD, USA). APCs were re-stimulated with fresh irradiated KCD40Ls on day 7, after washing with PBS and expanding into a whole 24-well plate. On day 12, APC purity was assessed by CD19+ CD86+ expressing cells using flow cytometry and were used for T cell stimulation after >90% purity. APCs were either restimulated up to 5 weeks or cryopreserved for re-expansion as necessary.

HPV CTL stimulation by autologous APCs

Antigen-specific T-cells were generated by stimulating healthy donor B-cell APCs by peptide pulsing with previously identified immunogenic HPV16 E6-3 (52-60, FAFRDLCIV) peptide. This specific peptide was targeted because previous data analysis showed that it was HLA-A2 restricted and ranked as moderate to highly immunogenic [92]. Peptide pulsing of APCs were done under BCM 5% human serum, with recombinant IL-4. Twenty four hours later, on day 1, APCs were washed with IMDM and incubated with thawed whole PBMCs at

a ratio of 1:3.65 (400,000 APCs : 1400,000 PBMCs) in a 24-well plate in BCM supplemented with 20U/mL recombinant human IL-2 (R&D Systems, MN, USA), 5ng/mL IL-7 (R&D Systems, MN, USA).On day 5, partial media exchange was performed by replacing half the well with fresh B-cell media and IL-2. On day 7, fresh APCs were peptide pulsed as described above in a new 24-well plate. On day 8, the PBMCs were stimulated with freshly peptide pulsed APCs. On day 13, fresh APCs were peptide pulsed as described above in a new 24-well plate. On day 14, expanded T-cells were restimulated with peptide- pulsed APCs similar to day 1 and day 8. T-cells were used for Elispot on day 10 and for flow analysis after day 15.

Elispot detection of IFNY secretion

Elispot detection assay was performed as previously described [143]. Briefly, sterile multiscreen Elispot plates, (Merck Millipore, Billerica, MA, USA) precoated overnight with 5μg/well anti-IFNY capture antibody (clone D1K, Mabtech, USA) in sterile 1X PBS. Eight days after stimulation, HPV+HNSCC PBMCs were subject to media change and IL-2, peptide (pools or individual) were added. Cells in each well were transferred to the Elispot plate and incubated at 37C 5% CO_2 incubator for 48 hours. Plates were washed with elispot buffer (PBS + 0.5% FBS) and incubated with 1μg/mL anti-IFNY secondary detection antibody (clone 7-B6-1, Mabtech, USA) for 2 hours at room temperature, washed and reincubated with 1μg/mL Streptavidin ALP conjugate for 1 hour at room temperature. The wells were washed again with elispot buffer and spots were developed by incubating for 8-10 minutes with detection buffer (33μL NBT, 16.5μL BCIP, in 100mM Tris-HCl pH 9, 1mM $MgCl_2$, 150mM NaCl). Plates were dried for 2 days and spots were read using the AID Elispot reader (Autoimmun Diagnostika GmbH, Germany). Average number of spot forming units for the triplicates were

calculated for each test peptide/pool and subtracted from background (either HIV-control peptide pool or PBS-DMSO controls).

Single-cell fluorescence-activated cell sorting (FACs) for T cells

Cells were washed once in 1x PBS, centrifuged at 550g for 5 min and re-suspended in 100μL cell staining buffer (BioLegend, CA, USA) with Human TruStain FcX (BioLegend, 2:50) for ten minutes. Cells were centrifuged at 550g for 5 min and resuspended in 100μL staining buffer containing anti-CD137, conjugated with phycoerythrin (PE, clone 4B4-1; Biolegend, USA), anti-CD8-Brilliant Violet 711 (clone SK1; Biolegend, 1:100), viability dye (Zombie Violet; Biolegend), anti-CD14-FITC (clone 63D3; BioLegend, 1:100), and anti-CD19-FITC (clone HIB19; BioLegend,1:100), CD14 and CD19 used for exclusion gates. Samples were covered and incubated for 30 min on ice, washed twice in PBS, and resuspended in 200ul PBS prior to analysis. For flow cytometric analysis, all samples were acquired with Attune flow cytometer (ThermoFisher Scientific, MA, USA) and analyzed using FlowJo software. Gates for expression of different phenotype markers were determined based on flow minus one (FMO) samples for each color after doublet discrimination. The CD8+CD137- population will be screened as well to help eliminate any background. Only samples with CD8+CD137+ events were used for single-cell fluorescence-activated cell sorting (FACS).

Single-Cell Human T-Cell Receptor Profiling

Stimulated T cells expressing CD8+ CD137+ phenotype were sorted into a 96-well plate and processed using SMARTer Human scTCR a/b Profiling Kit (Takara Bio, USA) (Figure 4.1). Briefly, this technology uses a combination of SMART (Switching Mechanism at 5' End of RNA Template) and 5'RACE to capture the V(D)J regions of TCR. Following single-cell sort, first-strand cDNA synthesis was performed in the 96-well plate using MMLV-derived SMARTScribeTM Reverse Transcriptase (RT). Using the MMLV-derived RT,

nontemplated nucleotides were added to the 5' end of each mRNA template allowing for the use of SMART-Seq Indexed Oligos (each containing a unique six-base in-line index) for template switching at the 5' end of each TCR transcript. cDNA amplification is performed using the provided cDNA Primer and SMART cDNA Primer that are complementary to the sequences previously added by the RT primer and SMART-Seq Oligos, respectively. Following cDNA amplification, samples were pooled, bead purified with Agencourt AMPure XP PCR Purification kit (Beckman Coulter, CA, USA), quantified using Agilent TapeStation 4200, then underwent two gene-specific PCRs. The first gene-specific PCR results in amplification of the entire variable and a portion of the constant region of TCRa/b. The second round of PCR further amplifies the full-length TCR variable region while also incorporating Illumina adapters for further demultiplexing. Samples are then again purified and validated with Tapestation D5000 and qPCR. Upon validation, pooled samples were sequenced on an Illumina MiSeq sequencer using the 600-cycle MiSeq Reagent Kit v3 (Illumina, Cat. No. MS-102-3003) with paired-end, 2 x 300 base pair reads.

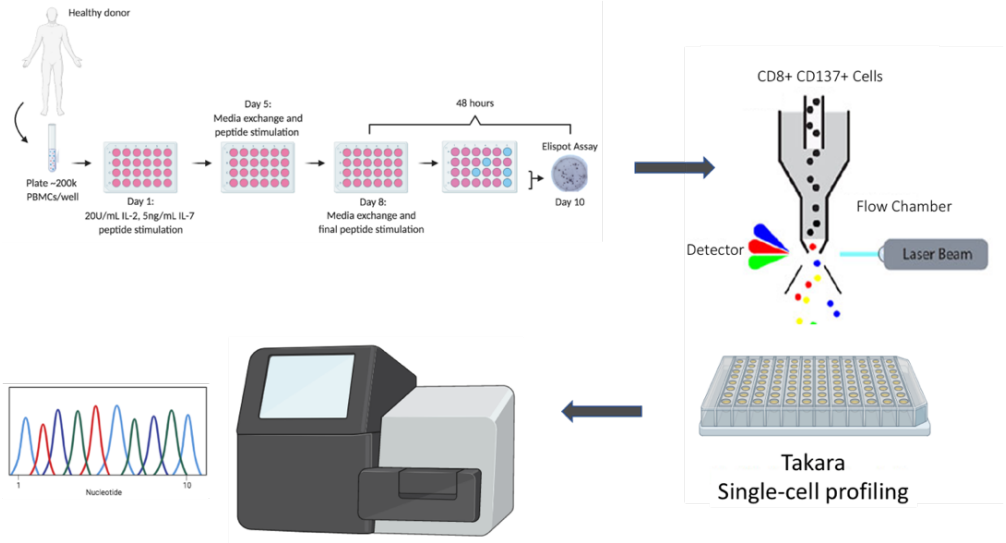

Figure 4.1: Methodology Overview of Single-Cell TCR Profiling. HPV CTLs are stimulated by autologous APCs and expanded. After day ten, cells are stained with target antibodies and sorted into a 96-well plate. Following RT-PCR and barcoding, samples are sent for next generation sequencing. Image created using BioRender.

TCR Modeling

The TCRpMHCmodels-1.0 server was used to predict the three-dimensional structure of TCR:pMHC complexes based off of our TCRαβ pairs. This tool assesses the amino acid sequences from each of the protein chains and selects the best templets for homology modeling.

CDR3 Alignments

We performed multiple sequence alignments on our retrieved TCRβ CDR3 sequences against TCRβ CDR3 sequences found in the ImmunoSeq T cell receptor database (https://clients.adaptivebiotech.com/immuneaccess). We calculated the pair-wise alignment score of each of our sequences against all of the CDR3 that were of the same length and derived from the same variable gene in the Immunoseq database for HPV-derived cancer. We selected the thirty highest scoring pairwise sequence alignments and performed multiple sequence alignments on those top thirty for each derived CDR3.

TCR Retroviral Construct Design

Paired TCRαβ nucleotide sequences derived from our Takara results were synthesized and subcloned into the HPV16 E6 MSGV1 retrovirus backbone (122727, Addgene) by GenScript Biotech (NJ, USA [6]. MSGV1-GFP and MSGV-FluM1 were also constructed as positive controls for transfection and transduction, respectively. The TCRα and TCRβ insert sequences were codon optimized for expression in mammalian cells. To prevent mispairings of TCR chains, we substituted human TCR constant regions for mouse TCR (mTCR) constant regions. In order to connect the TCRα and TCRβ in the same construct, a furin 2A self-cleaving peptide (P2A) was used as a linker between the two inserts (Figure 4.2).

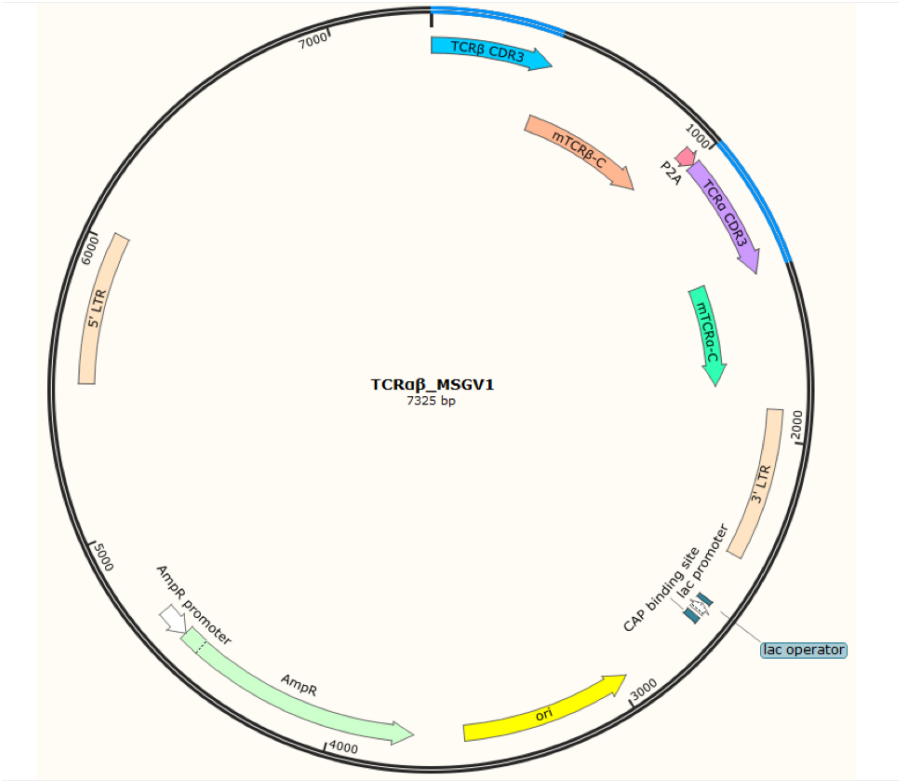

Figure 4.2: MSGV1 Plasmid Design with Incorporated Target TCR Sequences. TCRα and TCRβ constant regions were replaced with murine constant regions (mTCRα-C and mTCRβ-C). The full TCR sequence (V-D-J, V-J) containing the rearranged CDR3 was synthesized for TCRα and TCRβ, respectively. Additional plasmid features include the viral promoter within the 5' LTR and ampicillin resistance.

Transfecting TCR Retroviral Constructs

MSGV1-GFP, MSGV1-FluM1, and MSGV1-E6 retroviral supernatants were produced by co-transfecting each construct separately with Phoenix-GP packaging cell line (ATCC) and RD114 envelope plasmid (#17576, Addgene). Phoenix GP cells are a derivative of HEK 293 cells that express retroviral proteins, gag-pol. The cell line was cultured in Dulbecco's Modified Eagle's medium (DMEM) supplemented with 10% FBS and 1% penicillin/streptomycin (Life Technologies). On the day of transfection, Phoenix GP cells were harvested, counted, and diluted (1 x 10^5 cells/sample) in Opti-Mem reduced serum medium (ThermoFisher, USA). MSGV1 constructs were diluted in nuclease-free water and

brought to a concentration of approximately 1.2 micrograms. Constructs were added to Phoenix-GP cells in a total volume of 20ul and transferred to electroporation wells and run on the Lonza 4D Nucleofector, program A023 (Lonza, MD, USA). Transfected samples were transferred to 24-well plate containing antibiotic-free DMEM media supplemented with 10%FBS and incubated for two-three days before transduction (Figure 4.3)

T cell Transductions

Two days prior to transduction, PBMCs were brought into culture in BCM consisting of IMDM (Gibco, USA), 10% heat-inactivated human serum (Gemini Bio Products, CA, USA), 100mM HEPES (Sigma-Aldrich, CA, USA), and 2mM L-Glutamine (Gibco, USA). PBMCs were stimulated with 50 ng/mL of soluble anti-CD3 (OKT3) and 20U/ml of IL2 on the same day. Two days after transfections, we harvested retroviral supernatants from each construct in eight hour increments. After the third harvest, we plated the retroviral supernatants on retronectin coated plates (Takara Bio, USA). The previously stimulated PBMCs were added to the viral coated retronectin plates and incubated at 37C for five days. Expression of TCR constructs was verified by staining with anti-mTCR or tetramer, acquired with an Attune flow cytometer (ThermoFisher Scientific, MA, USA), and analyzed using FlowJo software (Figure 4.3).

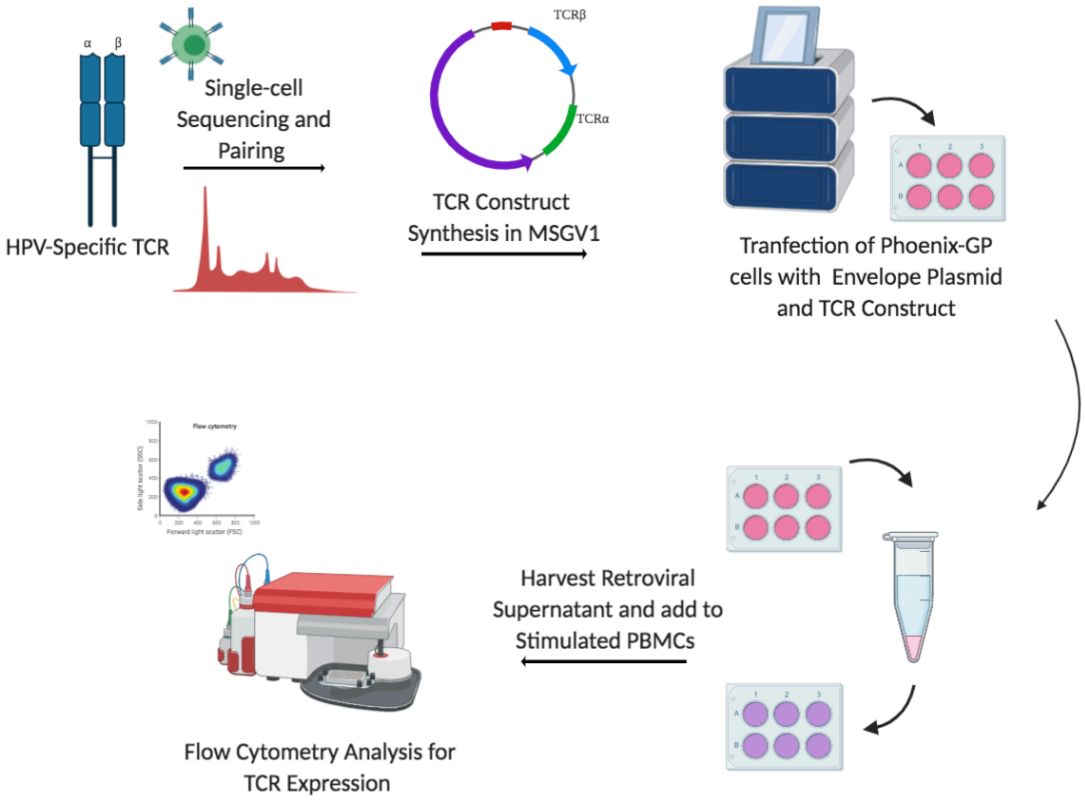

Figure 4.3: Methodology Overview of Transfecting Retroviral TCR Constructs and Transducing PBMCs. TCRαβ pairs were determined after single-cell sorting and Illumina sequencing then synthesized in retroviral vector, MSGV1. Retroviral TCR plasmids were transfected into Phoenix-GP packaging cells along with the RD114 envelope plasmid by electroporation. Two days post transfection, retroviral supernatant was harvested and placed on retronectin-coated plates. Stimulated PBMCs were added to the viral supernatants and analyzed by flow cytometry on day 4. Image created using BioRender.

Assess Function of TCR Constructs

We will assess TCR function with a previously established lab protocol for assessing cell cytotoxicity in HPV derived cell lines [92]. We currently have the following four HPV+HNSCC cell lines: SCC90, SCC47, SCC104, and 147T. The HLA- A*02:01+ HPV+HNSCC+ cell lines will be pre-labelled with 0.5μM CellTracker Green. We will then add the transduced TCR HPV-CTLs at ratio of 5:1 to the HPV+HNSCC cell line and incubate for 48 hours at 37 C, 5% CO_2. The co-cultured cells will be harvested and centrifuged. Cell

pellets will be washed and resuspended with 1mL 1X PBS and 2uL Propidium Iodide (ThermoFisher Scientific, MA, USA) then assess cell death by flow cytometry.

Results:

Healthy donor PBMCs can be stimulated with HPV-specific epitope. The first step to our approach of identifying T cell receptors specific to HPV16-E6-3 was to identify CTL-reactivity from healthy donor PBMCs. After generating autologous APCs from healthy individual PBMCs, we peptide pulsed them with HPV16 E6-3 (FAFRDLCIV) peptide and used an Elispot detection assay to measure interferon-gamma secretion The representative donor that elicited the strongest response to FluM1 followed by the CEF pool and then the A2-E6-3 peptide is shown below (Figure 4.4).

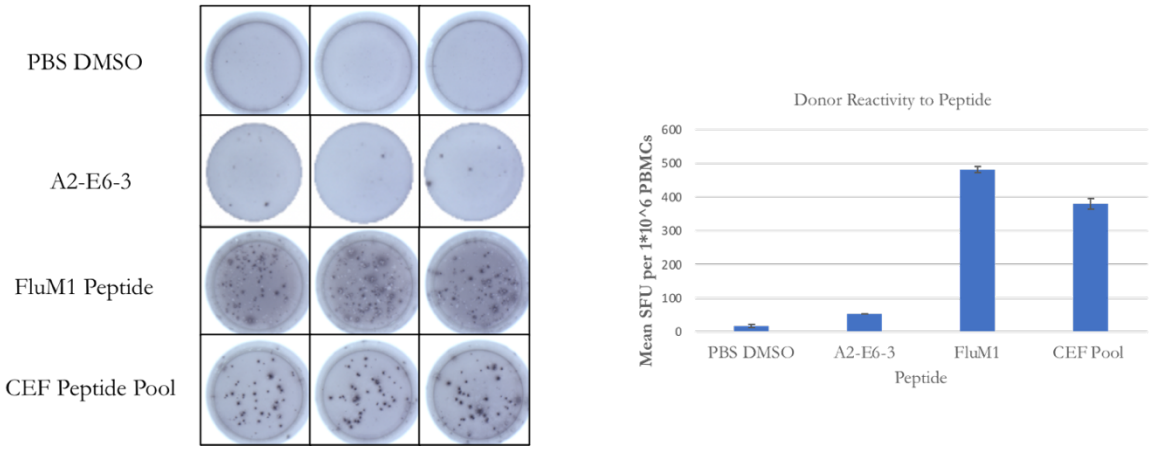

Figure 4.4: ELISpot Assay for Screening Healthy donor PBMCs to HPV16-E6-3 Epitope. ELlSpot assay results, measured by spot forming units (SFUs) per 10^6 PBMCs, determining FNγ secretion in response to HPV16-E6-3 in health donor PBMCs . FluM1 and CEF pool were used as positive controls. PBS DMSO was used as the negative control.

CD8+CD137+ T cell populations were generated after A2-E6-3 stimulations of donor PBMCs then single-cell sorted by FACS. Upon identifying donor PBMCs that could generate reactivity to A2-E6-3, we moved forward with a second set of stimulations to generate a population of T cells that we could use for single-cell sorting. After two rounds of peptide stimulations, we were able to expand HPV specific cytotoxic lymphocytes populations from donor PBMCs and further stained them with cell surface markers to distinguish recently activated CTL, CD8+CD137 phenotype (Figure 4.5).

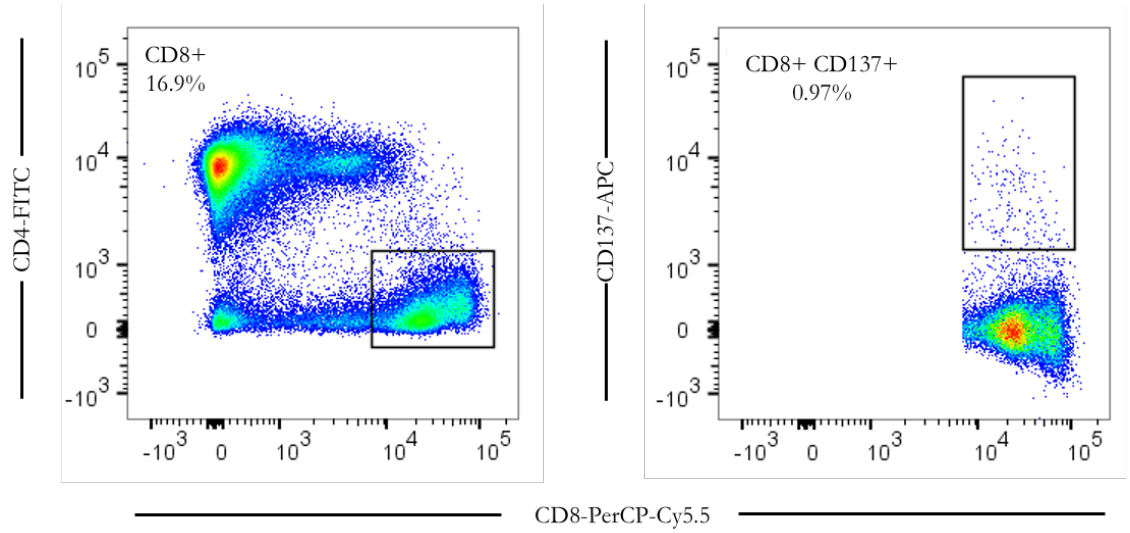

Figure 4.5: HPV16 E6 Specific T-cells Stimulated from an HLA-A*02:01 Healthy Donor. Representative flow cytometry plots of activated CD8+ T-cells generated when stimulating healthy donor APCs by peptide pulsing with specific HPV16-E6-3 epitope. Gated left: CD8+ cells events, gated right: CD8+ CD137+ T cells.

Single-cell TCR profiling of E2-E6-3 stimulated donor PBMCs generated ten unique TCRαβ pairs. Single-cell sorting double positive (CD8+CD137+) cells into a 96-well plate (Takara, Bio) allowed for individual RT-PCR reactions of TCRα and TCRβ from a single-cell. Incorporating inline barcodes and adapter ligations allowed for downstream demultiplexing during next gen sequencing. Sequence analysis yielded ~300 bp of targeted TCR sequencing, covering the CDR3 region of the TCR. Further sequence analysis showed

that we were able to retrieve ten unique TCRαβ pairs derived from stimulated donor PBMCs (Table 4.1). The retrieved TCRα sequences had redundant variable gene usage with TRAV13-1, TRAV13-2, and TRAV38 being the most frequent. However, retrieved TCRβ sequences exhibited more variation in gene usage with only two variable genes (TRBV2, TRBV18) showing up more than once. There was a unique CDR3 distribution of TCRβ sequences, even in the variable genes that showed up more than once, with an average CDR3 length of about 45 nucleotides (Table 4.2). However, the CDR3 distribution in TCR**α** was less variable, the redundant genes resulted in the same CDR3 sequences.

Variable Gene	Paired Sequences
TRAV 5	GGAGAGGATGTGGAGCAGAGTCTTTTCCTGAGTGTCCGAGAGGGAGACAGCTCCGTTATAAACTGCACTTACACAGACAGCTCCTCCACCTACTTATAC TGGTATAAGCAAGAACCTGGAGCAGGTCTCCAGTTGCTGACGTATATTTTTTCAAATATGGACATGAAACAAGACCAAAGACTCACTGTTCTATTGAATA AAAAGGATAAACATCTGTCTCTGCGCATTGCAGACACCCAGACTGGGGACTCAGCTATCTACTTCTGTGCAGAGATTCCGACCTCAGGAACCTACAAATA CATCTTTGGAACAGGCACCAGGCTGAAGGTTTTAGCAA
TRBV 7-8	GGTGCTGGAGTCTCCCAGTCCCCTAGGTACAAAGTCGCAAAGAGAGGACAGGATGTAGCTCTCAGGTGTGATCCAATTTCGGGTCATGTATCCCTTTTT TGGTACCAACAGGCCCTGGGGCAGGGGCCAGAGTTTCTGACTTATTTCCAGAATGAAGCTCAACTAGACAAATCGGGGCTGCCCAGTGATCGCTTCTTT GCAGAAAGGCCTGAGGGATCCGTCTCCACTCTGAAGATCCAGCGCACACAGCAGGAGGACTCCGCCGTGTATCTCTGTGCCAGCAGTATACCTCGGCG GGCGGTAAGCTCCTACAATGAGCAGTTCTTCGGGCCAGGGACACGGCTCACCGTGCTAG
TRAV 13-1	GGAGAGAATGTGGAGCAGCATCCTTCAACCCTGAGTGTCCAGGAGGGAGACAGCGCTGTTATCAAGTGTACTTATTCAGACAGTGCCTCAAACTACTTC CCTTGGTATAAGCAAGAACTTGGAAAAAGACCTCAGCTTATTATAGACATTCGTTCAAATGTGGGCGAAAAGAAAGACCAACGAATTGCTGTTACATTG AACAAGACAGCCAAACATTTCTCCCTGCACATCACAGAGACCCAACCTGAAGACTCGGCTGTCTACTTCTGTGCAGCAAGTATCAGAAAGGGCGGATCT GAAAAGCTGGTCTTTGGAAAGGGAACGAAACTGACAGTAAACCCAT
TRBV 12-4	GATGCTGGAGTTATCCAGTCACCCCGGCACGAGGTGACAGAGATGGGACAAGAAGTGACTCTGAGATGTAAACCAATTTCAGGACACGACTACCTTTTC TGGTACAGACAGACCATGATGCGGGGACTGGAGTTGCTCATTTACTTTAACAACAACGTTCCGATAGATGATTCAGGGATGCCCGAGGATCGATTCTCA GCTAAGATGCCTAATGCATCATTCTCCACTCTGAAGATCCAGCCCTCAGAACCCAGGGACTCAGCTGTGTACTTCTGTGCCAGCAGTTTCTTCGGACTAG CGGGAGTAAATGAGCAGTTCTTCGGGCCAGGGACACGGCTCACCGTGCTAG
TRAV 13-1	GGAGAGAATGTGGAGCAGCATCCTTCAACCCTGAGTGTCCAGGAGGGAGACAGCGCTGTTATCAAGTGTACTTATTCAGACAGTGCCTCAAACTACTTC CCTTGGTATAAGCAAGAACTTGGAAAAGACCTCAGCTTATTATAGACATTCGTTCAAATGTGGGCGAAAAGAAAGACCAACGAATTGCTGTTACATTGA ACAAGACAGCCAAACATTTCTCCCTGCACATCACAGAGACCCAACCTGAAGACTCGGCTGTCTACTTCTGTGCAGCAAGTATCAGAAAGGGCGGATCTG AAAAGCTGGTCTTTGGAAAGGGAACGAAACTGACAGTAAACCCAT
TRBV 29-1	AGTGCTGTCATCTCTCAAAAGCCAAGCAGGGATATCTGTCAACGTGGAACCTCCCTGACGATCCAGTGTCAAGTCGATAGCCAAGTCACCATGATGTTC TGGTACCGTCAGCAACCTGGACAGAGCCTGACACTGATCGCAACTGCAAATCAGGGCTCTGAGGCCACATATGAGAGTGGATTTGTCATTGACAAGTTT CCCATCAGCCGCCCAAACCTAACATTCTCAACTCTGACTGTGAGCAACATGAGCCCTGAAGACAGCAGCATATATCTCTGCAGCGGAATTGACAGCATCT CCTACGAGCAGTACTTCGGGCCGGGCACCAGGCTCACGGTCACAG
TRAV 13-2	GGAGAGAGTGTGGGGCTGCATCTTCCTACCCTGAGTGTCCAGGAGGGTGACAACTCTATTATCAACTGTGCTTATTCAAACAGCGCCTCAGACTACTTC ATTTGGTACAAGCAAGAATCTGGAAAAGGTCCTCAATTCATTATAGACATTCGTTCAAATATGGACAAAAGGCAAGGCCAAAGAGTCACCGTTTTATTG AATAAGACAGTGAAACATCTCTCTCTGCAAATTGCAGCTACTCAACCTGGAGACTCAGCTGTCTACTTTTGTGCAGAGAAAGGTAGGCAGAACGACTACA AGCTCAGCTTTGGAGCCGGAACCACAGTAACTGTAAGAGCAA
TRBV 2	GAACCTGAAGTCACCCAGACTCCCAGCCATCAGGTCACACAGATGGGACAGGAAGTGATCTTGCGCTGTGTCCCCATCTCTAATCACTTATACTTCTATT GGTACAGACAAATCTGGGGGCAGAAAGTCGAGTTTCTGGTTTCCTTTTATAATAATGAAATCTCAGAGAAGTCTGAAATATTCGATGATCAATTCTCAG TTGAAAGGCCTGATGGATCAAATTTCACTCTGAAGATCCGGTCCACAAAGCTGGAGGACTCAGCCATGTACTTCTGTGCCAGCAGTTGGGACAGTTACA ATGAGCAGTTCTTCGGGCCAGGGACACGGCTCACCGTGCTAG
TRAV 13-2	GGAGAGAGTGTGGGGCTGCATCTTCCTACCCTGAGTGTCCAGGAGGGTGACAACTCTATTATCAACTGTGCTTATTCAAACAGCGCCTCAGACTACTTC ATTTGGTACAAGCAAGAATCTGGAAAAGGTCCTCAATTCATTATAGACATTCGTTCAAATATGGACAAAAGGCAAGGCCAAAGAGTCACCGTTTTATTG AATAAGACAGTGAAACATCTCTCTCTGCAAATTGCAGCTACTCAACCTGGAGACTCAGCTGTCTACTTTTGTGCAGAGAAGGTGGGAAACACACCTCTTG TCTTTGGAAAGGGCACAAGACTTTCTGTGATTGCAA
TRBV 18	AATGCCGGCGTCATGCAGAACCCAAGACACCTGGTCAGGAGGAGGGGACAGGAGGTAAGACTGAGATGCAGCCCAATGAAAGGACACAGTCATGTTT ACTGGTATCGGCAGCTCCCAGAGGAATGTCTGAAATTCATGGTTTATCTCCAGAAAGAAAATATCATAGATGAGTCAGGAATGCCAAAGGAACGATTTT CTGCTGAATTTCCCAAAGAGGGCCCCAGCATCCTGAGGATCCAGCAGGTAGTGCGAGGAGATTCGGCAGCTTATTTCTGTGCCAGCTCCCCGTACCAG GAGACCCAGTACTTCGGGCCAGGCACGCGGCTCCTGGTGCTCG
TRAV 13-2	GGAGAGAGTGTGGGGCTGCATCTTCCTACCCTGAGTGTCCAGGAGGGTGACAACTCTATTATCAACTGTGCTTATTCAAACAGCGCCTCAGACTACTTC ATTTGGTACAAGCAAGAATCTGGAAAAGGTCCTCAATTCATTATAGACATTCGTTCAAATATGGACAAAAGGCAAGGCCAAAGAGTCACCGTTTTATTG AATAAGACAGTGAAACATCTCTCTCTGCAAATTGCAGCTACTCAACCTGGAGACTCAGCTGTCTACTTTTGTGCAGAGAAAGGTAGGCAGAACGACTACA AGCTCAGCTTTGGAGCCGGAACCACAGTAACTGTAAGAGCAA
TRBV 4-2	GAAACGGGAGTTACGCAGACACCAAGACACCTGGTCATGGGAATGACAAATAAGAAGTCTTTGAAATGTGAACAACATCTGGGGCATAACGCTATGTA TTGGTACAAGCAAAGTGCTAAGAAGCCACTGGAGCTCATGTTTGTCTACAACTTTAAAGAACAGACTGAAAACAACAGTGTGCCAAGTCGCTTCTCACCT GAATGCCCCAACAGCTCTCACTTATTCCTTCACCTACACACCCTGCAGCCAGAAGACTCGGCCCTGTATCTCTGTGCCAGCAGCCAGGCTTCCTGGACCG CGGAGTCCTATGGCTACACCTTCGGTTCGGGGACCAGGTTAACCGTTGTAG
TRAV 13-2	GGAGAGAGTGTGGGGCTGCATCTTCCTACCCTGAGTGTCCAGGAGGGTGACAACTCTATTATCAACTGTGCTTATTCAAACAGCGCCTCAGACTACTTC ATTTGGTACAAGCAAGAATCTGGAAAAGGTCCTCAATTCATTATAGACATTCGTTCAAATATGGACAAAAGGCAAGGCCAAAGAGTCACCGTTTTATTG AATAAGACAGTGAAACATCTCTCTCTGCAAATTGCAGCTACTCAACCTGGAGACTCAGCTGTCTACTTTTGTGCAGAGAAAGGTAGGCAGAACGACTACA AGCTCAGCTTTGGAGCCGGAACCACAGTAACTGTAAGAGCAA
TRBV 10-3	GATGCTGGAATCACCCAGAGCCCAAGACACAAGGTCACAGAGACAGGAACACCAGTGATTCTGAGATGTCACCAGACTGAGAACCACCGCTATATGTAC TGGTATCGACAAGACCCGGGGCATGGGCTGAGGCTGATCCATTACTCATATGGTGTTAAAGATACTGACAAAGGAGAAGTCTCAGATGGCTATAGTGT CTCTAGATCAAAGACAGAGGATTTCCTCCTCACTCTGGAGTCCGCTACCAGCTCCCAGACATCTGTGTACTTCTGTGCCATCAGTGATGAGACATCGCAG GTTTACGAGCAGTACTTCGGGCCGGGCACCAGGCTCACGGTCACAG
TRAV 30	CAACAACCAGTGCAGAGTCCTCAAGCCGTGATCCTCCGAGAAGGGGAAGATGCTGTCATCAACTGCAGTTCCTCCAAGGCTTTATATTCTGTACACTGG TACAGGCAGAAGCATGGTGAAGCACCCGTCTTCCTGATGATATTACTGAAGGGTGGAGAACAGAAGGGTCATGAAAAAATATCTGCTTCATTTAATGAA AAAAAGCAGCAAAGCTCCCTGTACCTTACGGCCTCCCAGCTCAGTTACTCAGGAACCTACTTCTGCGGCACTCACGCAATGAGGGGTGCTACAAACAAG CTCATCTTTGGAACTGGCACTCTGCTTGCTGTCCAGCCAA
TRBV 27	GAAGCCCAAGTGACCCAGAACCCAAGATACCTCATCACAGTGACTGGAAAGAAGTTAACAGTGACTTGTTCTCAGAATATGAACCATGAGTATATGTCCT GGTATCGACAAGACCCAGGGCTGGGCTTAAGGCAGATCTACTATTCAATGAATGTTGAGGTGACTGATAAGGGAGATGTTCCTGAAGGGTACAAAAGT CTCTCGAAAAGAGAAGAGGAATTTCCCCCTGATCCTGGAGTCGCCCAGCCCCAACCAGACCTCTCTGTACTTCTGTGCCAGCAGTTTCAGTCCTAGCGG GGGATATAATGAGCAGTTCTTCGGGCCAGGGACACGGCTCACCGTGCTAG
TRAV 38-1	GCCCAGACAGTCACTCAGTCTCAACCAGAGATGTCTGTGCAGGAGGCAGAGACTGTGACCCTGAGTTGCACATATGACACCAGTGAGAATAATTATTAT TTGTTCTGGTACAAGCAGCCTCCCAGCAGGCAGATGATTCTCGTTATTCGCCAAGAAGCTTATAAGCAACAGAATGCAACGGAGAATCGTTTCTCTGTG AACTTCCAGAAAGCAGCCAAATCCTTCAGTCTCAAGATCTCAGACTCACAGCTGGGGGACACTGCGATGTATTTCTGTGCTTTCATGGAGAGTTATAACA CCGACAAGCTCATCTTTGGGACTGGGACCAGATTACAAGTCTTTCCAA
TRBV 6-6	AATGCTGGTGTCACTCAGACCCCAAAATTCCGCATCCTGAAGATAGGACAGAGCATGACACTGCAGTGTACCCAGGATATGAACCATAACTACATGTACT GGTATCGACAAGACCCAGGCATGGGGCTGAAGCTGATTTATTATTCAGTTGGTGCTGGTATCACTGATAAAGGAGAAGTCCCGAATGGCTACAACGTC TCCAGATCAACCACAGAGGATTTCCCGCTCAGGCTGGAGTTGGCTGCTCCCTCCCAGACATCTGTGTACTTCTGTGCCAGCAGTTACTGGGGGAAAGAG ACCCAGTACTTCGGGGCCAGGCACGCGGCTCCTGGTGCTCG
TRAV 38-1	GCCCAGACAGTCACTCAGTCTCAACCAGAGATGTCTGTGCAGGAGGCAGAGACTGTGACCCTGAGTTGCACATATGACACCAGTGAGAATAATTATTAT TTGTTCTGGTACAAGCAGCCTCCCAGCAGGCAGATGATTCTCGTTATTCGCCAAGAAGCTTATAAGCAACAGAATGCAACGGAGAATCGTTTCTCTGTG AACTTCCAGAAAGCAGCCAAATCCTTCAGTCTCAAGATCTCAGACTCACAGCTGGGGGACACTGCGATGTATTTCTGTGCTTTCGTTGATAATAATGCAG GCAACATGCTCACCTTTGGAGGGGGAACAAGGTTAATGGTCAAACCCC
TRBV 2	GAACCTGAAGTCACCCAGACTCCCAGCCATCAGGTCACACAGATGGGACAGGAAGTGATCTTGCGCTGTGTCCCCATCTCTAATCACTTATACTTCTATT GGTACAGACAAATCTTGGGGCAGAAAGTCGAGTTTCTGGTTTCCTTTTATAATAATGAAATCTCAGAGAAGTCTGAAATATTCGATGATCAATTCTCAGT TGAAAGGCCTGATGGATCAAATTTCACTCTGAAGATCCGGTCCACAAAGCTGGAGGACTCAGCCATGTACTTCTGTGCCAGCAGTGATCCCGGGACTAG CGCCTACAATGAGCAGTTCTTCGGGCCAGGGACACGGCTCACCGTGCTAG

Table 4.1: Single-cell T-cell receptor sequencing results. Ten TCRαβ pairs were identified from healthy donor PBMCs stimulated with HPV16-E6-3 epitope. The TCRα and TCRβ variable genes are listed (left) with the nucleotide sequence (right) containing V-J or V-D-J genes for TCRα and TCRβ, respectively.

TRAV	TRAJ	CDR3α	TRBV	TRBD	TRBJ	CDR3β
5	40	CAEIPTSGTYKYIF	7-8	2	2-1	CASSIPRRAVSSYNEQFF
13-1	57	CASSFFGLAGVNEQFF	12-4	2	2-1	CAASIRKGGSEKLVF
13-1	57	CAASIRKGGSEKLVF	29-1	1	2-7	CSGIDSISYEQYF
13-2	20	CAEKGRQNDYKLSF	2	1	2-1	CASSWDSYNEQFF
13-2	29	CAEKLGNTPLVF	18	--	2-5	CASSPYQETQYF
13-2	20	CAEKGRQNDYKLSF	4-2	--	1-2	CASSQASWTAESYGYTF
13-2	20	CAEKGRQNDYKLSF	10-3	--	2-7	CAISDETSQVYEQYF
30	32	CGTHAMRGATNKLIF	27	2	2-1	CASSFSPSGGYNEQFF
38-1	34	CAFMESYNTDKLIF	6-6	1	2-5	CASSYWGKETQYF
38-1	39	CAFVDNNAGNMLTF	2	2	2-1	CASSDPGTSAYNEQFF

Table 4.2: *TCR*αβ Gene Distribution and Respective CDR3 Amino Acid Sequences. TCRα sequences are listed with the corresponding TCRβ sequence (rows). The individual variable (TRAV) and joining gene (TRAJ) for TCRα are designated in each column followed by the variable (TRBV), diversity (TRBD), and joining (TRBJ) gene for the TCRβ. Each CDR3 amino acid sequence is listed following the specific *TCR*α or *TCR*β genes.

TCR:pMHC homology modeling provided predictions of which TCRαβ pairs may have the best binding interface to HPV A2-E6-3 peptide. The nucleotide sequences retrieved from out paired TCR sequences were translated into amino acid sequences and submitted for homology modeling. The top two ranked TCR pairs (Figure 4.6) were chosen as the most likely to bind to p:MHC because it had the strongest predicted electrostatic binding interface; the lowest free energy and the strongest predicted contribution from electrostatic interactions.

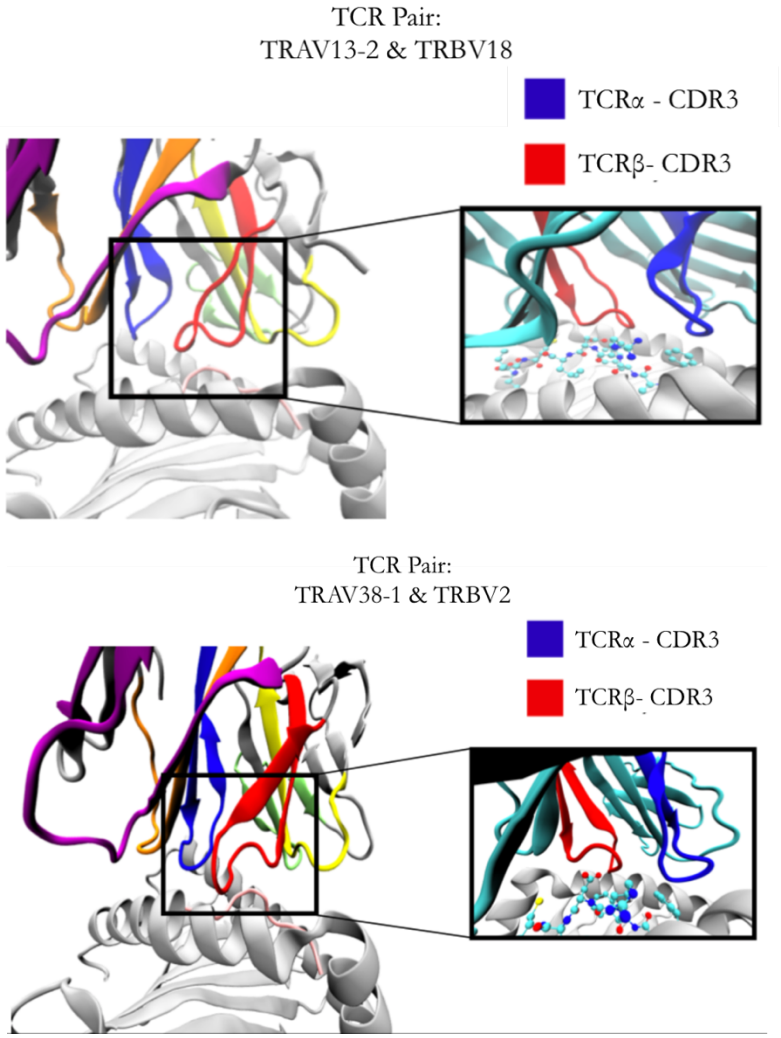

Figure 4.6: TCR:pMHC Homology Modeling of Retrieved TCRαβ Pairs to HPV A2-E6-3 Epitope. Representative comparative modeling of TCRαβ with target pMHC proteins demonstrating the binding interfaces between TCRα-CDR3 (blue), TCRβ-CDR3 (red), and the p:MHC complex (white).

Multiple sequence alignments provide a perfect pair-wise score to previously identified TCRβ CDR3 in HPV cervical cancer. In an effort to determine if any of our retrieved CDR3 sequences had been previously identified in other HPV associated cancers, we generated multiple sequence alignments. We compared our CDR3 sequences to previously analyzed data available on ImmunoSeq Analyzer database. The CDR3 that we used to compare were derived from a study that investigated the TCR repertoire between women who were able to clear cervical HPV infections versus those who could not [154]. While doing the alignments, we chose the top thirty CDR3 from the HPV set for each of our retrieved CDR3 and did and pairwise score to see how close the sequences would be. From the ten different CDR3 that we retrieved, we got a perfect match in TRBV 18 (CASSPYQETQYF). The CDR3 derived from cervical HPV infected patients were ranked from highest scoring (top) to lowest (bottom) (Figure 4.7)

TRBV18

TRBV7-8

TRBV12-4

TRBV29-1

TRBV2

TRBV4-2

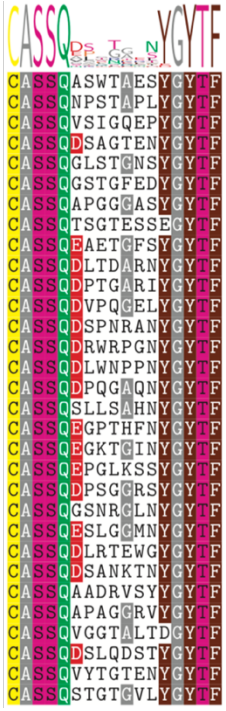

TRBV10-3

TRBV27

TRBV6-6

Figure 4.7: Multiple Sequence Alignments of Retrieved TCRβ CDR3 Against Published CDR3 in the ImmunoSeq Database. Our ten unique TCRβ CDR3 amino acid sequences were aligned to TCRβ CDR3 amino acid sequences found in women with HPV derived cervical infections. The retrieved CDR3 sequence is listed first (top) followed by a ranking of the most similar CDR3 sequence (top) to least similar (bottom) derived from ImmunoSeq.

Discussion:

HPV associated cancers, including cervical, colorectal, and head and neck cancer require the presence of a persistent HPV infection [93]. Although some virus specific proteins may be lost during integration into the host genome, expression of E2, E6, and E7 can be detected in varying degrees during infection [67]. The expression of virus specific proteins even post integration make HPV a great model for antigen targeting; these viral proteins should be restricted to malignant cells eliminating off-tumor toxicities [6, 58]. The presence of viral specific proteins within HPV-associated cancers suggests that these tumors could potentially be targeted with T cell therapies.

In previous studies, our lab identified high to moderately immunogenic HPV16 E2, E6, and E7 epitopes present in HPV+HNSCC [92]. Moving forward, I worked to expand antigen-specific T cells from healthy donor PBMCs through ex vivo stimulations with an HLA-A2

restricted E6-3 derived epitope. The goal was to isolate and profile TCR gene usage within an HPV stimulated population, thus identifying potential TCR pairs for adoptive cell therapies.

Using previously established *in vitro* stimulation protocols, we were able to generate an HPV-specific cytotoxic lymphocyte population that we further phenotyped and isolated by fluorescence activated cell sorting. Sorted CD8+CD137+ populations were amplified, processed, purified, and sent for next generation sequencing. Sequencing results allowed for the identification of ten unique paired TCRαβ sequences along with their respective CDR3 sequences, elucidating the variation in diversity of TCR in the context of E6-3 peptide. Based on homology modeling of the TCR;pMHC binding interfaces, we predict that two of our ten paired TCR (TRAV13-2 /TRBV18 and TRAV38-1/TRBV2), may be the best candidate for binding E2-E6-3 peptide.

Aligning our retrieved TCRβ CDR3 amino acids to previously reported CDR3 derived from individuals with a cervical HPV infection, we were able to perfectly match the CDR3 CASSPYQETQYF. The perfect alignment of our retrieved CDR3 to those found in a cervical HPV infected population may suggest a uniquely shared gene usage (TRBV 18) and CDR3 in HPV- associated infections. In a 2013 study investigating the TCR repertoire of tumor infiltrating lymphocytes in colon and rectal cancer, the same TCRβ CASSPYQETQYF CDR3 was observed in two out of fifteen patients [155]. While colon and rectal cancers are not necessarily HPV derived, 88% of anal cancers are linked to HPV infections [156] . While the study did not provide detail regarding where within the rectum the tissue was collected, it may be possible that T cells activated from an anal HPV-derived infection could have been detected, considering the anatomical proximity of the rectum and anus. Another explanation for the shared CDR3 sequence is that the individuals in the study may have had a previous or current HPV infection, influencing the expansion of this specific clonotype. The prevalence

of this CDR3 in HPV associated disease suggest that it is may be a TCR specific for HPV antigen and warrants further exploration.

To assess which individual could potentially benefit from TCR therapy specific to this epitope, I investigated the conservation of our HPV16-E6-3 target epitope across high risk HPV types (Table 4.3). Sequence analysis demonstrated that our target epitope (FAFRDLCIV) was unique to HPV16 and not conserved in the other HPV high risk types, suggesting that these TCR could be used to target individuals (expressing HLA-A2) specifically infected with HPV16.

HPV Type	E6 Amino Acid Sequence
16	MHQKRTAMFQDPQERPRKLPQLCTELQTTIHDIILECVYCKQQLLRREVYDFAFRDLCIVYRDGNPYAVCDKCLKFYSKISEYRHYCYSLY GTTLEQQYNKPLCDLLIRCINCQKPLCPEEKQRHLDKKQRFHNIRGRWTGRCMSCCRSSRTRRETQL
18	MARFEDPTRRPYKLPDLCTELNTSLQDIEITCVYCKTVLELTEVFEFAFKDLFVVYRDSIPHAACHKCIDFYSRIRELRHYSDSVYGDTLEKL TNTGLYNLLIRCLRCQKPLNPAEKLRH LNEKRRFHNIAGHYRGQCHSCCNRARQERLQRRRETQV
31	MFKNPAERPRKLHELSSALEIPYDELRLNCVYCKGQLTETEVLDFAFTDLTIVYRDDTPHGVCTKCLRFYSKVSEFRWYRYSVYGTTLEKLT NKGICDLLIRCITCQRPLCPEEKQRHLD KKKRFHNIGGRWTGRCIACWRRPRTETQV
33	MFQDTEEKPRTLHDLCQALETTIHNIELQCVECKKPLQRSEVYDFAFADLTVVYREGNPFGICKLCLRFLSKISEYRHYNYSVYGNTLEQT VKKPLNEILIRCIICQRPLCPQEKKRHVD LNKRFHNISGRWAGRCAACWRSRRRETAL
35	MFQDPAERPYKLHDLCNEVEESIHEICLNCVYCKQELQRSEVYDFACYDLCIVYREGQPYGVCMKCLKFYSKISEYRWYRYSVYGETLEKQ CNKQLCHLLIRCITCQKPLCPVEKQRHLE EKKRFHNIGGRWTGRCMSCWKPTRRETEV
45	MARFDDPKQRPYKLPDLCTELNTSLQDVSIACVYCKATLERTEVYQFAFKDLCIVYRDCIAYAACHKCIDFYSRIRELRYYSNSVYGETLEKI TNTELYNLLIRCLRCQKPLNPAEKRRH LKDKRRFHSIAGQYRGQCNTCCDQARQERLRRRRETQV
52	MFEDPATRPRTLHELCEVLEESVHEIRLQCVQCKKELQRREVYKFLFTDLRIVYRDNNPYGVCIMCLRFLSKISEYRHYQYSLYGKTLEERV KKPLSEITIRCIICQTPLCPEEKERHVN ANKRFHNIMGRWTGRCSECWRPRPVTQV
58	MFQDAEEKPRTLHDLCQALETSVHEIELKCVECKKTLQRSEVYDFVFADLRIVYRDGNPFAVCKVCLRLLSKISEYRHYNYSLYGDTLEQT LKKCLNEILIRCIICQRPLCPQEKKRHVD LNKRFHNISGRWTGRCAVCWRPRRRQTQV

Table 4.3 E6 Protein Conservation across High Risk HPV Types. The E6 protein sequence (right) derived from each respective high rics HPV type (left). The E6-3 epitope analyzed in this study is highlighted in yellow.

Future direction:

The GFP, FLuM1-TCR, and HPV-TCR constructs have all been designed for insert into MSGV1 plasmid. We currently have the GFP and FluM1-TCR constructs and are running experiments to test for successful expression. After confirming that the constructs have been correctly designed and can express in PBMCs, future work will be to have the HPV-TCR constructs synthesized and assess their functional capability.

CHAPTER 5

DISCUSSION

The global prevalence of HPV induced cancers, which accounts for 5% of all cancers worldwide, has revamped efforts to better understand persistent HPV infection in relation to adaptive immunity [157]. Previous studies have established that HPV-associated cancers express multiple oncogenic proteins (E6, and E7) [56]. Thus, effort have been aimed at developing immune therapies targeting E6 and E7 [6, 150, 151]. HPV16-E2, a transcriptional regulatory gene, has not been as heavily investigated as a candidate for immunotherapies because it is thought that protein expression is lost after genome integration [67]. However, current research has shown that in in comparison to cervical cancer, HPV+ HNSCCs have lower rates of genome integration as well as less interruption of E2 [67, 158]. As these findings suggest that subsets of HPV+ HNSCCs may express E2 in addition to E6 and E7, it emphasizes the importance of expanding candidates for targeted therapy to E2 epitopes in addition to E6 and E7.

Identifying a landscape of immunogenic epitopes is an important factor in developing targeted therapy however, it only provides a partial view of the immunologic landscape in HPV associated cancers. In order to more fully understand HPV immunology, it is critical to identify and characterize the subset of cells responsible for identifying and clearing viral infections and cancer, CD8+Tcells. Studies have shown that CD8+Tcells are necessary for viral clearance and in their absence or dysfunction, viral infections become persistent and lead to disease [125, 137]. T cell dysfunction has been confirmed in chronic infections derived from HIV, HBV, and HCV; illuminating the probability that T cell dysfunction could also be a factor in chronic HPV infections and associated cancers [125, 138]. Importantly, research and clinical trials have demonstrated that exhausted CD8+T cells could potentially be restored

with PD-L1/CTLA-4 blockade, essentially "releasing the breaks" on the T cells allowing them to perform their cytolytic function [159–161]. While checkpoint blockade inhibitors may serve as an important therapeutic in HPV+HNSCC, additional efforts have revamped in identifying the specific CD8+Tcell receptors that could recognize HPV targets and trigger an immune response. Targeted TCR therapies, which are widely investigated for their specificity and programmability, may serve as a better method for customizing treatment for late-stage cancers, such as HPV+HNSCC and invites further research.

There have been tremendous advancements in developing molecular approaches for analyzing TCR diversity in bulk and sorted populations. Next generation sequencing has revolutionized the analysis capabilities for evaluating immune repertoires [109]. While current approaches have their individual strengths and pitfalls, researchers can use a combination of approaches for optimal results. In an effort to combine previously established techniques with novel modifications, we aimed to develop a more streamlined method of retrieving and sequencing paired TCR sequences. In project one, I worked on modifying a new method for capturing and pairing TCR mRNA species from individual cells. While the original method was optimized for murine TCR, I was able to adapt the technology to capture human TCR mRNA. The overall goal of the project was to be able to demonstrate that the DNA origami nanoprobe complex could capture, barcode, and link TCRαβ at the single-cell level. Importantly, we wanted to develop the methodology in a framework that that did not require expensive and specialized equipment. I was able to modify the DNA origami nanoprobe complex, optimize the process for transfection into a human T cell line, and successfully capture and recover paired TCRα and TCRβ mRNA. Future goals for this methodology would be to optimize the system to barcode and pair an extensive repertoire of TCR gene sequences from a polyclonal population within a single experiment.

In project two, my colleagues used predictive algorithms to identify HPV16-E2, E6, and E7 immunogenic epitopes in HPV+HNSCC patient PBMCs. Several of the highly to moderately immunogenic predicted epitopes proved to be novel in the context of HPV+HNSCC and HLA-restriction. This work provided a very comprehensive landscape of immunodominant epitopes derived from functionally important HPV proteins E2, E6, and E7. After identifying a landscape of immunogenic HPV epitopes, I worked to optimize a method to detect low frequency HPV-specific CTLs, determined whether these CTLs were tumor specific (expression of memory cell surface markers), and assessed overall T cell dysfunction (expression of multiple exhaustion markers). From this study, I was able to detect low frequency HPV-specific CTLs as confirmed through tetramer binding, I showed that HPV+HNSCC patients exhibited increased E7 or E2-specific levels of CD8+T cell exhaustion. Prior to this study, T cell dysfunction in the context of HPV+HNSCC had not yet been described.

In project three, I took previously established methods developed in our laboratory to expand and isolate CD8+T cells reactive to HPV target epitope E6-3. The goal was to perform a single-cell analysis of the TCRαβ repertoire generated in response to this previously defined immunogenic epitope. Our sequencing results provided ten unique TCRαβ pairs with respective CDR3 sequences. In an effort to determine the frequency of our retrieved TCRβ CDR3 sequences in other HPV infections, I performed sequence alignments against previously published TCRβ CDR3 derived from women with HPV cervical infections. The TRBV18 CDR3 (CASSPYQETQYF) alignments resulted in a perfect match in the HPV database set but HLA status of those cases is not known. Further research into the prevalence of CASSPYQETQYF showed that it also appeared in colon and rectal cancers. While these cancers are not associated with HPV infections, it is possible that these donors did have an

HPV infection that influenced the expansion of this particular CDR3 subset, suggesting that TRBV18/CASSPYQETQYF may be specific to HPV associated infection and disease and further warrants additional experiments to test the functional capability of this TCR to HPV. Epitope conservation analysis across HPV high risk types revealed that our targeted E6-3 epitope was only conserved in HPV16; suggesting that our HLA-A2 restricted E6-3 protein would be a potential candidate for individuals infected with HPV16 but no other high-risk subtypes. In order to develop a TCR therapy that could target a heterogeneous population, a broad range of immunogenic epitopes across various HLA's would need to be developed.

REFERENCES

1. Graham S V. (2010) Human papillomavirus: Gene expression, regulation and prospects for novel diagnostic methods and antiviral therapies. Future Microbiol. 5:1493–1506

2. Senba M, Mori N (2012) Mechanisms of virus immune evasion lead to development from chronic inflammation to cancer formation associated with human papillomavirus infection. Oncol Rev

3. Spence T, Bruce J, Yip KW, Liu FF (2016) HPV associated head and neck cancer. Cancers (Basel) 8:. https://doi.org/10.3390/cancers8080075

4. The Nobel Prize in Physiology or Medicine 2008

5. Finlay BB, McFadden G (2006) Anti-immunology: Evasion of the host immune system by bacterial and viral pathogens. Cell 124:767–782

6. Draper LM, Kwong MLM, Gros A, et al (2015) Targeting of HPV-16+ epithelial cancer cells by TCR gene engineered T cells directed against E6. Clin Cancer Res 21:4431–4439. https://doi.org/10.1158/1078-0432.CCR-14-3341

7. Kellie S, Al-Mansour Z (2017) Overview of the Immune System. In: Micro- and Nanotechnology in Vaccine Development. Elsevier Inc., pp 63–81

8. Thompson MR, Kaminski JJ, Kurt-Jones EA, Fitzgerald KA (2011) Pattern recognition receptors and the innate immune response to viral infection. Viruses 3:920–940

9. Chaplin DD (2010) Overview of the immune response. J Allergy Clin Immunol 125:S3. https://doi.org/10.1016/j.jaci.2009.12.980

10. Kenneth Murphey CW (2017) Janeway's Immunobiology 9th Edition . In: Book. https://www.amazon.com/Janeways-Immunobiology-Kenneth-Murphy/dp/081534550X. Accessed 9 Oct 2020

11. Beutler B (2004) Innate immunity: An overview. Mol Immunol 40:845–859. https://doi.org/10.1016/j.molimm.2003.10.005

12. Parkin J, Cohen B (2001) An overview of the immune system. Lancet 357:1777–1789. https://doi.org/10.1016/S0140-6736(00)04904-7

13. Volanakis JE (1982) COMPLEMENT ACTIVATION BY C-REACTIVE PROTEIN COMPLEXES. Ann N Y Acad Sci 389:235–250. https://doi.org/10.1111/j.1749-6632.1982.tb22140.x

14. Kimbrell DA, Beutler B (2001) The evolution and genetics of innate immunity.

Nat. Rev. Genet. 2:256–267

15. Modlin RL (2012) Innate immunity: Ignored for decades, but not forgotten. In: Journal of Investigative Dermatology. Nature Publishing Group, pp 882–886

16. Abul Abbas ALSP (2014) Cellular and Molecular Immunology - 8th Edition, 8th ed. Elsevier Health Sciences

17. Yatim KM, Lakkis FG (2015) A brief journey through the immune system. Clin J Am Soc Nephrol 10:1274–1281. https://doi.org/10.2215/CJN.10031014

18. Masopust D, Vezys V, Wherry EJ, Ahmed R (2007) A brief history of CD8 T cells. Eur J Immunol 37:S103–S110. https://doi.org/10.1002/eji.200737584

19. Joglekar A V., Li G (2020) T cell antigen discovery. Nat. Methods

20. Gowans JL, Uhr JW (1966) The carriage of immunological memory by small lymphocytes in the rat. J Exp Med 124:1017–1030. https://doi.org/10.1084/jem.124.5.1017

21. Voskoboinik I, Whisstock JC, Trapani JA (2015) Perforin and granzymes: Function, dysfunction and human pathology. Nat. Rev. Immunol. 15:388–400

22. Bjorkman PJ, Saper MA, Samraoui B, et al (1987) Structure of the human class I histocompatibility antigen, HLA-A2. Nature 329:506–512. https://doi.org/10.1038/329506a0

23. Zhang J, Chen Y, Qi J, et al (2012) Narrow Groove and Restricted Anchors of MHC Class I Molecule BF2*0401 Plus Peptide Transporter Restriction Can Explain Disease Susceptibility of B4 Chickens. J Immunol 189:4478–4487. https://doi.org/10.4049/jimmunol.1200885

24. Bjorkman PJ, Burmeister WP (1994) Structures of two classes of MHC molecules elucidated: crucial differences and similarities. Curr Opin Struct Biol 4:852–856. https://doi.org/10.1016/0959-440X(94)90266-6

25. Blum JS, Wearsch PA, Cresswell P (2013) Pathways of antigen processing. Annu. Rev. Immunol. 31:443–473

26. Peter Parham (2009) The Immune System, 3rd Edition: 9780815341468: Medicine & Health Science , 3rd ed. Garland Science

27. Murphy KCW (2016) Janeway's Immunobiology 9, 9th ed. Garland Science

28. Abele R, Tampé R (1999) Function of the transport complex TAP in cellular immune recognition. Biochim. Biophys. Acta - Biomembr. 1461:405–419

29. La Gruta NL, Gras S, Daley SR, et al (2018) Understanding the drivers of MHC restriction of T cell receptors. Nat Rev Immunol 18:467–478. https://doi.org/10.1038/s41577-018-0007-5

30. Courtney AH, Lo WL, Weiss A (2018) TCR Signaling: Mechanisms of Initiation and Propagation. Trends Biochem. Sci. 43:108–123

31. Wucherpfennig KW, Gagnon E, Call MJ, et al (2010) Structural biology of the T-cell receptor: insights into receptor assembly, ligand recognition, and initiation of signaling. Cold Spring Harb. Perspect. Biol. 2:5140–5141

32. Garcia KC (2012) Reconciling views on T cell receptor germline bias for MHC. Trends Immunol. 33:429–436

33. Davis MM, Bjorkman PJ (1988) T-cell antigen receptor genes and T-cell recognition. Nature 334:395–402

34. Olaru A, Petrie HT, Livák F (2005) Beyond the 12/23 Rule of VDJ Recombination Independent of the Rag Proteins. J Immunol 174:6220–6226. https://doi.org/10.4049/jimmunol.174.10.6220

35. Ma Y, Lu H, Schwarz K, Lieber MR (2005) Cell Cycle Repair of Double-Strand DNA Breaks by the Human Nonhomologous DNA End Joining Pathway: The Iterative Processing Model. https://doi.org/10.4161/cc.4.9.1977

36. Arstila TP, Casrouge A, Baron V, et al (1999) A direct estimate of the human αβ T cell receptor diversity. Science (80-) 286:958–961. https://doi.org/10.1126/science.286.5441.958

37. Robins HS, Srivastava SK, Campregher P V., et al (2010) Overlap and effective size of the human CD8+ T cell receptor repertoire. Sci Transl Med 2:47ra64. https://doi.org/10.1126/scitranslmed.3001442

38. Laydon DJ, Bangham CRM, Asquith B (2015) Estimating T-cell repertoire diversity: Limitations of classical estimators and a new approach. Philos Trans R Soc B Biol Sci 370:. https://doi.org/10.1098/rstb.2014.0291

39. Nikolich-Žugich J, Slifka MK, Messaoudi I (2004) The many important facets of T-cell repertoire diversity. Nat. Rev. Immunol. 4:123–132

40. Pannetier C, Cochet M, Darche S, et al (1993) The sizes of the CDR3 hypervariable regions of the murine T-cell receptor β chains vary as a function of the recombined germ-line segments. Proc Natl Acad Sci U S A 90:4319–4323. https://doi.org/10.1073/pnas.90.9.4319

41. Even J, Lim A, Puisieux I, et al (1995) T-cell repertoires in healthy and diseased human tissues analysed by T-cell receptor β-chain CDR3 size determination:

evidence for oligoclonal expansions in tumours and inflammatory diseases. Res Immunol 146:65–80. https://doi.org/10.1016/0923-2494(96)80240-9

42. Brownlie RJ, Zamoyska R (2013) T cell receptor signalling networks: Branched, diversified and bounded. Nat. Rev. Immunol. 13:257–269

43. Smith-Garvin JE, Koretzky GA, Jordan MS (2009) T cell activation. Annu. Rev. Immunol. 27:591–619

44. Dobosz P, Dzieciątkowski T (2019) The Intriguing History of Cancer Immunotherapy. Front. Immunol. 10:2965

45. Magalhaes I, Carvalho-Queiroz C, Hartana CA, et al (2019) Facing the future: challenges and opportunities in adoptive T cell therapy in cancer. Expert Opin. Biol. Ther. 19:811–827

46. Chen DS, Mellman I (2013) Oncology meets immunology: The cancer-immunity cycle. Immunity 39:1–10

47. Ben-Avi R, Farhi R, Ben-Nun A, et al (2018) Establishment of adoptive cell therapy with tumor infiltrating lymphocytes for non-small cell lung cancer patients. Cancer Immunol Immunother 67:1221–1230. https://doi.org/10.1007/s00262-018-2174-4

48. Rohaan MW, Wilgenhof S, Haanen JBAG Adoptive cellular therapies: the current landscape. https://doi.org/10.1007/s00428-018-2484-0

49. Wang Z, Cao YJ (2020) Adoptive Cell Therapy Targeting Neoantigens: A Frontier for Cancer Research. Front. Immunol. 11:176

50. P J Spiess JCYSAR (1987) In vivo antitumor activity of tumor-infiltrating lymphocytes expanded in recombinant interleukin-2 - PubMed. J Natl Cancer Inst

51. Rosenberg SA, Restifo NP, Yang JC, et al (2008) Adoptive cell transfer: A clinical path to effective cancer immunotherapy. Nat. Rev. Cancer 8:299–308

52. Schumacher TN, Schreiber RD (2015) Neoantigens in cancer immunotherapy. Science (80-.). 348:69–74

53. Ott PA, Hu Z, Keskin DB, et al (2017) An immunogenic personal neoantigen vaccine for patients with melanoma. Nature 547:217–221. https://doi.org/10.1038/nature22991

54. Tran E, Robbins PF, Lu Y-C, et al (2016) T-Cell Transfer Therapy Targeting Mutant KRAS in Cancer. N Engl J Med 375:2255–62. https://doi.org/10.1056/NEJMoa1609279

55. Fesnak AD, June CH, Levine BL (2016) Engineered T cells: The promise and challenges of cancer immunotherapy. Nat. Rev. Cancer 16:566–581

56. Tognon MG, Akgül B, Banks L, Gheit T (2019) Mucosal and Cutaneous Human Papillomavirus Infections and Cancer Biology. Front Oncol | www.frontiersin.org 1:355. https://doi.org/10.3389/fonc.2019.00355

57. Marur S, D'Souza G, Westra WH, Forastiere AA (2010) HPV-associated head and neck cancer: A virus-related cancer epidemic. Lancet Oncol. 11:781–789

58. Li W, Qi Y, Cui X, et al (2018) Characteristic of HPV Integration in the Genome and Transcriptome of Cervical Cancer Tissues. Biomed Res Int 2018:. https://doi.org/10.1155/2018/6242173

59. Riemer AB, Keskin DB, Zhang G, et al (2010) A conserved E7-derived cytotoxic T lymphocyte epitope expressed on human papillomavirus 16-transformed HLA-A2+ epithelial cancers. J Biol Chem 285:29608–29622. https://doi.org/10.1074/jbc.M110.126722

60. Doorbar J, Egawa N, Griffin H, et al (2015) Human papillomavirus molecular biology and disease association. Rev Med Virol 25:2–23. https://doi.org/10.1002/rmv.1822

61. Koneva LA, Zhang Y, Virani S, et al (2018) HPV integration in HNSCC correlates with survival outcomes, immune response signatures, and candidate drivers. Mol Cancer Res 16:90–102. https://doi.org/10.1158/1541-7786.MCR-17-0153

62. Oh ST, Longworth MS, Laimins LA (2004) Roles of the E6 and E7 Proteins in the Life Cycle of Low-Risk Human Papillomavirus Type 11. J Virol 78:2620–2626. https://doi.org/10.1128/jvi.78.5.2620-2626.2004

63. Yim E-K, Park J-S (2005) The Role of HPV E6 and E7 Oncoproteins in HPV-associated Cervical Carcinogenesis. Cancer Res Treat 37:319. https://doi.org/10.4143/crt.2005.37.6.319

64. Doorbar J, Quint W, Banks L, et al (2012) The biology and life-cycle of human papillomaviruses. Vaccine 30:. https://doi.org/10.1016/j.vaccine.2012.06.083

65. Lawrence MS, Sougnez C, Lichtenstein L, et al (2015) Comprehensive genomic characterization of head and neck squamous cell carcinomas. Nature 517:576–582. https://doi.org/10.1038/nature14129

66. Pinatti LM, Walline HM, Carey TE (2018) Human Papillomavirus Genome Integration and Head and Neck Cancer. J Dent Res 97:691–700. https://doi.org/10.1177/0022034517744213

67. Parfenov M, Pedamallu CS, Gehlenborg N, et al (2014) Characterization of HPV

and host genome interactions in primary head and neck cancers. Proc Natl Acad Sci U S A 111:15544–15549. https://doi.org/10.1073/pnas.1416074111

68. Lechien JR, Descamps G, Seminerio I, et al (2020) HPV involvement in the tumor microenvironment and immune treatment in head and neck squamous cell carcinomas. MDPI AG

69. Torre LA, Bray F, Siegel RL, et al (2015) Global cancer statistics, 2012. CA Cancer J Clin 65:87–108. https://doi.org/10.3322/caac.21262

70. Gillison ML, D'Souza G, Westra W, et al (2008) Distinct risk factor profiles for human papillomavirus type 16-positive and human papillomavirus type 16-negative head and neck cancers. J Natl Cancer Inst 100:407–420. https://doi.org/10.1093/jnci/djn025

71. Boscolo-Rizzo P, Del Mistro A, Bussu F, et al (2013) New insights into human papillomavirus-associated head and neck squamous cell carcinoma. Acta Otorhinolaryngol. Ital. 33:77–87

72. Curado MP, Boyle P (2013) Epidemiology of head and neck squamous cell carcinoma not related to tobacco or alcohol. Curr. Opin. Oncol. 25:229–234

73. O'Sullivan B, Huang SH, Su J, et al (2016) Development and validation of a staging system for HPV-related oropharyngeal cancer by the International Collaboration on Oropharyngeal cancer Network for Staging (ICON-S): a multicentre cohort study. Lancet Oncol 17:440–451. https://doi.org/10.1016/S1470-2045(15)00560-4

74. Huang SH, Xu W, Waldron J, et al (2015) Refining American joint committee on cancer/union for international cancer control TNM stage and prognostic groups for human papillomavirus-related oropharyngeal carcinomas. J Clin Oncol 33:836–845. https://doi.org/10.1200/JCO.2014.58.6412

75. Smith EM, Pawlita M, Rubenstein LM, et al (2010) Risk factors and survival by HPV-16 E6 and E7 antibody status in human papillomavirus positive head and neck cancer. Int J Cancer 127:111–117. https://doi.org/10.1002/ijc.25015

76. Smith EM, Ritchie JM, Summersgill KF, et al (2003) AGE, SEXUAL BEHAVIOR AND HUMAN PAPILLOMAVIRUS INFECTION IN ORAL CAVITY AND OROPHARYNGEAL CANCERS. https://doi.org/10.1002/ijc.11633

77. Wood ZC, Bain CJ, Smith DD, et al (2017) Oral human papillomavirus infection incidence and clearance: A systematic review of the literature. J. Gen. Virol. 98:519–526

78. de Martel C, Plummer M, Vignat J, Franceschi S (2017) Worldwide burden of

cancer attributable to HPV by site, country and HPV type. Int J Cancer 141:664–670. https://doi.org/10.1002/ijc.30716

79. Zhou C, Tuong ZK, Frazer IH (2019) Papillomavirus Immune Evasion Strategies Target the Infected Cell and the Local Immune System. Front Oncol 9:. https://doi.org/10.3389/fonc.2019.00682

80. Steinbach A, Riemer AB (2018) Immune evasion mechanisms of human papillomavirus: An update. Int J Cancer 142:224–229. https://doi.org/10.1002/ijc.31027

81. de Ruiter EJ, Ooft ML, Devriese LA, Willems SM (2017) The prognostic role of tumor infiltrating T-lymphocytes in squamous cell carcinoma of the head and neck: A systematic review and meta-analysis. Oncoimmunology 6:. https://doi.org/10.1080/2162402X.2017.1356148

82. Wansom D, Light E, Thomas D, et al (2012) Infiltrating lymphocytes and human papillomavirus-16-associated oropharyngeal cancer. Laryngoscope 122:121–127. https://doi.org/10.1002/lary.22133

83. Monie A, Hung CF, Roden R, Wu TC (2008) Cervarix^{TM}:A vaccine for the prevention of HPV 16, 18-associated cervical cancer. Biol. Targets Ther. 2:107–113

84. Chatterjee A (2014) The next generation of HPV vaccines: nonavalent vaccine V503 on the horizon. Expert Rev Vaccines 13:1279–1290. https://doi.org/10.1586/14760584.2014.963561

85. Hirth JM, Chang M, Resto VA, et al (2017) Prevalence of oral human papillomavirus by vaccination status among young adults (18–30 years old). Vaccine 35:3446–3451. https://doi.org/10.1016/j.vaccine.2017.05.025

86. Chaturvedi AK, Graubard BI, Broutian T, et al (2018) Effect of prophylactic human papillomavirus (HPV) vaccination on oral HPV infections among young adults in the United States. J Clin Oncol 36:262–267. https://doi.org/10.1200/JCO.2017.75.0141

87. Beachler DC, Kreimer AR, Schiffman M, et al (2016) Multisite HPV16/18 Vaccine Efficacy Against Cervical, Anal, and Oral HPV Infection. J Natl Cancer Inst 108:302. https://doi.org/10.1093/jnci/djv302

88. Melchers WJ, Herbrink P, Walboomers JM, et al (1989) Optimization of human papillomavirus genotype detection in cervical scrapes by a modified filter in situ hybridization test. J Clin Microbiol 27:

89. Abreu ALP, Souza RP, Gimenes F, Consolaro MEL (2012) A review of methods for detect human Papillomavirus infection. Virol. J. 9:1–9

90. Stephen JK, Divine G, Chen KM, et al (2012) Significance of p16 in site-specific HPV positive and HPV negative HNSCC. Cancer Clin Oncol 2:. https://doi.org/10.5539/cco.v2n1p51

91. Cuschieri K, Wentzensen N (2008) Human papillomavirus mRNA and p16 detection as biomarkers for the improved diagnosis of cervical neoplasia. Cancer Epidemiol. Biomarkers Prev. 17:2536–2545

92. Krishna S, Ulrich P, Wilson E, et al (2018) Human papilloma virus specific immunogenicity and dysfunction of CD8+ T cells in head and neck cancer. Cancer Res 78:6159–6170. https://doi.org/10.1158/0008-5472.CAN-18-0163

93. Gillison ML, Chaturvedi AK, Anderson WF, Fakhry C (2015) Epidemiology of human papillomavirus-positive head and neck squamous cell carcinoma. J. Clin. Oncol. 33:3235–3242

94. Ferris RL, Blumenschein G, Fayette J, et al (2016) Nivolumab for recurrent squamous-cell carcinoma of the head and neck. N Engl J Med 375:1856–1867. https://doi.org/10.1056/NEJMoa1602252

95. Chow LQM, Haddad R, Gupta S, et al (2016) Antitumor activity of pembrolizumab in biomarker-unselected patients with recurrent and/or metastatic head and neck squamous cell carcinoma: Results from the phase Ib KEYNOTE-012 expansion cohort. J Clin Oncol 34:3838–3845. https://doi.org/10.1200/JCO.2016.68.1478

96. Barrett DM, Grupp SA, June CH (2015) Chimeric Antigen Receptor– and TCR-Modified T Cells Enter Main Street and Wall Street. J Immunol 195:755–761. https://doi.org/10.4049/jimmunol.1500751

97. Anderson KS, Dahlstrom KR, Cheng JN, et al (2015) HPV16 antibodies as risk factors for oropharyngeal cancer and their association with tumor HPV and smoking status. Oral Oncol 51:662–667. https://doi.org/10.1016/j.oraloncology.2015.04.011

98. Zhang Y, Zhang Y, Zhu Y, et al Tools for fundamental analysis functions of TCR repertoires: a systematic comparison. Brief Bioinform 21:1706–1716. https://doi.org/10.1093/bib/bbz092

99. Li H, Ye C, Ji G, Han J (2012) Determinants of public T cell responses. Cell Res. 22:33–42

100. Price DA, West SM, Betts MR, et al (2004) T cell receptor recognition motifs govern immune escape patterns in acute SIV infection. Immunity 21:793–803. https://doi.org/10.1016/j.immuni.2004.10.010

101. Page DB, Yuan J, Redmond D, et al (2016) Deep sequencing of T-cell receptor

DNA as a biomarker of clonally expanded TILs in breast cancer after immunotherapy. Cancer Immunol Res 4:835–844. https://doi.org/10.1158/2326-6066.CIR-16-0013

102. Sims JS, Grinshpun B, Feng Y, et al (2016) Diversity and divergence of the glioma-infiltrating T-cell receptor repertoire. Proc Natl Acad Sci U S A 113:E3529–E3537. https://doi.org/10.1073/pnas.1601012113

103. Han Y, Li H, Guan Y, Huang J (2016) Immune repertoire: A potential biomarker and therapeutic for hepatocellular carcinoma. Cancer Lett. 379:206–212

104. Cui J-H, Lin K-R, Yuan S-H, et al (2018) TCR Repertoire as a Novel Indicator for Immune Monitoring and Prognosis Assessment of Patients With Cervical Cancer. Front Immunol 9:2729. https://doi.org/10.3389/fimmu.2018.02729

105. Reuben A, Zhang J, Chiou SH, et al (2020) Comprehensive T cell repertoire characterization of non-small cell lung cancer. Nat Commun 11:. https://doi.org/10.1038/s41467-019-14273-0

106. Rizvi NA, Hellmann MD, Snyder A, et al (2015) Mutational landscape determines sensitivity to PD-1 blockade in non-small cell lung cancer. Science (80-) 348:124–128. https://doi.org/10.1126/science.aaa1348

107. Govindan R, Ding L, Griffith M, et al (2012) Genomic landscape of non-small cell lung cancer in smokers and never-smokers. Cell 150:1121–1134. https://doi.org/10.1016/j.cell.2012.08.024

108. Gameiro SF, Ghasemi F, Barrett JW, et al (2018) Treatment-naïve HPV+ head and neck cancers display a T-cell-inflamed phenotype distinct from their HPV-counterparts that has implications for immunotherapy. Oncoimmunology 7:. https://doi.org/10.1080/2162402X.2018.1498439

109. Rosati E, Dowds CM, Liaskou E, et al (2017) Overview of methodologies for T-cell receptor repertoire analysis. BMC Biotechnol 17:. https://doi.org/10.1186/s12896-017-0379-9

110. Ciupe SM, Devlin BH, Markert ML, Kepler TB (2013) Quantification of total T-cell receptor diversity by flow cytometry and spectratyping. BMC Immunol 14:35. https://doi.org/10.1186/1471-2172-14-35

111. Six A, Mariotti-Ferrandiz ME, Chaara W, et al (2013) The past, present, and future of immune repertoire biology - the rise of next-generation repertoire analysis. Front Immunol 4:. https://doi.org/10.3389/fimmu.2013.00413

112. Gorski J, Yassai M, Zhu X, et al (1994) Circulating T cell repertoire complexity in normal individuals and bone marrow recipients analyzed by CDR3 size spectratyping. Correlation with immune status. J Immunol 152:

113. Robins HS, Campregher P V., Srivastava SK, et al (2009) Comprehensive assessment of T-cell receptor β-chain diversity in αβ T cells. Blood 114:4099–4107. https://doi.org/10.1182/blood-2009-04-217604

114. De Simone M, Rossetti G, Pagani M (2018) Single Cell T Cell Receptor Sequencing: Techniques and Future Challenges. Front Immunol 9:1638. https://doi.org/10.3389/fimmu.2018.01638

115. Howie B, Sherwood AM, Berkebile AD, et al (2015) High-throughput pairing of T cell receptor α and β sequences. Sci Transl Med 7:301ra131-301ra131. https://doi.org/10.1126/scitranslmed.aac5624

116. Han A, Glanville J, Hansmann L, Davis MM (2014) Linking T-cell receptor sequence to functional phenotype at the single-cell level. Nat Biotechnol 32:684–692. https://doi.org/10.1038/nbt.2938

117. Munson DJ, Egelston CA, Chiotti KE, et al (2016) Identification of shared TCR sequences from T cells in human breast cancer Using emulsion RT-PCR. Proc Natl Acad Sci U S A 113:8272–8277. https://doi.org/10.1073/pnas.1606994113

118. Faint JM, Pilling D, Akbar AN, et al (1999) Quantitative flow cytometry for the analysis of T cell receptor Vβ chain expression. J Immunol Methods 225:53–60. https://doi.org/10.1016/S0022-1759(99)00027-7

119. Kebschull JM, Zador AM (2015) Sources of PCR-induced distortions in high-throughput sequencing data sets. Nucleic Acids Res 43:. https://doi.org/10.1093/nar/gkv717

120. Kivioja T, Vähärautio A, Karlsson K, et al (2012) Counting absolute numbers of molecules using unique molecular identifiers. Nat Methods 9:72–74. https://doi.org/10.1038/nmeth.1778

121. Rothemund PWK (2006) Folding DNA to create nanoscale shapes and patterns. Nature 440:297–302. https://doi.org/10.1038/nature04586

122. Hu Q, Li H, Wang L, et al (2019) DNA Nanotechnology-Enabled Drug Delivery Systems. Chem. Rev. 119:6459–6506

123. Schoettle L, Blattman J, Yan H, et al (2017) Bowties, Barcodes, and DNA Origami; A Novel Approach for Paired-Chain Immune Receptor Repertoire Analysis. Arizona State University

124. Fields B (2013) Fields virology, 6th ed. Wolters Kluwer Health/Lippincott Williams & Wilkins, Philadelphia

125. Rosendahl Huber S, van Beek J, de Jonge J, et al (2014) T cell responses to viral infections – opportunities for peptide vaccination.

https://doi.org/10.3389/fimmu.2014.00171

126. Mueller SN, Rouse BT (2008) Immune responses to viruses. In: Clinical Immunology. Elsevier Ltd, pp 421–431

127. Huber SR, van Beek J, de Jonge J, et al (2014) T cell responses to viral infections - opportunities for peptide vaccination. Front Immunol 5:. https://doi.org/10.3389/fimmu.2014.00171

128. Matloubian M, Concepcion RJ, Ahmed R (1994) CD4+ T cells are required to sustain CD8+ cytotoxic T-cell responses during chronic viral infection. J Virol 68:8056–8063. https://doi.org/10.1128/jvi.68.12.8056-8063.1994

129. Thimme R, Wieland S, Steiger C, et al (2003) CD8+ T Cells Mediate Viral Clearance and Disease Pathogenesis during Acute Hepatitis B Virus Infection. J Virol 77:68–76. https://doi.org/10.1128/jvi.77.1.68-76.2003

130. Jones RB, Walker BD (2016) HIV-specific CD8+ T cells and HIV eradication. J Clin Invest 126:455–463. https://doi.org/10.1172/JCI80566

131. Boldogh I, Albrecht T, Porter DD (1996) Persistent Viral Infections. University of Texas Medical Branch at Galveston

132. Zhou F, Chen JZ, Zhao KN (2013) Human papillomavirus 16-encoded E7 protein inhibits IFN-γ-mediated MHC class I antigen presentation and CTL-induced lysis by blocking IRF-1 expression in mouse keratinocytes. J Gen Virol 94:2504–2514. https://doi.org/10.1099/vir.0.054486-0

133. Bottley G, Watherston OG, Hiew YL, et al (2008) High-risk human papillomavirus E7 expression reduces cell-surface MHC class I molecules and increases susceptibility to natural killer cells. Oncogene 27:1794–1799. https://doi.org/10.1038/sj.onc.1210798

134. D'Souza G, Kreimer AR, Viscidi R, et al (2007) Case–Control Study of Human Papillomavirus and Oropharyngeal Cancer. N Engl J Med 356:1944–1956. https://doi.org/10.1056/NEJMoa065497

135. Wherry EJ, Kurachi M (2015) Molecular and cellular insights into T cell exhaustion. Nat. Rev. Immunol. 15:486–499

136. Wherry EJ, Blattman JN, Murali-Krishna K, et al (2003) Viral Persistence Alters CD8 T-Cell Immunodominance and Tissue Distribution and Results in Distinct Stages of Functional Impairment. J Virol 77:4911–4927. https://doi.org/10.1128/jvi.77.8.4911-4927.2003

137. Saeidi A, Zandi K, Cheok YY, et al (2018) T-cell exhaustion in chronic infections: Reversing the state of exhaustion and reinvigorating optimal protective immune

responses. Front Immunol 9:2569. https://doi.org/10.3389/fimmu.2018.02569

138. Shin H, Wherry EJ (2007) CD8 T cell dysfunction during chronic viral infection. Curr. Opin. Immunol. 19:408–415

139. Wherry EJ, Ha SJ, Kaech SM, et al (2007) Molecular Signature of CD8+ T Cell Exhaustion during Chronic Viral Infection. Immunity 27:670–684. https://doi.org/10.1016/j.immuni.2007.09.006

140. Barber DL, Wherry EJ, Masopust D, et al (2006) Restoring function in exhausted CD8 T cells during chronic viral infection. Nature 439:682–687. https://doi.org/10.1038/nature04444

141. Gupta PK, Godec J, Wolski D, et al (2015) CD39 Expression Identifies Terminally Exhausted CD8+ T Cells. PLoS Pathog 11:. https://doi.org/10.1371/journal.ppat.1005177

142. Chowell D, Krishna S, Becker PD, et al (2015) TCR contact residue hydrophobicity is a hallmark of immunogenic CD8+ T cell epitopes. Proc Natl Acad Sci U S A 112:E1754–E1762. https://doi.org/10.1073/pnas.1500973112

143. Krishna S, Anderson KS (2016) T-cell epitope discovery for therapeutic cancer vaccines. In: Methods in Molecular Biology. Humana Press Inc., pp 779–796

144. Roberts AD, Ely KH, Woodland DL (2005) Differential contributions of central and effector memory T cells to recall responses. J Exp Med 202:123–133. https://doi.org/10.1084/jem.20050137

145. Zur Hausen H (1991) Viruses in human cancers. Science (80-) 254:1167–1173. https://doi.org/10.1126/science.1659743

146. Hudnall SD (2014) Viruses and human cancer. Springer New York

147. PK G, J G, D W, et al (2015) CD39 Expression Identifies Terminally Exhausted CD8+ T Cells. PLoS Pathog 11:. https://doi.org/10.1371/JOURNAL.PPAT.1005177

148. Markowitz LE, Gee J, Chesson H, Stokley S (2018) Ten Years of Human Papillomavirus Vaccination in the United States

149. Fakhry C, Westra WH, Li S, et al (2008) Improved survival of patients with human papillomavirus-positive head and neck squamous cell carcinoma in a prospective clinical trial. J Natl Cancer Inst 100:261–269. https://doi.org/10.1093/jnci/djn011

150. Kenter GG, Welters MJP, Valentijn ARPM, et al (2009) Vaccination against HPV-16 Oncoproteins for Vulvar Intraepithelial Neoplasia. N Engl J Med 361:1838–

1847. https://doi.org/10.1056/NEJMoa0810097

151. Trimble CL, Morrow MP, Kraynyak KA, et al (2015) Safety, efficacy, and immunogenicity of VGX-3100, a therapeutic synthetic DNA vaccine targeting human papillomavirus 16 and 18 E6 and E7 proteins for cervical intraepithelial neoplasia 2/3: A randomised, double-blind, placebo-controlled phase 2b trial. Lancet 386:2078–2088. https://doi.org/10.1016/S0140-6736(15)00239-1

152. Woodsworth DJ, Castellarin M, Holt RA (2013) Sequence analysis of T-cell repertoires in health and disease. Genome Med 5:. https://doi.org/10.1186/gm502

153. Li B, Li T, Pignon JC, et al (2016) Landscape of tumor-infiltrating T cell repertoire of human cancers. Nat Genet 48:725–732. https://doi.org/10.1038/ng.3581

154. Lang Kuhs KA, Lin S-W, Hua X, et al (2018) T cell receptor repertoire among women who cleared and failed to clear cervical human papillomavirus infection: An exploratory proof-of-principle study. PLoS One 13:e0178167. https://doi.org/10.1371/journal.pone.0178167

155. Sherwood AM, Emerson RO, Scherer D, et al (2013) Tumor-infiltrating lymphocytes in colorectal tumors display a diversity of T cell receptor sequences that differ from the T cells in adjacent mucosal tissue. Cancer Immunol Immunother 62:1453–1461. https://doi.org/10.1007/s00262-013-1446-2

156. Wang CJ, Sparano J, Palefsky JM (2017) HIV/AIDS, HPV and Anal Cancer. Surg Oncol Clin N Am 26:17. https://doi.org/10.1016/J.SOC.2016.07.010

157. Dorrell L, Hellner K (2017) Recent advances in understanding and preventing human papillomavirus-related disease. F1000Research 6

158. Akagi K, Li J, Broutian TR, et al (2014) Genome-wide analysis of HPV integration in human cancers reveals recurrent, focal genomic instability. Genome Res 24:185–199. https://doi.org/10.1101/gr.164806.113

159. Barber DL, Wherry EJ, Masopust D, et al (2006) Restoring function in exhausted CD8 T cells during chronic viral infection. Nature 439:682–687. https://doi.org/10.1038/nature04444

160. Pardoll DM (2012) The blockade of immune checkpoints in cancer immunotherapy. Nat Rev Cancer 12:252–264. https://doi.org/10.1038/nrc3239

161. Robert C, Schachter J, Long G V., et al (2015) Pembrolizumab versus ipilimumab in advanced melanoma. N Engl J Med 372:2521–2532. https://doi.org/10.1056/NEJMoa1503093